

# IMPACT OF DISTRIBUTED GENERATION ON UNBALANCED POWER SYSTEMS

By

Edy Ernesto Jiménez Toribio

A thesis submitted in partial fulfillment of the requirements for the degree of

MASTER OF SCIENCE  
in  
ELECTRICAL ENGINEERING  
(Power Systems)

UNIVERSITY OF PUERTO RICO  
MAYAGÜEZ CAMPUS  
2009

Approved by:

\_\_\_\_\_  
Lionel R. Orama-Exclusa, Ph.D.  
Member, Graduate Committee

\_\_\_\_\_  
Date

\_\_\_\_\_  
Erick E. Aponte, Eng. D  
Member, Graduate Committee

\_\_\_\_\_  
Date

\_\_\_\_\_  
Efrain O'Neill-Carrillo, Ph.D.  
Chairperson, Graduate Committee

\_\_\_\_\_  
Date

\_\_\_\_\_  
Juan Romero, PhD  
Representative of Graduate Studies

\_\_\_\_\_  
Date

\_\_\_\_\_  
Benjamín Colucci, Ph.D.  
Interim Dean of Engineering and  
Acting Chairman of the Department

\_\_\_\_\_  
Date

## **ABSTRACT**

The interconnection of Distributed Generation (DG) units to a utility grid changes the configuration of traditional distribution networks. Today, DG has been one of the key driving forces in the evolution of distribution system analysis, which has been traditionally perceived as modelling small radially-connected systems with simple power flow methods. Despite its apparently simple structure, the distribution system is considerably more complex than transmission systems due to a mixture of three-phase, two-phase, and single-phase lines and transformers. This work developed more accurate modeling of unbalanced power systems to determine the impact of DG technologies on voltage regulation, taking into consideration the total system losses. The analysis was conducted with a full three-phase model because unbalanced conditions affect the behavior of the entire distribution system under high penetration of DG. A detailed mathematical formulation of line models and voltage dependency of loads was presented in order to achieve a better understanding of the distribution system characteristics. Also, a detailed description of the step voltage regulator control system was presented and related with the three-phase model of transformer banks. The IEEE 13 Node and 4 Node Test Feeders were selected to verify the validity of the proposed models. The complete simulation of the IEEE systems was carried out with the calculation program DIgSILENT.

## RESUMEN

Independientemente del beneficio que la Generación Distribuida (GD) puede proporcionar, la interconexión de estas unidades de generación con la red de distribución cambia la configuración de estos sistemas tradicionales. Hoy en día, las unidades de GD han sido uno de los motores clave en la evolución del análisis de los sistemas de distribución, los cuales han sido tradicionalmente percibidos como pequeños sistemas conectados radialmente y analizados con métodos simples de flujo de potencia. A pesar de su estructura, aparentemente sencilla, el sistema de distribución es mucho más complejo que los sistemas de transmisión debido a una mezcla de alimentadores trifásicos y monofásicos, interconectados mediante transformadores con innumerables configuraciones posibles. Este trabajo ha modelado de forma correcta dichos sistemas para determinar el impacto de una alta penetración de GD sobre la regulación de voltaje, teniendo en cuenta las pérdidas totales del sistema. Una formulación matemática detallada de los modelos de la línea y la dependencia de voltaje de la carga se presentó con el fin de lograr una mejor comprensión de las características del sistema de distribución. Además, una amplia descripción del sistema de control del regulador de voltaje relacionado con el modelo trifásico de los bancos de transformadores. Los Alimentadores Radiales de Prueba (13 y 4 Nodos) de la IEEE fueron seleccionados para verificar la validez de los modelos propuestos. La simulación completa de los Alimentadores de prueba de la IEEE se llevo a cabo con el programa DIgSILENT.

*Dedicated to Haydeli and Rufo, my parents*

## **ACKNOWLEDGMENTS**

First, I want to thank God for giving me life, and for blessing me in all ways through my academic preparation. Thanks to Dr. Efraín O’Neill-Carrillo, chairman of my graduate committee, for his support and guidance. Thanks Dr. O’Neill for your time and patience and for giving me the opportunity of being one of your graduate students. I also want to express my gratitude to Dr. Erick Aponte and Dr. Lionel Orama-Exclusa for serving as member of my graduate committee and for their valuable advice during the course of the master program. I would like to thank my fellows in graduate school for their friendship, and to my girlfriend, for her unconditional love and support. I am especially grateful to Alfredo Cuello-Reyna for his advice and encouragement.

Special thanks to my parents, Haydeli and Rufo, for their support and consideration in all of my studies. Also to my sister Ada and my brother Jose Luis for being always there in the most important times. Last but not least, I would like to thank my aunt Dionilda Toribio for her unconditional support.

# Table of Contents

ABSTRACT.....	ii
RESUMEN .....	iii
ACKNOWLEDGMENTS .....	v
LIST OF TABLES .....	viii
LIST OF FIGURES.....	ix
CHAPTER 1 .....	1
INTRODUCTION.....	1
1.1 Research Objectives .....	2
1.2 Thesis Outline .....	3
CHAPTER 2 .....	4
LITERATURE REVIEW .....	4
2.1 Beginning of the Electrical Industry .....	4
2.2 Distributed Generation .....	5
2.3 Driving Forces for DG Technologies .....	7
2.4 Impact of DG on Distribution Systems .....	10
2.5 Impact of DG on Voltage Regulation.....	12
2.6 Impact of DG on Overcurrent Protection.....	13
2.7 Islanding Considerations .....	15
2.8 DG Interconnection Transformer Considerations.....	17
CHAPTER 3 .....	23
REALISTIC POWER SYSTEM MODELING FOR DISTRIBUTED GENERATION .....	23
3.1 IEEE Radial Distribution Test Feeder Simulation.....	23
3.2 Load Models .....	25
3.3 Overhead and Underground Line Models.....	26
3.4 Distribution Transformer Models .....	32
3.5 Voltage Regulator Model .....	37
3.6 IEEE 13 Node Test Feeder Unbalanced Power-Flow.....	42
3.7 IEEE 4 Node Test Feeder Model.....	46
3.8 Overcurrent Protection Model .....	48
3.9 PWM Converter Model .....	63

CHAPTER 4 .....	66
DISTRIBUTED GENERATION UNDER.....	66
UNBALANCED CONDITIONS .....	66
4.1    Introduction .....	66
4.2    Impact of SVR and Shunt Capacitors on Voltage Regulation.....	70
4.3    Impact of DG Integration on the Original System.....	76
4.4    Case Study I: DG Interconnection at Phase A (N_652).....	79
4.5    Case Study II: DG Interconnection at Phase C (N_611).....	82
4.6    Case Study III: Three-Phase DG Interconnection .....	84
CHAPTER 5 .....	88
CONCLUSIONS AND FUTURE WORK .....	88
5.1    Conclusions .....	88
5.2    Future Work.....	90
References.....	91

## LIST OF TABLES

Table 2. 1: Characteristics and Costs of electric power generation technologies [9] [17].....	8
Table 2. 2: Interconnection system response to abnormal voltages [11].....	12
Table 2. 3: Characteristic of three-phase transformer connections used for DG applications [37].....	18
Table 3. 1: Spot Load Data [39] [4] .....	26
Table 3. 2: Distributed Load Data [39] [4]. .....	26
Table 3. 3: Overhead and underground line configuration data [39] [4] .....	31
Table 3. 4: Standard Distribution Transformer Sizes [23].....	33
Table 3. 5: Category of transformer ratings [46].....	33
Table 3. 6: Distribution transformer short-circuit withstand capability [46] .....	33
Table 3. 7: IEEE 13 node test feeder Transformer’s data [39].....	36
Table 3. 8: ANSI C84.1 Service voltage ranges for a normal 3-wire 120/240 volts service to a user. Adapted from [23].....	37
Table 3. 9: Line drop compensator parameters [49] [51] .....	41
Table 3. 10: Step voltage regulator data [39].....	42
Table 3. 11: Unbalanced Power Flow results for the IEEE 13 node test feeder .....	45
Table 3. 12: Three-Phase Transformer Data [56].....	47
Table 3. 13: Closed Connection Load Data [56].....	47
Table 3. 14: Unbalanced load flow results for the IEEE 4 node test feeder with <i>Grounded-Y/Delta Step-Down</i> Transformer Bank. ....	47
Table 3. 15: Relay Designations .....	50
Table 3. 16: IEEE Standardized Relay Curve Equations Constants [61] .....	51
Table 3. 17: Full load current magnitudes per phase for the IEEE 13 Node Test Feeder.....	56
Table 3. 18: Unbalanced Three-phase fault currents for the IEEE 13 Node test feeder .....	57
Table 3. 19: Single-phase-to-ground fault currents for the IEEE 13 node test feeder.....	59
Table 3. 20: Maximum continuous and fault current magnitudes for the device location.....	60
Table 3. 21: Melting Time-Current characteristics of E Rated Links [69] .....	61
Table 3. 22: Device Rating for F1 to F8, E Rated [70].....	62
Table 3. 23: Maximum Rating Capabilities for SMC-40 Fuse [70].....	62

## LIST OF FIGURES

Figure 2. 1: Traditional electric utility structure .....	4
Figure 2. 2: New conception of electric industry. Integration of DG technologies.....	6
Figure 2. 3: Emissions from Energy Consumption at Conventional Power Plants and CHP Plants, 1996 through 2007, Data extracted from U.S. Department of Energy [19] .....	9
Figure 2. 4: Decision making summary when considering DG interconnection to a power system. Adapted from [22] [24].....	11
Figure 2. 5: Impact of DG integration on a typical distribution feeder overcurrent protection .....	14
Figure 2. 6: Voltage developed when systems are 180° out of phase .....	16
Figure 2. 7: Islanding detection techniques classification. Adapted from [33] [34] .....	16
Figure 2. 8: Neutral shift during single line to ground (SLG) fault and phasor representation. Adapted from [23] [36] [37]. .....	19
Figure 2. 9: Ground fault contribution from DG interconnected using grounded-Y (utility) / delta (DG) transformer. Adapted from [37] .....	20
Figure 3. 1: IEEE 13 Node Distribution Test Feeder Online Diagram [39].....	24
Figure 3. 2: Transposition Cycle [41].....	26
Figure 3. 3: Conductors and images. The conductors I' and j' represent the ground image [3]. .....	27
Figure 3. 4: Overhead line spacing ID-(500,505,510).....	30
Figure 3. 5: Underground Line Spacing. ....	30
Figure 3. 6: Basic transformer model. Adapted from [43].....	32
Figure 3. 7: Typical distribution transformer with two-bushing primary and center-tapped 120/240 volts three-bushing secondary .....	35
Figure 3. 8: Three-phase distribution transformer connections. Adapted from [23].....	35
Figure 3. 9: Standard Delta/Grounded-wye connection with voltages .....	36
Figure 3. 10: Type B step-voltage regulator and control circuit. Adapted from [49].....	38
Figure 3. 11: Line Drop Compensator Circuit .....	40
Figure 3. 12: IEEE 13 node test feeder online diagram from DIgSILENT workspace. ....	44
Figure 3. 13: IEEE 4 Node Test Feeder Online Diagram .....	46
Figure 3. 14: Composite Frame of a Time-Overcurrent Relay. Adapted from [54].....	49
Figure 3. 15: Extremely Inverse Relay curves following the IEEE standardized characteristics .....	50
Figure 3. 16: Typical ac connections of a protective relay with its DC trip circuit.....	51
Figure 3. 17: Tentative location of overcurrent protection on the IEEE 13 Node Test Feeder.....	53
Figure 3. 18: Principle of the Superposition Method. Adapted from [68].....	54
Figure 3. 19: Behavior of the Short-Circuit Current far from the Generator .....	55
Figure 3. 20: Location of Three-Phase Short Circuit Calculations .....	57
Figure 3. 21: Electromagnetic Transient behavior of a three-phase fault at node RG-60 .....	58
Figure 3. 22: TCC Coordination for S&C SMU-40 fuses and ABB/Westinghouse CO-7 Moderately Inverse Overcurrent Relay .....	61
Figure 3. 23: Sinusoidal pulse-width modulation .....	64

Figure 3. 24: DG Interface Control operated as a constant power source with unity power factor operation [77].	65
Figure 4. 1: Single-phase and Three-Phase DG integration considering individual home projects and multi-megawatt three-phase PV arrays. Adapted from [75].	67
Figure 4. 2: Electronically coupled DER unit: Dispatchable DG plus batteries storage	68
Figure 4. 3: SVR and Shunt Capacitors Location on the IEEE 13 Node Test Feeder.	70
Figure 4. 4: Current Tap Position of the SVRs for Cases II and III	71
Figure 4. 5: Voltage profile of the Main Feeder per phase. (1, 1) phase A; (1, 2) phase B; (2, 1) phase C; and (2, 2) phases A-B-C for Cases II-III	72
Figure 4. 6: Grounded Wye Three-phase Line.	73
Figure 4. 7: Kilowatts losses per phase and Total losses for Cases II and III.	74
Figure 4. 8: Modification of the IEEE 13 Node Test Feeder to Evaluate the Impact of DG on Voltage Regulation.	76
Figure 4. 9: Original Three-phase Voltage Profile of the Main Feeder.	78
Figure 4. 10: Voltage profile of the Main Feeder and SVR Tap Positions for DG Interconnection at Phase A	80
Figure 4. 11: Active power losses of the system for DG interconnection at Phase A	81
Figure 4. 12: Active Power Losses of the System for DG Interconnection at Phase C	82
Figure 4. 13: Voltage profile of the Main Feeder and SVR Tap Positions for DG Interconnection at Phase C	83
Figure 4. 14: Active Power Losses of the System for Three-phase DG Interconnection	84
Figure 4. 15: Voltage profile of the Main Feeder and SVR Tap Positions for Three-Phase DG Interconnection.	85
Figure 4. 16: Summary of Single-phase DGs Impact on phase A.	86
Figure 4. 17: Summary of Single-phase DGs Impact on phase C.	86

# CHAPTER 1

## INTRODUCTION

The electric utility industry can trace its beginnings to the early 1880s. The earliest distribution system surrounded Thomas Edison's 1882 Pearl Street Station in lower Manhattan, using direct current (DC) placing small generators right next to the load. The fast growth of electricity demand and the development of high-voltage power transmission lines using alternating current (AC) encouraged electric utilities to build larger generators near the primary energy source (e.g., coal mines, water dams, etc.) and use transmission lines to deliver electricity to load centers, sometimes over spans of hundreds of miles. As a result of this production scheme electric utilities made technological advances by constructing larger generating plants to capture economies of scale [1] [2].

The last decade has presented dramatic changes in world energy policies due to unstable prices of fossil fuels. The fast degradation of natural resources suggests that renewable forms of energy must be leading the future of the power generation industry. *Distributed Generation (DG)* systems are small-scale power generation technologies used to provide an alternative to or an improvement of the traditional electric power system. This includes a wide range of energy sources like wind, solar, biomass, and storage.

Regardless of the benefits that DG can provide, the interconnection of DG to utility grid changes the configuration of traditional distribution networks. Today, DG has been one of the key driving forces in the evolution of distribution system analysis, which has been traditionally perceived as modelling small radially-connected systems with simple power flow methods. Although this perception is true in many cases, things are changing.

Radial distribution feeders are characterized by having only one path for power to flow from the source to each customer, and the loading is unbalanced because of the large number of unequal single-phase loads that must be served. An additional unbalance is introduced by the nonequilateral conductor spacings of three-phase overhead and underground line segments. Traditional power flow studies for transmission networks assume a perfectly balanced system and line transposition, so that a single-phase equivalent system is used. This assumption cannot be made on distribution networks [3].

This thesis seeks to examine the impact of DG technologies on unbalanced power systems with an emphasis on voltage regulation. The analysis is conducted with a full three-phase (multi-phase) model because unbalances affect the whole behavior of the distribution system under scenarios of high penetration of DG. A detailed mathematical formulation of line models and voltage dependency of loads is presented, as well as the transformer banks and control system of the step voltage regulator. The IEEE 13 Node and 4 Node Test Feeders were selected to verify the validity of the proposed models. Also, a short-circuit analysis of the original system is developed in order to show the modeling of overcurrent protective devices. Through simulation, various types of DG (single-phase and Three-phase) have been interconnected with the distribution system at different penetration levels to analyze the voltage profile of the main feeder.

## **1.1 Research Objectives**

The IEEE Distribution System Analysis Subcommittee (DSAS) has developed a number of test feeders to serve as a common set of data that could be used by program developers and users to verify the accuracy of their solutions [4]. This thesis will examine the impact of DG interconnection on the IEEE 13 Node Test Feeder, taking into consideration the single-phase and three-phase integration. This thesis pays attention to a more accurate modeling of distribution systems to achieve results closer to reality and a better interpretation of DG behavior and impact.

The specific objectives of this work are the following:

1. Mathematical description and modeling of distribution power system devices, with particular emphasis on the control system for step voltage regulators.
2. Development of solving methods for power-flow and short-circuit analysis in distribution systems. The short-circuit analysis was made in order to establish guidelines for the coordination of overcurrent protection devices on unbalanced power systems.
3. Simulation of the IEEE 13 Node and 4 Node Test Feeders to verify the accuracy of the proposed models.
4. Integration of single-phase and three-phase DGs to the IEEE 13 Node Test Feeder taking into consideration different penetration levels. Establish differences between single-phase and three-phase DGs on unbalanced voltage regulation.

5. Present arguments in favor of a more accurate modeling of distribution networks to guarantee the validity of future impact studies on power systems.

## **1.2 Thesis Outline**

In Chapter 2 the evolution of the traditional power system is presented. Also, an overview is given of the state of the art in distribution system analysis with respect to considering DG in the medium voltage (MV) distribution system. Chapter 3 describes the mathematical model of distribution system elements (i.e., overhead and underground lines, loads, power transformers, and step voltage regulators). A comparison is made between the IEEE original test feeders and the modeled network to verify the validity of the simulation. Chapter 4 presents the Case Studies considered to state differences between the impact of single-phase and three-phase DGs on distribution systems. Finally, Chapter 5 presents general conclusions and future work.

## CHAPTER 2

### LITERATURE REVIEW

#### 2.1 Beginning of the Electrical Industry

The electric utility industry can trace its beginnings to the early 1880s. The earliest distribution system surrounded Thomas Edison's 1882 Pearl Street Station in lower Manhattan, using direct current (DC) and putting their small generators right next to the load. This method of distribution was so inefficient that most power plants had to be located within a mile of the place using the power. The generation was planned to meet demand, with a certain reserve margin for safety reasons [2] [5].

The fast growth of electricity demand and the development of high-voltage power transmission lines using alternating current (AC) encouraged electric utilities to build larger generators near the primary energy source (e.g., coal mines, water dams, etc.). Electric utilities made technological advances by constructing larger generating plants to capture economies of scale. It cost less to generate a kilowatt-hour (kWh) of electricity from a large plant than from a small plant. Under this structure, the Public Utility Holding Company Act of 1935 (PUHCA) limits the geographical scope of holding companies and creates vertically integrated utilities in monopoly service areas. Traditionally, these utilities own generation, transmission, and distribution facilities within their assigned service territories (Figure 2.1) [1].

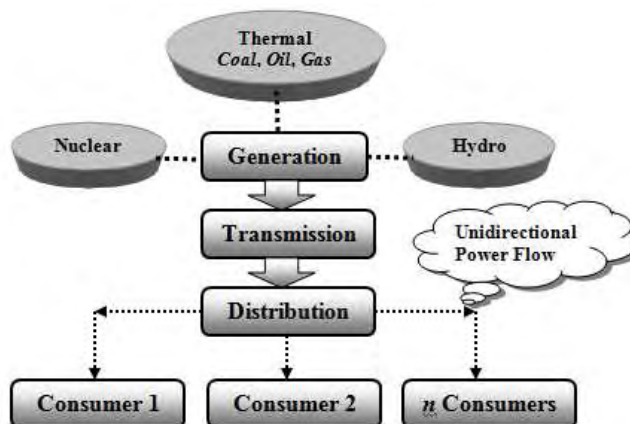


Figure 2. 1: Traditional electric utility structure

The 1978 Public Utility Regulatory Policies Act (PURPA) was the first step toward deregulation of the electric power industry. This law created a market for non-utility electric power producers forcing electric utilities to buy power from these producers at the avoided cost rate, which is the marginal cost for the same amount of energy acquired through another means such as construction of new production facility or purchase from an alternate supplier [6]. During the next few years the central system became three separate entities, energy suppliers, transmission companies and distribution utilities coordinated by the Independent System Operators (ISOs). In this context, Distributed Energy Resources (DER) has emerged as a promising option to meet growing customer needs for electric power.

## 2.2 Distributed Generation

Distributed generation is a new approach in the electric power industry and the analysis of the relevant literature has shown there is no generally accepted definition of distributed generation; the following different definitions are currently used:

1. *International Council on Large Electric Systems (CIGRÉ)* defines DG as [7] [8]:

- Not centrally planned.
- Today not centrally dispatched.
- Usually connected to the distribution network.
- Smaller than 50 or 100 MW.

2. *International Energy Agency (IEA)* [9]:

Distributed generation is generating plant serving a customer on-site or providing support to a distribution network, connected to the grid at distribution-level voltages. The technologies generally include engines, small (and micro) turbines, fuel cells, and photovoltaic systems. It generally excludes wind power, since that is mostly produced on wind farms rather than for on-site power requirements.

3. *US Department of Energy (US DOE)* [10]:

Distributed generation – small, modular electricity generators sited close to the customer load- can enable utilities to defer or eliminate costly investments in transmission and distribution (T&D) systems upgrades, and provides customers with better quality, more reliable energy supplies and a cleaner environment.

4. *Electric Power Research Institute (EPRI)* [8] [10]:

Distributed generation is small generation (1kW to 50MW) and/or energy storage devices typically sited near customer loads of distribution and sub-transmission substations.

5. *Institute of Electrical and Electronic Engineers (IEEE)* [11]:

The Standard for Interconnecting Distributed Resources with Electric Power System of IEEE, define distributed generation like electric generation facilities connected to an Area EPS (Electrical Power System) through a point of common coupling; a subset of distributed resources. EPS areas are facilities that deliver electric power to a load that serves Local EPS. The point where a Local EPS is connected to the Area EPS receives the name of Point of Common Coupling (PCC). Finally, the IEEE defines Distributed Resources (DR) as sources of electric power that are not directly connected to a bulk power transmission system. DR includes generators and energy storage systems.

There is not a clear consensus finding a proper definition for DG, but every attempt given by each organization consider location and rated capacity. Figure 2.2 shows that DG can be connected directly to distribution network, not necessarily at customer busbar, so that a feeder with DG can be subjected to bidirectional flows, i.e., DG power generation exceeds customer needs or customer demand is higher than DG production. DG should not be confused with renewable generation. High penetration of certain DG technologies can contribute to air pollution problems and greenhouse effect.

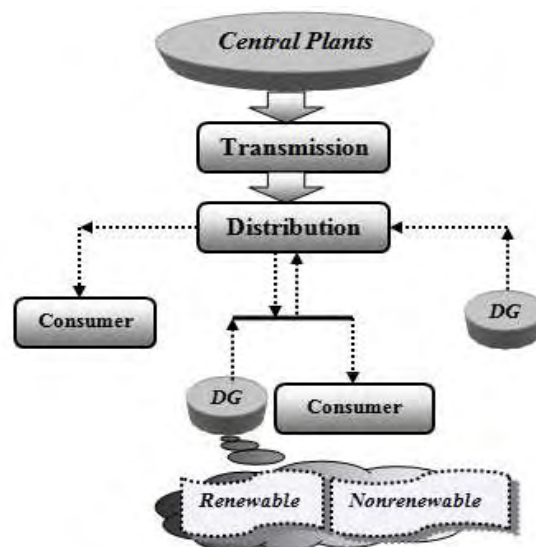


**Figure 2. 2:** New conception of electric industry. Integration of DG technologies

## 2.3 Driving Forces for DG Technologies

In the last decade, distributed generation is attracting a renewed interest and policy attention. The International Energy Agency identifies five major external forces influencing utility business strategy and decisions [9] [12]:

### 1. *Electricity market liberalization.*

In a liberalized market it is very important to adapt to the evolving regulatory issues in a flexible way. These regulations impact the use of distributed generation, including net metering, interconnection access, stranded costs, etc. Therefore, new suppliers are identifying niche markets for best DG implementation (i.e. enhance reliability, CHP applications). Also DG provides bigger flexibility than large central power plants because of their small sizes [13]. Before approval of the Energy Policy Act of 2005, utilities were required to purchase qualifying facilities (QFs) power at avoided cost. This requirement was eliminated for QFs operating in competitive wholesale markets meeting certain requirements established by the Federal Energy Regulatory Commission (FERC) [14] [15].

### 2. *Developments in DG technology.*

Recent technical advances are also increasing interest in DG power units. The use of DG allows a flexible reaction to the changing market, implementing DG for continuous or peak shaving use. The Table 2.1 shows a brief summary of available DG technologies, characteristics and typical cost per kilowatt-hour.

### 3. *Constraints on the construction of new transmission lines.*

The construction of ever larger central power plants is more difficult with the pass of the years. Since it is more convenient to transport energy in its electric form, fossil thermal plants are sited close to raw fuel sources and require the construction of complex and capital-intensive transmission networks [16]. It is becoming more difficult to receive the right-of-way or the permits allowing the construction of *T&D* systems.

### 4. *Increased customer demand for highly reliable electricity.*

Reliability problems refer to sustain interruptions (outages). A standard often cited for highly reliable power is “*six nines*” of reliability (i.e. 99.9999%), equivalent to 30 seconds of outage per year. Since radial distribution network protection is one of the main causes for service outages, on-site DG and storage devices could be employed to guarantee a continuous energy supply.

**Table 2. 1:** Characteristics and Costs of electric power generation technologies [9] [17]

<b>Technology</b>	<b>Typical Characteristics</b>	<b>Typical Energy Costs (U.S. cents/kilowatt-hour)</b>
<b>Industrial Generation/cost at 60% Load Factor</b>		
Internal Combustion Engine	<i>System size: 5 kW-10 MW; efficiency for large diesel systems up to 43%</i>	6-11
Gas Turbines	<i>System size: 1-20 MW; commonly used in CHP applications</i>	6-9
Microturbine	<i>System Size: 35 kW-1 MW</i>	7-9
<b>Renewable Technologies</b>		
<b>Power Generation</b>		
Large hydro	<i>Plant size: 10-18000 MW</i>	3-4
Small hydro	<i>Plant size: 1-10 MW</i>	4-7
On-shore wind	<i>Turbine size: 1-3 MW Blade diameter: 60-100 meters</i>	5-8
Off-shore wind	<i>Turbine size: 1.5-5 MW Blade diameter: 70-125 meters</i>	8-12
Biomass power	<i>Plant size: 1-20 MW</i>	5-12
Geothermal power	<i>Plant size: 1-100 MW, Type: binary, single and double-flash, natural steam</i>	4-7
Solar PV (module)	<i>Cell type and efficiency: single-crystal 17%; polycrystalline 15%; amorphous silicon 10%; thin film 9-12%</i>	----
Rooftop solar PV	<i>Peak Capacity: 2-5 kilowatts-peak</i>	20-80
Concentrating Solar Thermal Power (CSP)	<i>Plant size: 50-500 MW (trough), 10-20 MW (tower); Types: trough, tower, dish</i>	12-18
<b>Hot Water/Heating</b>		
Biomass heat	<i>Plant size: 1-20 MW</i>	1-6
Solar hot water/heating	<i>Size: 2-5 m<sup>2</sup> (household); 20-200 m<sup>2</sup> (medium/multi-family) ; 0.5-2 MWth (large/district heating); Types: evacuated tube, flat-plate</i>	2-20 (household) 1-15 (medium) 1-8 (large)
Geothermal heating/cooling	<i>Plant capacity: 1-10 MW; Types: heat pumps, direct use, chillers</i>	0.5-2
<b>Rural (off-grid) Energy</b>		
Mini-hydro	<i>Plant capacity: 100-1000 kW</i>	5-10
Micro-hydro	<i>Plant capacity: 1-100 kW</i>	7-20
Biomass gasifier	<i>Size: 20-5000 kW</i>	8-12
Small wind turbine	<i>Turbine size: 3-100 kW</i>	15-25
Household wind turbine	<i>Turbine size: 0.1-3 kW</i>	15-35
Solar home system	<i>System size: 20-100 watts</i>	40-60

5. Environmental concerns.

As electricity demand was increasing Mega projects of hydroelectric power plants were developed. Most of these power plants involved large dams which flooded big areas of land to provide water storage and therefore a constant supply of electricity. It is becoming increasingly difficult for developers to build new dams because of opposition from environmentalists and people living on the land to be flooded. On the other hand, fossil fuel thermal power plants bring air pollution problems difficult to ignore. The imposition of carbon emission penalties on fossil fuel plants encourages the adoption of renewable based energy generation to substitute carbon power generation (*substitution effect*). This will decrease the energy demand due to an increase in the average electricity price (*price effect*) [18].

Figure 2.3 shows the emissions from energy consumption at conventional power plants and CHP plants from 1996 through 2007. Two dates have been identified: 1997, Kyoto Protocol was initially adopted, and entered into force on February 16, 2005.

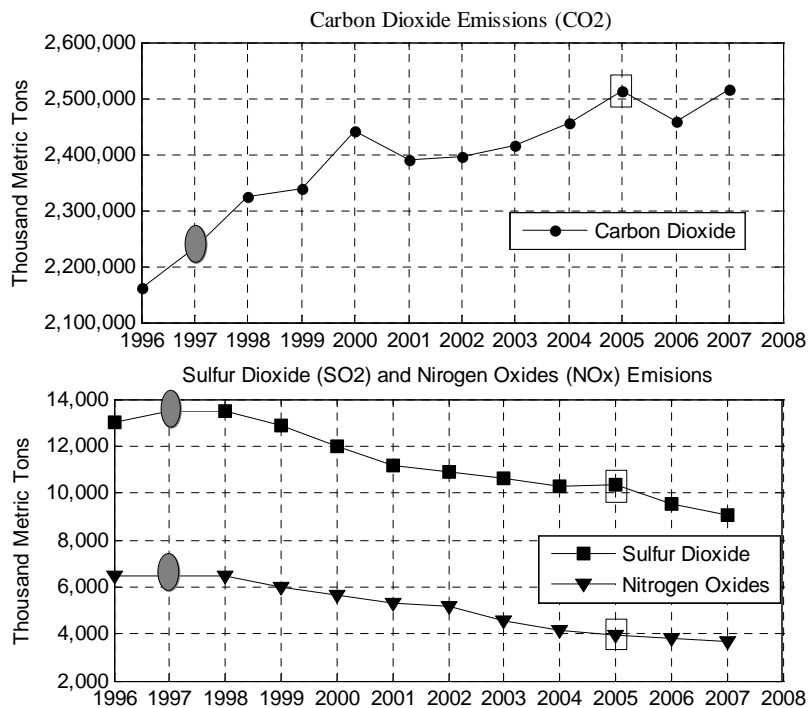


Figure 2. 3: Emissions from Energy Consumption at Conventional Power Plants and CHP Plants, 1996 through 2007, Data extracted from U.S. Department of Energy [19]

## 2.4 Impact of DG on Distribution Systems

The interconnection of DG to utility grid changes the configuration of traditional distribution networks, creating problems to protection schemes. The high penetration of DG can have a significant impact on the T&D system creating bidirectional power flows (usually flows from higher voltage to lower voltage levels, i.e. transmission to distribution). The degree of this impact depends on many factors, including the size of DR units, location on the T&D system, loading, system configuration and time at which DG units are dispatched. However, DG may provide benefits [20] [21]:

- Emergency Backup during sustained utility outages.
- Value of energy savings through peak shaving.
- Reduced voltage sags.
- Postpone potential utility capacity addition, and congestion of transmission line infrastructure.
- Renewable forms of DG helps to reduce pollutants sent to the atmosphere.
- Line loss reduction, among others.

Distributed generation can also impact the distribution economics decisions and technical planning. Utility distribution planners balance various design and operating factors to provide a distribution system that is reliable, safe and cost effective. Distribution engineers tend to focus on technology and on the different factors of getting the technology to work in a power system. R. Dugan and K. Price say that engineering analysis deals with the “*how*” aspect of DR application on distribution systems, while economist deals with the “*why*” [22].

The successful integration of DG units into the power system requires effective coordination with the system design and operation practices. So that integration considers the entire electric power system and how the DG influences its behavior under normal and abnormal conditions. Interconnection practices are those dealing with the specific DG elements required for a good operation of the unit, i.e. control relays, transformer interfaces, disconnecting switches, converters (DC-DC), and inverters (DC-AC), among others [23]. Figure 2.4 shows the relation in the decision making before the integration of a DG with the distribution network, between economical and technical aspects.

R. Dugan has enumerated the following four screens as reliable indicators of potential problems analyzing a DG proposal: *Voltage change screen, overcurrent contribution screen, open conductor screen and islanding screen* [24]. Figure 2.4 shows that interconnections issues of a DG installation can be done considering screening applications as mentioned above, when distribution engineers have a relatively short time to realize the evaluation (2-4 weeks), or a detailed analysis for longer periods. Most of publications related to DR have focused its efforts on the bottom “*How to make it work?*”, but several DG projects could be discouraged in the feasibility stage.

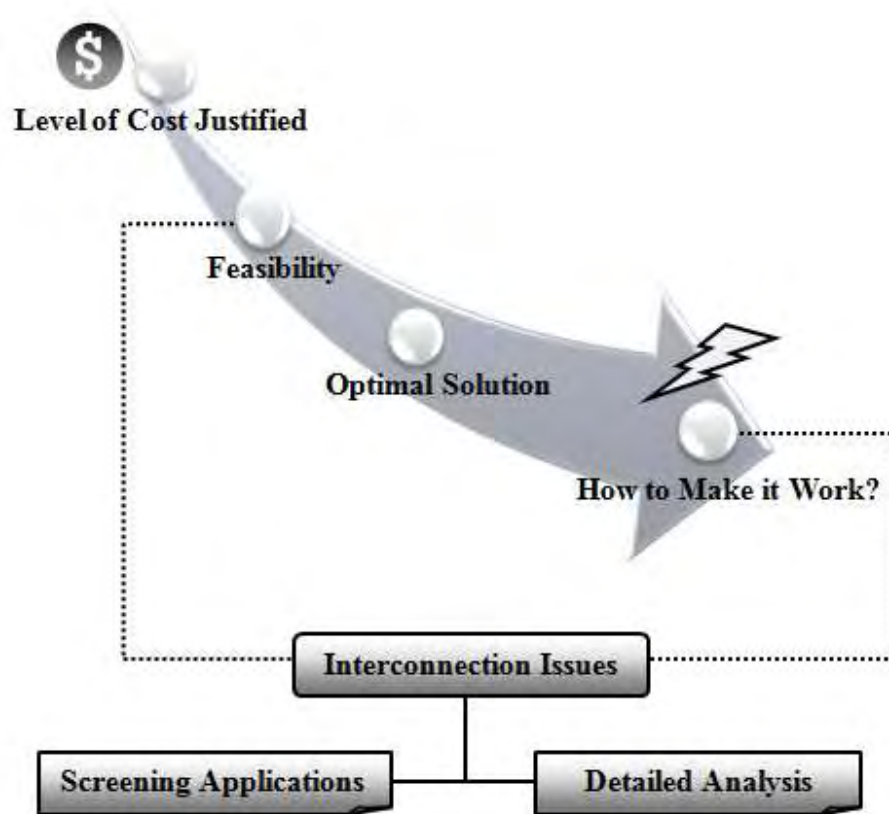


**Figure 2. 4:** Decision making summary when considering DG interconnection to a power system. Adapted from [22] [24]

## 2.5 Impact of DG on Voltage Regulation

The load on a distribution feeder varies in different ways in time, the voltage drop between the substation and the user will vary. In order to maintain the user's voltages within an acceptable range, the voltage at the substation needs to change as the load changes. This is accomplished firstly with the initial design scheme or "fixed design" (i.e. conductor selection, substation and distribution transformer tap settings and fixed capacitor banks) and secondly by voltage control equipment such as automatic Load Tap Changers (LTC), step-type voltage regulators (SVR), and switched capacitors [25].

The IEEE Standard 1547-2003 4.1.1 establishes the following [11] [26]: "*The DR shall not actively regulate the voltage at the PCC. The DR shall not cause the Area EPS service voltage at other Local EPSs to go outside the requirements of ANSI C84.1-1995, Range A*". When any voltage is a range given in Table 2.2, the DR shall cease to energize the utility grid.

**Table 2. 2:** Interconnection system response to abnormal voltages [11]

Voltage Range (% of base voltage) <sup>1)</sup>	Clearing Time(s) <sup>2)</sup>
$V < 50$	0.16
$50 \leq V < 88$	2.00
$110 < V < 120$	1.00
$V \geq 120$	0.16

1 Base voltages are the nominal system voltages stated in ANSI C84.1-1995

2 DR  $\leq$  30 kW, maximum clearing times; DR  $>$  30 kW, default clearing times

Depending on DG size and technology the disconnection can represent a sudden change in generation, affecting adversely the voltage level. If DG is able to produce reactive power can increase or decrease the voltage at PCC. Inverters in PV systems usually work to unity power factor. Induction generators (wind) have lagging power factor, and allocate a capacitor bank to compensate reactive consumption is a common practice. If the voltage variations exceed 5% (ANSI C84.1-2006) when DG is disconnected, it means that DG is too large for the capacity of the feeder under consideration. Another issue is the possible unbalanced voltage drops induced by single-phase loads and its impacts on customers with critical three-phase loads.

## 2.6 Impact of DG on Overcurrent Protection

One of the most common types of studies in distribution systems is the short circuit analysis, because it is essential for determining overcurrent protection device settings. Typically, distribution networks are design for radial operation, which allows the use of protection system without directional discrimination [27]. Therefore, during that time the systems were protected with overcurrent-based protective equipment, including circuit breakers with overcurrent relays, reclosers and fuses. The integration of DR to medium voltage networks means that the grid cannot longer be considered as a radial system.

All DG should disconnect in the first reclose interval so that the utility fault clearing equipment can proceed normally. The presence of DG in the circuit can cause the fuse blowing, because of the current coming from the utility supply (considered during the fixed design) and other component from the DG, which depends on DG technology, size and location, among other factors [28]. A group of current source inverter (CSI) operating in parallel with the utility offset the grid current, rather than control of voltage. The high switching frequency of grid-tied inverters has important implications, one of them is that contribution to fault current can be terminated quickly when the fault is detected, stopping the switching signal. This usually takes place before the current reaches two times rated current to protect the transistor switches.

In radial distribution feeders most failures can be cleared by automatic reclosing, which has been a very successful means to enhance the quality of supply. The impact of autoreclosing is based on the extinction of the arc during the dead time of the reclosing sequence, as established by K. Kauhaniemi [29] [30]. The time from energizing the trip coil to the reclosing of the breaker contacts on an instantaneous reclose cycle is a function of the breaker design: typical values are 20-30 cycles. Otherwise the arc will reignite immediately after the reclosing. On an average, the de-energized time for the fault arc to de-ionize and re-strike is given by [31]:

$$t = \frac{kV}{34.5} + 10.5 \text{cycles}$$

This formula applies where all three phases are opened and there is no trapped energy, such as from shunt reactors, or induction from parallel lines. For single-pole trip-reclose operation, longer deionizing times are required, for energy coupled from unopened phases can keep the arc active [32].

Reclosers that are employed for fuse saving interrupt the fault current very quickly, i.e. 1.5-3 cycle interruption, and many overcurrent devices have a 6-10 cycle time delay. Therefore, if the DG remains on line, out of phase reclosing can also result in transient overvoltage and high electromechanical torques on customer equipment, e.g. rotating generators can accelerate or decelerate when the utility supply is disconnected causing out of phase reclosing. Typical impacts from the integration of DR to distribution network overcurrent protection include [23]:

- Nuisance fuse blowing, particularly related to fuse-saving schemes affected by the added current supplied by the DR ( $DG_1$  &  $DG_2$ ), as shown in Figure 2.5 in the fault  $F2$ . This occurs if the  $FUSE$  is coordinated with the upstream breaker  $CB1$  in a fuse-saving practice. The objective is that  $CB1$  clear the fault  $F2$  before the damage or melting of  $FUSE$ .
- False tripping operations by upstream breakers, reclosers, sectionalizers, or fuses due to downstream DR generation. The fault  $F3$  shown in Figure 2.5 is able to cause  $CB1$  false tripping (health feeder).
- Failure of sectionalizers to operate when they should because the DR keeps a line energized.  $DG_2$  located downstream of the sectionalizer in Figure 2.5 can feed faults upstream the *auto-sectionalizing* device and confuse the protection logic, see fault  $F1$ .

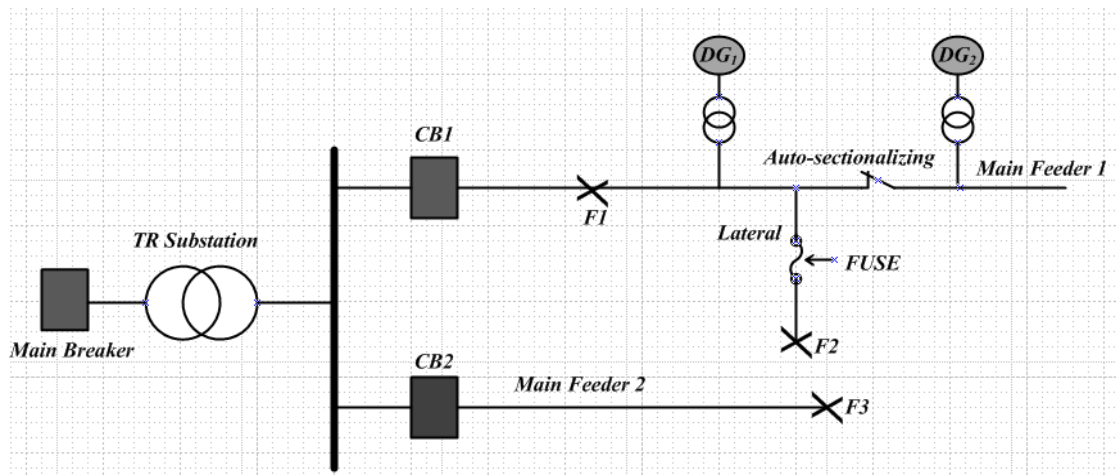


**Figure 2. 5:** Impact of DG integration on a typical distribution feeder overcurrent protection

## 2.7 Islanding Considerations

Islanding occurs when a portion of the distribution system becomes electrically isolated from the remainder of the power system, and continues energized by DG connected to the isolated area. Synchronous generators can sustain islanded conditions as long as the load is small or closely to the generation. Induction generators are incapable of sustain an isolated area, but they can become self-excited if there is sufficient amount of capacitance at their output terminals. The possibility of a power electronic converter based technology depends on the type of inverter (VSI or CSI) and the control method. From the perspective of the requirements of the load supplied from the DR, voltage magnitude, frequency, and grounding must be maintained within an acceptable range. Therefore, unintentional islanding could have severe implications; some of them are as follows [33]:

- Line worker safety can be threatened by the DG sources feeding a system after the utility grid is disconnected.
- Public safety can be compromised as the utility does not have the capability of de-energizing the DG sources energizing the downed lines.
- The voltage and frequency provided to the customers connected to the island are out of utility's control.
- Protection systems on the island are likely to be uncoordinated, due to change in the short circuit current availability. An island may also prevent the clearing of fault currents on the systems leading to reliability reduction and possible conductor burn-downs.
- The islanded system may be inadequately grounded by the DG interconnection.
- Utility breakers or the circuit reclosures may reconnect the island to the utility system when out of phase, causing over currents and CB tripping, see Figure 2.6.

In order to achieve adequate safety and reliability level of the distribution system, anti-islanding protection is usually considered necessary. There are many rules and guidelines from country to country, but similar considerations are often given, e.g. DG should disconnect from the network in the case of abnormality in voltage or frequency; if one or more phases are disconnected from the grid supply the DG units should be rapidly disconnected from the network; or if automatic reclosing is applied, the DG units must disconnect before reclosure.

Due to the reasons mentioned above it is very important detect an islanding condition quickly and accurately. The islanding detection methods can be broadly classified into remote and local techniques, as shown in Figure 2.7. Remote islanding detection techniques are based on communication between utilities and DGs; hence they are expensive methods, e.g. Supervisory Control and Data Acquisition (SCADA) can be used for that. Local techniques rely on the information and data at the DG site, like voltage, frequency, etc. Local methods can be divided into active, passive and hybrid techniques [34].

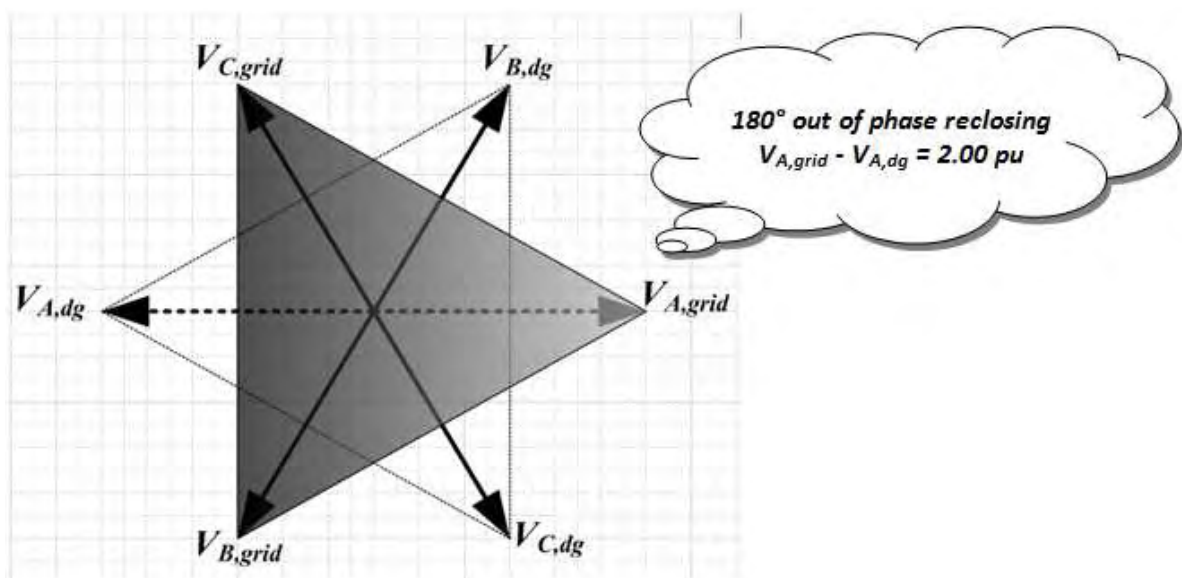


Figure 2. 6: Voltage developed when systems are 180° out of phase

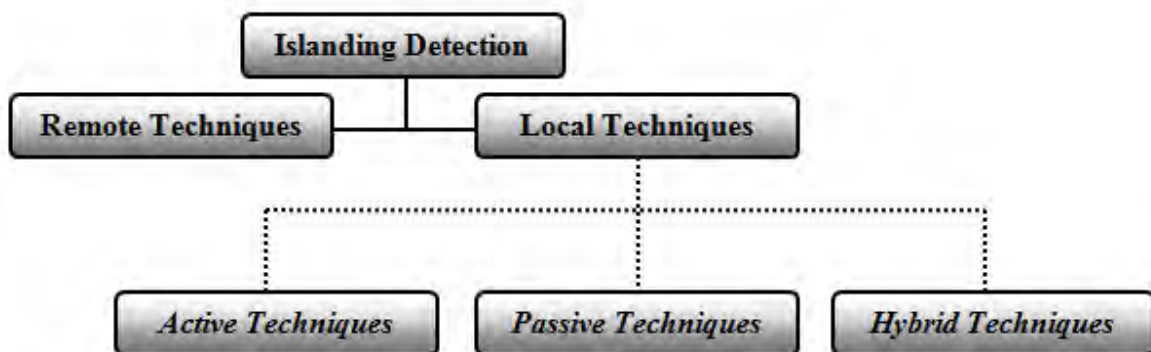


Figure 2. 7: Islanding detection techniques classification. Adapted from [33] [34]

Passive methods work measuring system parameters such as variations in voltage, frequency, harmonic distortion, etc; because these parameters vary greatly when the system is islanded. With active methods, islanding can be detected even under the perfect match of generation and load, which is not possible in case of the passive detection schemes. Active methods directly interact with the power system operation by introducing perturbations. The basic idea of an active detection technique is that this small perturbation causes a significant change in system parameters when the DG is islanded, while the change is negligible when the DG is grid-connected.

For customers who own DG, islanding can represent the continuity of operation under several emergency conditions, which increases the reliability of the supply. However, there are many differences between short-time perturbations and long interruptions or blackouts. In the case of long-duration interruptions, the scheme is based on the disconnection of its non-essential loads until a source/load balance is reached (*load shedding*), therefore, re-synchronization when the utility power is restored must be carried out. In general, the main interest of customers having their own DG is in short-time perturbations in order to keep the DG/utility connection, avoiding any needed action due to disconnection and subsequent re-synchronization [35].

## **2.8 DG Interconnection Transformer Considerations**

The DG interconnection transformer plays a key role in how a three-phase DR affects the utility grid and how the utility may impact the DR. Isolation transformer of DG is a special transformer installed at the exit of DG when DG with large capacity needs to be interconnected, where voltage transformation is not its main function, and by selecting proper connection modes and parameters of transformer the following functions can be obtained [36]:

- Prevent injecting DC current to grid, because direct current does not cause change of magnetic flux in the transformer core.
- Clear 3<sup>rd</sup> harmonics and voltage fluctuation on other users on the distribution grid.
- Make sure the DG-side can detect the fault during system fault and limit short circuit current to prevent protection disoperation.
- Prevent resonance overvoltage and steady state overvoltage at DG-side during system fault. Table 2.3 shows advantages and disadvantages between some transformer connections used for DG interconnection.

**Table 2. 3:** Characteristic of three-phase transformer connections used for DG applications [37]

<b>Transformer Connections</b>	<b>Advantages</b>	<b>Disadvantages</b>
<i>Grounded-Y(Utility) / Grounded-Y (DG)</i>	<i>Less concern of ferroresonance in cable-fed installations. More economic fusing than similarly rated delta connected primary winding. No phase shift in system voltages (relying); can detect primary side voltages with low-voltage relays. Good for power converters that cannot be grounded.</i>	<i>The DG sees the imbalance that utility system sees. Will directly pass zero-sequence harmonic currents (3<sup>rd</sup>). DG may feed into any type of fault that is on utility system. Utility will supply fault current for internal generator faults, increasing fault damage. Does not necessarily provide an effectively grounded source when islanded, the reference will be provided by generator and/or load.</i>
<i>Delta (Utility) / Grounded-Y (DG)</i>	<i>Third harmonics from DG do not reach the utility system. Provides some isolation from voltage sags due to utility-side single line-ground (SLG) faults. Do not feed directly into utility-side SLG faults.</i>	<i>Very prone to ferroresonance in cable-fed installations, especially during open conductor fault. 3<sup>rd</sup> harmonics in the DG side may cause excessive current in DG-side neutral. If islanded on SLG fault, can subject utility arresters to overvoltages. Difficult to detect some utility-side SLG faults from the DG-side by voltage relying alone.</i>
<i>Grounded-Y (Utility) / Delta (DG)</i>  <i>This connection is also known as a “grounding transformer” or a “ground source”</i>	<i>Protection schemes are well understood. Third harmonic currents are blocked by the delta winding. Utility side faults are generally more readily detected, because the transformer itself participates in all ground faults. This generally allows the DG to disconnect more quickly. In case of islanding this connection helps the DG to present an effectively grounded source to the utility distribution system and avoid the resonance and over voltage issues of other connections.</i>	<i>The 3<sup>rd</sup> harmonic currents in the utility system from other sources will tend to flow into transformers with this connection. Contribute strongly to all ground faults. Contribute to sympathetic tripping of the feeder breaker for faults on other feeders. Utilities may have to change relying depending on whether a transformer of this type is connected or disconnected.</i>

The use of a delta winding on one or both sides prevents the flow of zero-sequence current through the transformer; hence, this helps to limit the impact of ground faults on the DG unit. On the other hand, if the delta winding is on the utility primary side and island develops, serious overvoltages could be imposed on the islanded section of the distribution feeder during ground fault conditions, as shown in Figure 2.8. This could damage surge arresters, operate distribution transformer fuses, and cause serious overvoltage problems for customer loads. It is important to note that many industrial installations are served by delta (utility)/ grounded-y transformers and these are the types of systems where many DR units are being considered for installation. The phasor diagram illustrated on Figure 2.8 shows the neutral shift due to a non-effective grounded system. This can be avoided with a grounded-y connection in the utility-side of the DG transformer, but under the risk that the DG may feed into any type of fault that is on the utility system.

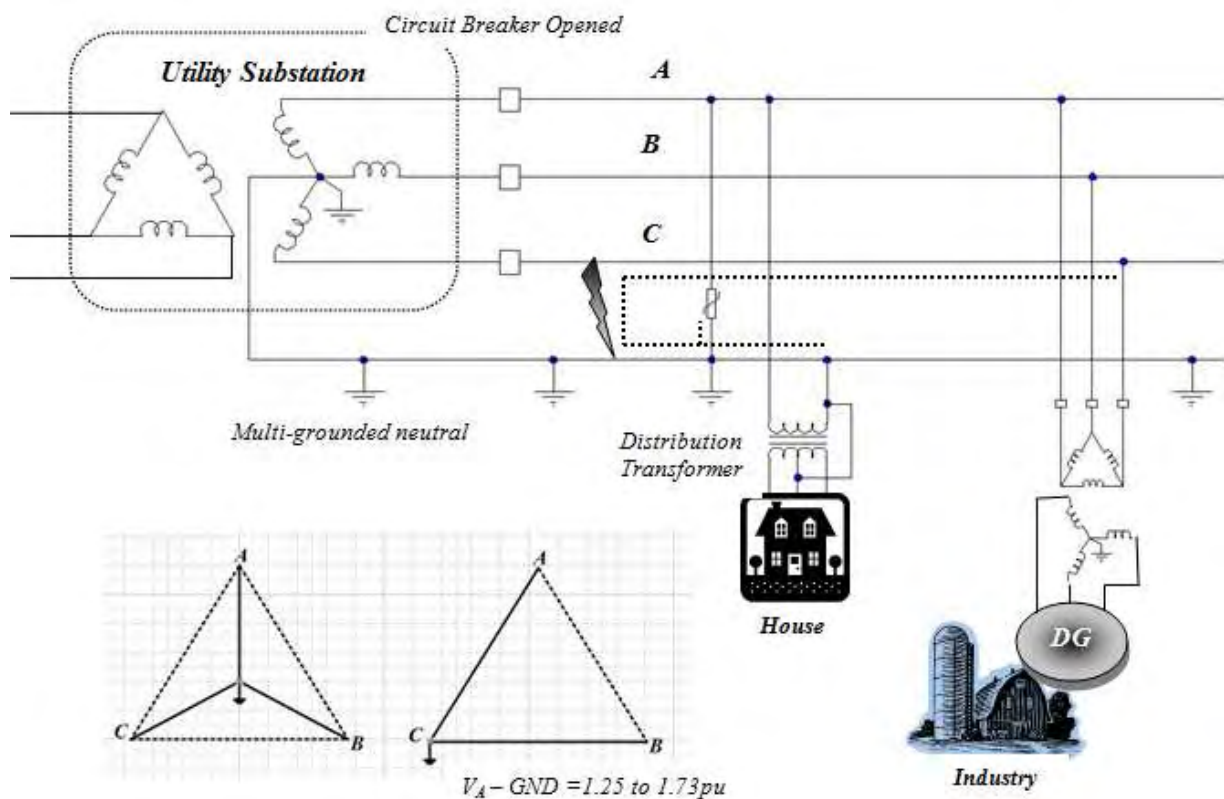


**Figure 2. 8:** Neutral shift during single line to ground (SLG) fault and phasor representation. Adapted from [23] [36] [37].

The grounded-Y (Utility)/delta (DG) connection it is not permitted on most utility distribution systems without considerable study. The main reason is that the ground fault contribution from the transformer alone can be sufficient to affect the ground fault coordination of the utility breakers and reclosers, which do not typically use directional relays [25]. This is shown in Figure 2.9.

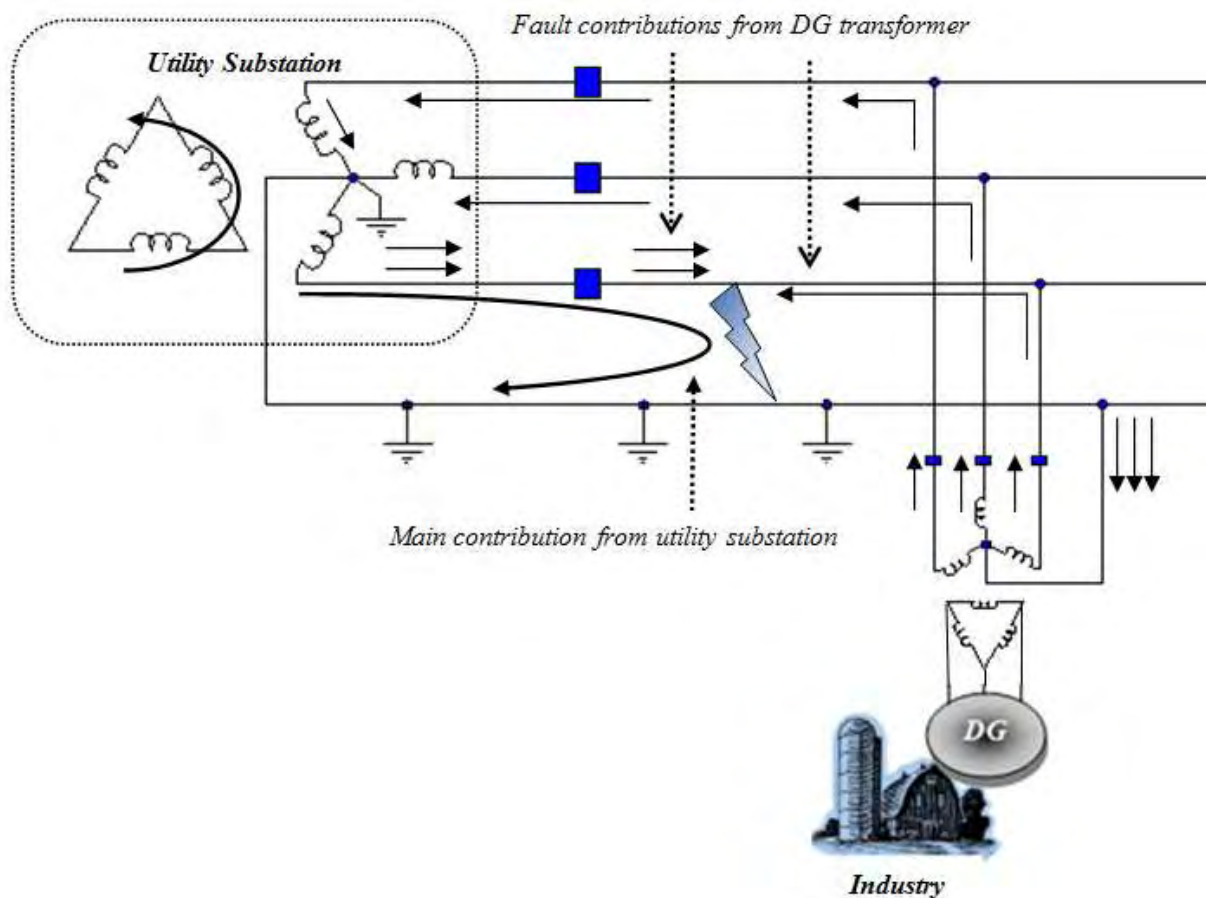


**Figure 2. 9:** Ground fault contribution from DG interconnected using grounded-Y (utility) / delta (DG) transformer.

Adapted from [37]

A neutral reactor is recommended to be added to this connection to make it more compatible with typical distribution networks by limiting fault currents, unbalance currents and harmonic currents. If neutral reactor is sized properly, the Grounded-Y (utility)/Delta (DG) transformer connection can provide an effectively grounded DG interface under all circumstances. However, the addition of future DG with this transformer connection may affect

the optimal neutral reactor selection. Three conflicting goals must be accomplished to find the proper size of neutral grounding reactor [37]:

1. High enough to limit the maximum fault current contribution.
2. High enough to limit circulating currents for continuous operation in unbalanced conditions.
3. Low enough to maintain an effectively grounded system.

In order to be low enough to maintain an effectively grounded system the following criteria must be met:

$$\frac{X_0}{X_1} \leq 3 \qquad \frac{R_0}{X_1} \leq 1$$

To keep the system effectively grounded during a possible islanding condition the reactor size needs to be limited to the value calculated below:

$$X_N \leq X_{T1} + X_{G1} - \frac{X_{T0}}{3}$$

Where,

$X_N$ =Neutral Reactance

$X_{T0}$ = Transformer zero-sequence reactance

$X_{T1}$ = Transformer positive-sequence reactance

$X_{G1}$ = Generator Positive-sequence reactance.

Ferroresonance can occur with DG as the energy source in the circuit during islanding conditions. The peak voltage during this ferroresonance can reach three to four per units. The most susceptible transformer connections are the ungrounded ones. Grounded Y transformers are not immune, but overvoltages are considerably lower than with ungrounded ones, usually ranging from 120 to 200 percent [38,37]. There are four conditions necessary for DG islanding ferroresonance to occur:

1. The generator must be operating in an islanded state.
2. The generator must be capable of supplying the island load.
3. Sufficient capacitance must be available on the island to resonate (usually 30-400% of the generator rating).
4. A transformer must be present on the island to serve as the non-linear reactance.

The true validity of the benefits obtained from DR has been subject of so much debate and discussion. Based on the literature analysis exposed above, the interconnection of DG units presents the following common challenges:

1. Unintentional islanding with concerns about reliability, safety and power quality.
2. Fault current produced by DG units may reduce current seen by feeder relay (protection under reach).
3. DG can cause tripping of healthy feeders adjacent to faulted feeder.
4. Depending on number and type of generator, fault level can increase or decrease.
5. Overvoltage caused by reverse power flow, ferroresonance or SLG fault in a non-effective grounded system.
6. Harmonic distortion (inverter-based technology).

## **CHAPTER 3**

# **REALISTIC POWER SYSTEM MODELING FOR DISTRIBUTED GENERATION**

### **3.1 IEEE Radial Distribution Test Feeder Simulation**

Distribution system analysis has been traditionally perceived as modelling small radially-connected systems with simple power flow methods. Although this perception is true in many cases, things are changing. Despite its apparently simple structure, the distribution system is considerably more complex than transmission systems due to a mixture of three-phase, two-phase, and single-phase lines and transformers interconnected in every imaginable way. The IEEE Distribution System Analysis Subcommittee (DSAS) has developed a number of test feeders to make available a common set of data that could be used by program developers and users to verify the accuracy of their solutions. The complete data and solutions for all of the test feeders can be downloaded from the internet [4].

The analysis of a distribution feeder will typically consist of a study under normal steady-state conditions (power-flow analysis), and a study under short-circuit conditions (short-circuit analysis). Radial distribution feeders are characterized by having only one path for power to flow from the source to each customer, and the loading is unbalanced because of the large number of unequal single-phase loads that must be served. An additional unbalance is introduced by the nonequilateral conductor spacings of three-phase overhead and underground line segments. Traditional power flow studies for transmission networks assume a perfectly balanced system and line transposition, so that a single-phase equivalent system is used, this assumption cannot be made on distribution networks.

Today so many digital computer programs have been developed for the analysis of unbalanced three-phase radial distribution feeders. This time is implemented the calculation program PowerFactory, as written by DIgSILENT (**D**igital **S**imuLation and **E**lectrical **N**eTwork calculation program), because of the options presented by this software in the modeling of distribution power system components. Also DIgSILENT provides several generator models for distributed generation interconnection analysis.

Figure 3.1 shows the IEEE 13 Node Distribution Test Feeder oneline diagram. The aim of this work is to model this test feeder and study the behavior of the original system under high penetration of distributed generation. This feeder can be divided into “*Series Components*” (line segments, transformers and voltage regulators) and “*Shunt Components*” (spot loads, distributed loads and capacitor banks). The following characteristics are displayed by this particular test system [39]:

- A. Short and relatively highly loaded for a 4.16 kV feeder
- B. One substation voltage regulator consisting of three single-phase units connected in wye.
- C. Overhead and underground lines with variety of phasing
- D. Shunt capacitor banks
- E. In-line transformer
- F. Unbalanced spot and distributed loads.

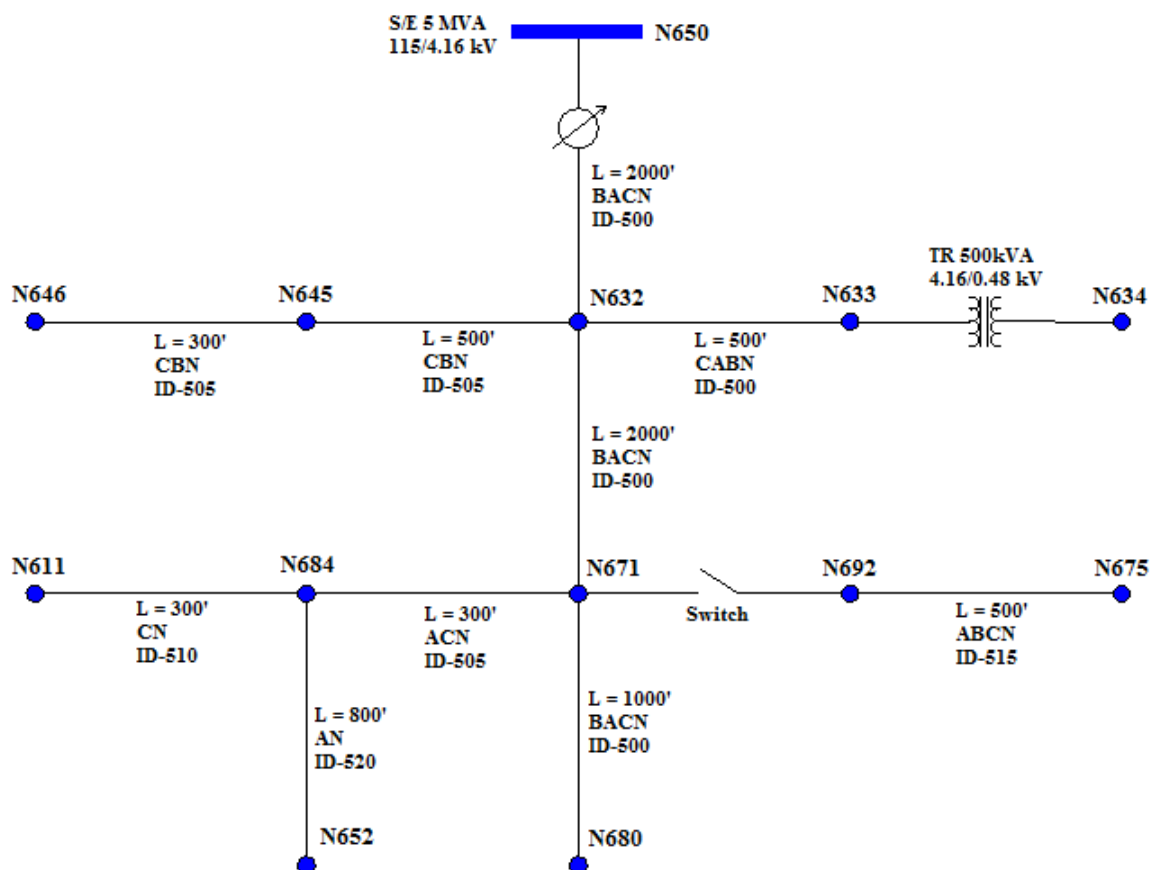


Figure 3. 1: IEEE 13 Node Distribution Test Feeder Oneline Diagram [39].

### 3.2 Load Models

The electrical representation of loads in a distribution node is a complicated task. There is a high diversity and number of devices such as fluorescent and incandescent lamps, refrigerators, heaters, compressors, motors, furnaces, etc. The load models are classified into “static models” and “dynamic models”. A static load model expresses the characteristics of the load at any instant of time as algebraic functions of the bus voltage magnitude and frequency at that instant. The voltage dependency of loads has been represented by the exponential model as follows [40]:

$$\begin{aligned} P &= P_0 \left( \frac{V}{V_0} \right)^a \\ Q &= Q_0 \left( \frac{V}{V_0} \right)^b \end{aligned} \quad (3.1)$$

Where  $P$  is the active power and  $Q$  the reactive power of the load in the considered node when the voltage magnitude is  $V$ . The subscript 0 indicates initial operating conditions. The exponents “ $a$ ” and “ $b$ ” can be 0, 1, or 2, to represent constant power, constant current, or constant impedance characteristics, respectively. There is an alternative model to represent the voltage dependency of loads know as “polynomial model”:

$$\begin{aligned} P &= P_0 \left[ p_1 \left( \frac{V}{V_0} \right)^2 + p_2 \left( \frac{V}{V_0} \right) + p_3 \right] \\ Q &= Q_0 \left[ q_1 \left( \frac{V}{V_0} \right)^2 + q_2 \left( \frac{V}{V_0} \right) + q_3 \right] \end{aligned} \quad (3.2)$$

The parameters of this model are the coefficients  $p_1$  to  $p_3$  and  $q_1$  to  $q_3$ , so it is referred to as the “ZIP model”, composed of constant impedance (Z), constant current (I) and constant power (P) components. The general load model of DIGSILENT allows to introduce the coefficient value for each term taking into account that the sum of the coefficients of the equation must be equal to one. Tables 3.1 and 3.2 shows the magnitude of active and reactive power for the IEEE system under consideration, also shows the configuration (WYE or DELTA) and the load model (ZIP).

*Spot Loads*, see Table 3.1, are located at a node and can be three-phase, two-phase, or single-phase, and connected in Wye or Delta. On the other hand, *Distributed Loads* are those considered uniformly distributed along the line, this type of load is modeled connecting two

thirds of the load at one quarter of the line and the remaining load at the end of the line [3]. The capacitor banks are modeled as constant admittance connected to a particular node.

**Table 3. 1:** Spot Load Data [39] [4]

Node	Load	Ph-1	Ph-1	Ph-2	Ph-2	Ph-3	Ph-3
	Model	kW	kVAr	kW	kVAr	kW	kVAr
634	<i>Y-PQ</i>	160	110	120	90	120	90
645	<i>Y-PQ</i>	0	0	170	125	0	0
646	<i>D-Z</i>	0	0	230	132	0	0
652	<i>Y-Z</i>	128	86	0	0	0	0
671	<i>D-PQ</i>	385	220	385	220	385	220
675	<i>Y-PQ</i>	485	190	68	60	290	212
692	<i>D-I</i>	0	0	0	0	170	151
611	<i>Y-I</i>	0	0	0	0	170	80
<b>TOTAL</b>		<b>1158</b>	<b>606</b>	<b>973</b>	<b>627</b>	<b>1135</b>	<b>753</b>

**Table 3. 2:** Distributed Load Data [39] [4].

Node A	Node B	Load	Ph-1	Ph-1	Ph-2	Ph-2	Ph-3	Ph-3
		Model	kW	kVAr	kW	kVAr	kW	kVAr
632	671	<i>Y-PQ</i>	17	10	66	38	117	68

### 3.3 Overhead and Underground Line Models

The series impedance of overhead and underground lines is composed of the resistance of the conductors and the self and mutual inductive reactances resulting from magnetic fields created by the current flow in each line. When the conductors of a three-phase line are not spaced equilaterally the flux linkages and the inductance of each phase is different and results in an unbalanced circuit. The balance can be restored exchanging the positions of the conductors at regular intervals along the line (each phase occupies the same physical position on the structure for one-third of the length of the line). That exchange of phase position is called *Transposition*, see Figure 3.2 [3] [41].

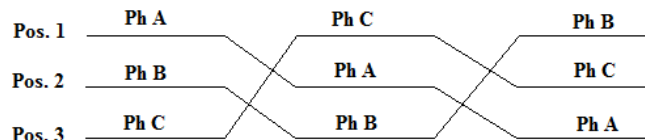


**Figure 3. 2:** Transposition Cycle [41].

The analysis of high-voltage transmission lines assumes line transposition and balanced loading. Transposition results in each conductor having the same average inductance over the whole cycle. Distribution systems are composed of single-phase, two-phase, and untransposed three-phase lines connected to unbalanced loads, then it is necessary to keep the idea of self and mutual impedance of the conductors taking into account the ground return path for the unbalanced currents. To make this possible it is employed the Carson's equations, published in a 1926's paper. Referring to Figure X.3, the original Carson's equations are given in Equations 3.3 and 3.4 [42].

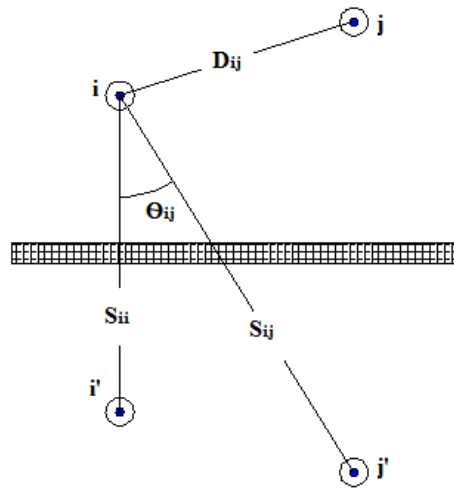


**Figure 3. 3:** Conductors and images. The conductors  $i'$  and  $j'$  represent the ground image [3].

Self impedance of conductor i:

$$\hat{z}_{ii} = r_i + 4\omega P_{ii}G + j \left[ X_i + 2\omega G \cdot \ln \frac{S_{ii}}{RD_i} + 4\omega Q_{ii}G \right] \Omega / \text{mile} \quad (3.3)$$

Mutual impedance between conductor i and j:

$$\hat{z}_{ij} = 4\omega P_{ij}G + j \left[ 2\omega G \cdot \ln \frac{S_{ij}}{D_{ij}} + 4\omega Q_{ij}G \right] \Omega / \text{mile} \quad (3.4)$$

Where

$z_{ii}$  = self impedance of conductor i in  $\Omega/\text{mile}$

$z_{ij}$  = mutual impedance between conductors I and j in  $\Omega/\text{mile}$

$r_i =$  resistance of conductor  $i$  in  $\Omega/\text{mile}$

$\omega = 2\pi f =$  system angular frequency in radians per second

$G = 0.1609344 \times 10^{-3}$   $\Omega/\text{mile}$

$RD_i =$  radius of conductor  $i$  in feet

$GMR_i =$  Geometric Mean Radius of conductor  $i$  in feet

$f =$  system frequency in Hertz

$\rho =$  resistivity of earth in  $\Omega\text{-meters}$

$D_{ij} =$  Distance between conductors  $i$  and  $j$  in feet

$S_{ij} =$  distance between conductor  $i$  and image  $j$  in feet

$\Theta_{ij} =$  angle between a pair of lines drawn from conductor  $i$  to its own image and to the image of conductor  $j$

$$X_i = 2\omega G \ln \frac{RD_i}{GMR_i} \Omega/\text{mile} \quad (3.5)$$

$$P_{ij} = \frac{\pi}{8} - \frac{1}{3\sqrt{2}} k_{ij} \cos(\theta_{ij}) + \frac{k_{ij}^2}{16} \cos(2\theta_{ij}) \cdot \left( 0.6728 + \ln \frac{2}{k_{ij}} \right) \quad (3.6)$$

$$Q_{ij} = -0.0386 + \frac{1}{2} \ln \frac{2}{k_{ij}} + \frac{1}{3\sqrt{2}} k_{ij} \cos(\theta_{ij}) \quad (3.7)$$

$$k_{ij} = 8.565 \times 10^{-4} \cdot S_{ij} \cdot \sqrt{\frac{f}{\rho}} \quad (3.8)$$

Before the implementation of Carson's equations there are two approximations done to the expressions of  $P_{ij}$  and  $Q_{ij}$  using only the first term of the variable  $P_{ij}$  and the first two terms of  $Q_{ij}$ .  $P_{ij}$  and  $Q_{ij}$  in Carson's paper are developed in an infinite series as function of  $K_{ij}$  and  $\Theta_{ij}$ , for practical applications  $K_{ij}$  does not have big magnitudes, thus these two assumptions are valid.

$$P_{ij} = \frac{\pi}{8} \quad (3.9)$$

$$Q_{ij} = -0.0386 + \frac{1}{2} \ln \frac{2}{k_{ij}} \quad (3.10)$$

The substitution of Equations (3.8), (3.9) and (3.10) into Equations (3.3) and (3.4) gives the Modified Carson's Equation, which are implemented to calculate the series impedance of overhead and underground lines. Considering a system frequency of 60Hz and an earth resistivity of 100  $\Omega$ -m the modified Carson's equations are [3],

$$\hat{z}_{ii} = r_i + 0.09530 + j0.12134 \left[ \ln \frac{1}{GMR_i} + 7.93402 \right] \Omega / mile \quad (3.11)$$

$$\hat{z}_{ij} = 0.09530 + j0.12134 \left[ \ln \frac{1}{D_{ij}} + 7.93402 \right] \Omega / mile \quad (3.12)$$

Equations (3.11) and (3.12) are used to calculate the elements of an  $n_{cond} \times n_{cond}$  primitive impedance matrix.

$$[\hat{Z}_{PRIMITIVE}] = \begin{bmatrix} \begin{bmatrix} \hat{Z}_{aa} & \hat{Z}_{ab} & \hat{Z}_{ac} \\ \hat{Z}_{ba} & \hat{Z}_{bb} & \hat{Z}_{bc} \\ \hat{Z}_{ca} & \hat{Z}_{cb} & \hat{Z}_{cc} \end{bmatrix} & \begin{bmatrix} \hat{Z}_{an1} & \hat{Z}_{an2} & \hat{Z}_{anm} \\ \hat{Z}_{bn1} & \hat{Z}_{bn2} & \hat{Z}_{bnm} \\ \hat{Z}_{cn1} & \hat{Z}_{cn2} & \hat{Z}_{cnm} \end{bmatrix} \\ \begin{bmatrix} \hat{Z}_{n1a} & \hat{Z}_{n1b} & \hat{Z}_{n1c} \\ \hat{Z}_{n2a} & \hat{Z}_{n2b} & \hat{Z}_{n2c} \\ \hat{Z}_{nma} & \hat{Z}_{nmb} & \hat{Z}_{nmc} \end{bmatrix} & \begin{bmatrix} \hat{Z}_{n1n1} & \hat{Z}_{n1n2} & \hat{Z}_{n1nm} \\ \hat{Z}_{n2n1} & \hat{Z}_{n2n2} & \hat{Z}_{n2nm} \\ \hat{Z}_{nmn1} & \hat{Z}_{nmn2} & \hat{Z}_{nmnm} \end{bmatrix} \end{bmatrix} \quad (3.13)$$

In partitioned form,

$$[\hat{Z}_{PRIMITIVE}] = \begin{bmatrix} \begin{bmatrix} \hat{Z}_{ij} \end{bmatrix} & \begin{bmatrix} \hat{Z}_{in} \end{bmatrix} \\ \begin{bmatrix} \hat{Z}_{nj} \end{bmatrix} & \begin{bmatrix} \hat{Z}_{nn} \end{bmatrix} \end{bmatrix} \quad (3.14)$$

Implementing Kron reduction technique, see Equation (3.15), the primitive impedance matrix is reduced to a 3x3 phase matrix consisting of the self and mutual equivalent impedances for the three phases in  $\Omega/mile$ .

$$[\hat{Z}_{abc}] = [\hat{Z}_{ij}] - [\hat{Z}_{in}] \cdot [\hat{Z}_{nn}]^{-1} \cdot [\hat{Z}_{nj}] \quad (3.15)$$

$$[\hat{Z}_{abc}] = \begin{bmatrix} \hat{Z}_{aa} & \hat{Z}_{ab} & \hat{Z}_{ac} \\ \hat{Z}_{ba} & \hat{Z}_{bb} & \hat{Z}_{bc} \\ \hat{Z}_{ca} & \hat{Z}_{cb} & \hat{Z}_{cc} \end{bmatrix} \Omega / mile \quad (3.16)$$

Figures 3.4 and 3.5 shows the spacing distances between the phase conductors and the neutral conductor for a particular *Spacing ID* number (overhead and underground lines).

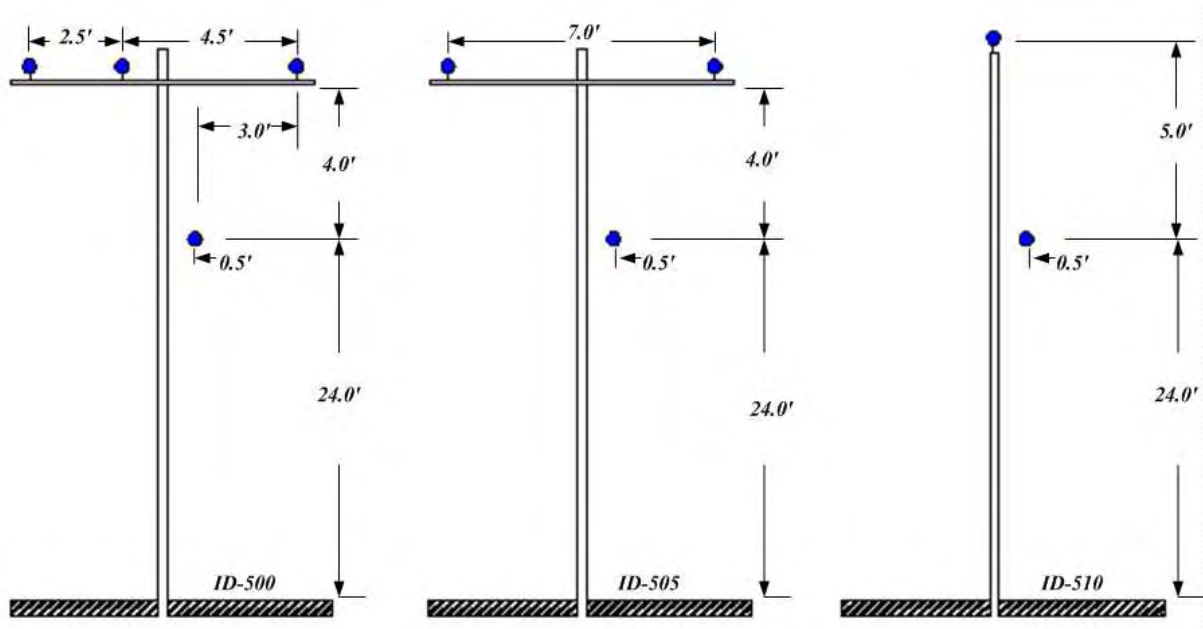


Figure 3. 4: Overhead line spacing ID-(500,505,510).

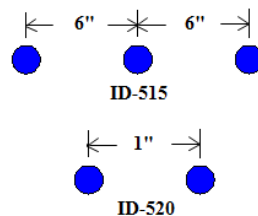


Figure 3. 5: Underground Line Spacing.

The IEEE test feeder simulation on DIgSILENT is realized for the line configurations specified. Most of the time the shunt capacitance of the line segment can be ignored, and this time has been preferred not to present the shunt admittance matrix, although it is included into calculations. The last assumption is made because the longest line segment in the system under consideration is approximately 0.38 miles, meaning that is a very short feeder. As an example, the expression bellow presents the shunt admittance matrix for *configuration 601*, see Table 3.3.

$$[B_{601}] = \begin{bmatrix} 6.2681 & -1.9872 & -1.2522 \\ -1.9872 & 5.9302 & -0.7379 \\ -1.2522 & -0.7379 & 5.6094 \end{bmatrix} \mu Siemens / mile$$

Table 3.3 shows the possible line configurations data for overhead and underground lines, followed by the equivalent matrix impedances for overhead lines (*configuration 601-605*) obtained from DIgSILENT.

**Table 3. 3:** Overhead and underground line configuration data [39] [4]

Configuration	Phasing	Phase	Neutral	Spacing
		ACSR	ACSR	ID
<b>601</b>	B A C N	556,500 26/7	4/0 6/1	500
<b>602</b>	C A B N	4/0 6/1	4/0 6/1	500
<b>603</b>	C B N	1/0	1/0	505
<b>604</b>	A C N	1/0	1/0	505
<b>605</b>	C N	1/0	1/0	510
<b>606</b>	A B C N	250,000 AA, CN	None	515
<b>607</b>	A N	1/0 AA, TS	1/0 Cu	520

*Configuration 601:*

$$z_{abc} = \begin{bmatrix} 0.3459 + 1.0135i & 0.1552 + 0.5003i & 0.1573 + 0.4225i \\ 0.1553 + 0.5003i & 0.3368 + 1.0432i & 0.1528 + 0.3841i \\ 0.1573 + 0.4225i & 0.1528 + 0.3841i & 0.3407 + 1.0303i \end{bmatrix} \Omega / mile$$

*Configuration 602:*

$$z_{abc} = \begin{bmatrix} 0.7520 + 1.1760i & 0.1573 + 0.4225i & 0.1553 + 0.5003i \\ 0.1573 + 0.4225i & 0.7468 + 1.1927i & 0.1528 + 0.3841i \\ 0.1553 + 0.5003i & 0.1528 + 0.3841i & 0.7429 + 1.2056i \end{bmatrix} \Omega / mile$$

*Configuration 603:*

$$z_{abc} = \begin{bmatrix} 0 & 0 & 0 \\ 0 & 1.3283 + 1.3415i & 0.2054 + 0.4587i \\ 0 & 0.2054 + 0.4587i & 1.3227 + 1.3513i \end{bmatrix} \Omega / mile$$

*Configuration 604:*

$$z_{abc} = \begin{bmatrix} 1.3227 + 1.3513i & 0 & 0.2054 + 0.4587i \\ 0 & 0 & 0 \\ 0.2054 + 0.4587i & 0 & 1.3283 + 1.3415i \end{bmatrix} \Omega / mile$$

*Configuration 605:*

$$z_{abc} = \begin{bmatrix} 0 & 0 & 0 \\ 0 & 0 & 0 \\ 0 & 0 & 1.3280 + 1.3420i \end{bmatrix} \Omega / mile$$

### 3.4 Distribution Transformer Models

The distribution transformer is one of the key elements to allow the widespread delivery of electric power today. In general, the distribution transformer serves as the final transition to the customer stepping the primary voltage down to a practical level suitable for utilization within most consumer devices and often providing a local grounding reference. Figure 3.6 shows the basic model of a single-phase transformer. The series resistance is mainly the resistance of the wires in each winding. The series reactance is the leakage impedance, and the shunt branch is the magnetizing branch (current that flows to magnetize the core). Most of the magnetizing current is reactive power, but it includes a real power component. Power is lost in the core through *hysteresis* and *Eddy currents*.

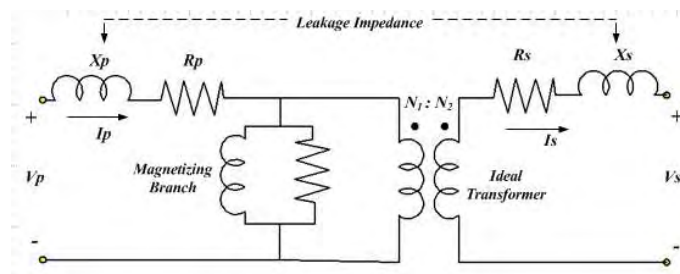


Figure 3. 6: Basic transformer model. Adapted from [43]

The magnetizing branch impedance is normally above 5000% on a transformer's base, so can be neglected in many cases. The core losses are often referred to as iron losses or no-load losses. The load losses are frequently called the wire losses or copper losses. The simplified transformer model, i.e. basic transformer model without magnetizing branch, is sufficient for most calculations including load flows; short-circuit calculations, motor starting, or unbalance. Small distribution transformers have low leakage reactances, some less than 1% on the transformer rating, and  $X/R$  ratios of 0.5 to 5. Larger power transformers used in distribution substations have higher impedances, usually on the order of 7 to 10% with  $X/R$  ratios between 10 and 40 [44] [45]. The leakage reactance is calculated by designers using the number of turns, the magnitudes of the current and the leakage field, and the geometry of the transformer. It is measured placing a short circuit on one winding of the transformer and increasing the voltage on the other winding until rated current flows in the windings. The voltage drop across this reactance results in the voltage at the load, and it is less than the ideal value determined by the turns ratio. The percentage decrease in the voltage is called "*regulation*", which is a function of the power factor of the load.

The understanding of distribution transformers characteristics, configurations, and applications is a critical issue for integrating DR to the system. This is because the most DR installations involve some type of existing distribution transformer interface. Distribution transformers are available in several standardized sizes as shown in Table 3.4, and its impedances are relatively low compared with substation transformers. The units under 50 kVA have impedances less than 2%, hence provides better voltage regulation and less voltage flicker under fluctuating loads. But lower impedance transformers increase fault currents on the secondary and these faults impact the primary side more.

**Table 3. 4:** Standard Distribution Transformer Sizes [23]

<b>Distribution Transformer Standard Ratings [kVA]</b>	
<b>Single Phase</b>	5, 10, 15, 25, 37.5, 50, 75, 100, 167, 250, 333, 500
<b>Three Phase</b>	30, 45, 75, 112.5, 150, 225, 300, 500

Four categories for the rating of transformers are recognized in the *IEEE Std. C57.12.00-2006*, see Table 3.5. For *Category I* distribution transformers, the duration of the short circuit shall be determined by the following Equation:

$$t = \frac{1250}{I^2}$$

Where  $I$  is the symmetrical current in multiples of the normal base current from Table 3.6

**Table 3. 5:** Category of transformer ratings [46]

<b>Category</b>	<b>Single Phase (kVA)</b>	<b>Three Phase (kVA)</b>
<b>I</b>	5-500	15-500
<b>II</b>	501-1667	501-5000
<b>III</b>	1668-10000	5001-30000
<b>IV</b>	Above 10000	Above 30000

**Table 3. 6:** Distribution transformer short-circuit withstand capability [46]

<b>Single-Phase Rating, kVA</b>	<b>Three-Phase Rating, kVA</b>	<b>Withstand Capability in per Unit of the Base Current (Symmetrical)<sup>a</sup></b>
5-25	15-75	40
37.5-110	112.5-300	35
167-500	500	25

<sup>a</sup> This table applies to all distribution transformers with secondary rated 600 V and below and distribution autotransformers with secondary rated above 600 V. Two winding distribution transformers with secondary rated above 600 V should be designed to withstand short circuits limited only by the transformer's impedance.

The standard connection arrangements and terminal markings for particular types of transformers are included in the *IEEE Std. C57.12.70-2000*. This standard specifies that the highest voltage winding shall be designated as HV or H; and the other windings, in order of decreasing voltage are designated as X, Y, and Z. In general, external terminal shall be distinguished from one another by marking each terminal with a capital letter, followed by a subscript number. The terminals of the H winding are marked H<sub>1</sub>, H<sub>2</sub>, H<sub>3</sub>, etc. The terminals of the X winding are marked X<sub>1</sub>, X<sub>2</sub>, X<sub>3</sub>, etc. A neutral terminal of a three-phase transformer shall be marked with the proper letter followed by the subscript 0, for example H<sub>0</sub>, X<sub>0</sub>, etc. A neutral terminal common to two or more windings of a single or three-phase transformer shall be marked with the combination of the proper winding letters, each followed by the subscript 0; for example H<sub>0</sub>X<sub>0</sub> [47].

The *polarity* for all liquid-insulated distribution transformers must be *subtractive*, except for those applicable sections of the *IEEE Std. C57.12.00-2006*, which specify *additive* polarity for single-phase transformers in sizes 200 kVA and smaller having high-voltage windings 8660 volts and below. An understanding of polarity is essential to correctly construct three-phase transformer banks and to properly parallel single or three-phase transformers with existing electrical systems. Knowledge of polarity is also required to connect potential and current transformers to power metering devices and protective relays. In practice, polarity refers to the way the leads are brought out of the transformer. For example, distribution transformers are *Additive Polarity* if the H<sub>1</sub> and X<sub>1</sub> bushings are physically placed diagonally. Since H<sub>1</sub> is always on the left, X<sub>1</sub> will be on the right-hand side of a transformer, see Figure 3.7.

The standard single-phase transformer connections is shown in Figure 3.7. The Standard secondary load voltage is 120/240 volts. The transformer's secondary terminals are marked according to the corresponding IEEE/ANSI standard, where the voltage X<sub>1</sub>-X<sub>2</sub> and X<sub>2</sub>-X<sub>3</sub> are each 120 volts. X<sub>1</sub>-X<sub>3</sub> is 240 volts. Most small-scale generation systems, such as PV, fuel cell or engine-generators will be connected at 240 volts at the service panel location of the customer site.

Almost all loads larger than a few kilowatts are three-phase loads. There are many types of three-phase connections used to serve three-phase loads on distribution systems. In general, permissible transformer connections is related to the type of service to be delivered and the type of primary supply.

Three-phase services may be three-wire or four-wire. The three-wire service is commonly called “*delta service*” and consists only of three-phase conductors, having no neutral conductor. The four-wire service is usually called “*wye service*” and includes a neutral conductor which is grounded at the service for 208Y/120 and 480Y/277 volts services. In some cases where the supply is outside the building served, may exist other ground point on the secondary side of the transformer. Some four-wire services are derived from a  $\Delta$  or open- $\Delta$  connected secondary with the center tap of one leg grounded, see Figure 3.8 [48].

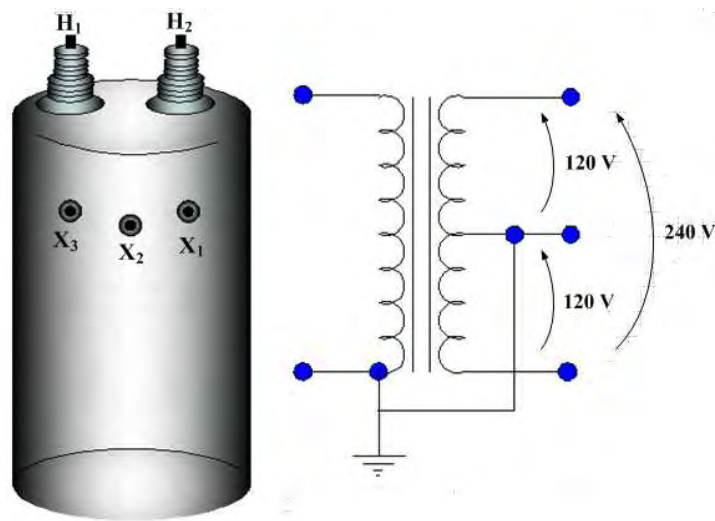


**Figure 3.7:** Typical distribution transformer with two-bushing primary and center-tapped 120/240 volts three-bushing secondary

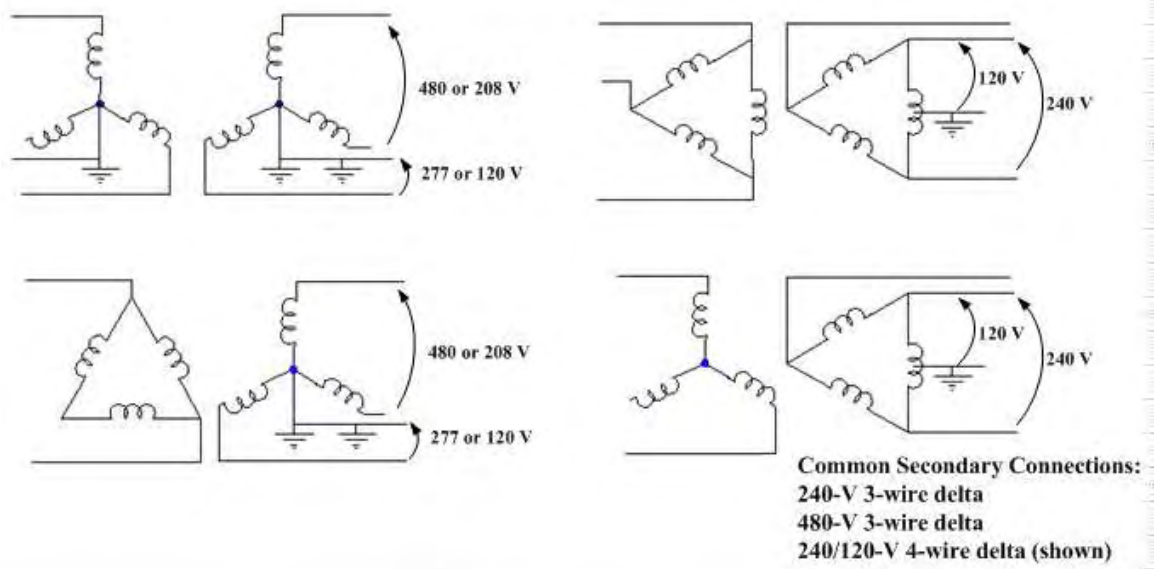


**Figure 3.8:** Three-phase distribution transformer connections. Adapted from [23]

It is assumed that all variations of wye-delta connections are connected in the “*American Standard Thirty-Degree*” connection. This standard stabilishes that the angular displacement between high-voltage and low-voltage phase of three-phase transformers with wye-delta or delta-wye connections shall be  $30^\circ$ , with the low voltage lagging the high voltage as shown in Figure 3.9. The angular displacement of a polyphase transformer is the time angle expressed in degrees between the line-to-neutral voltage of the reference identified high-voltage terminal  $H_1$  and the line-to-neutral voltage of the corresponding identified low-voltage terminal  $X_1$ . The positive sequence phasor diagrams of the voltages in Figure 3.9 show the relationships between the various positive sequence voltages. Care must be taken to observe the polarity marks on the individual transformer windings.

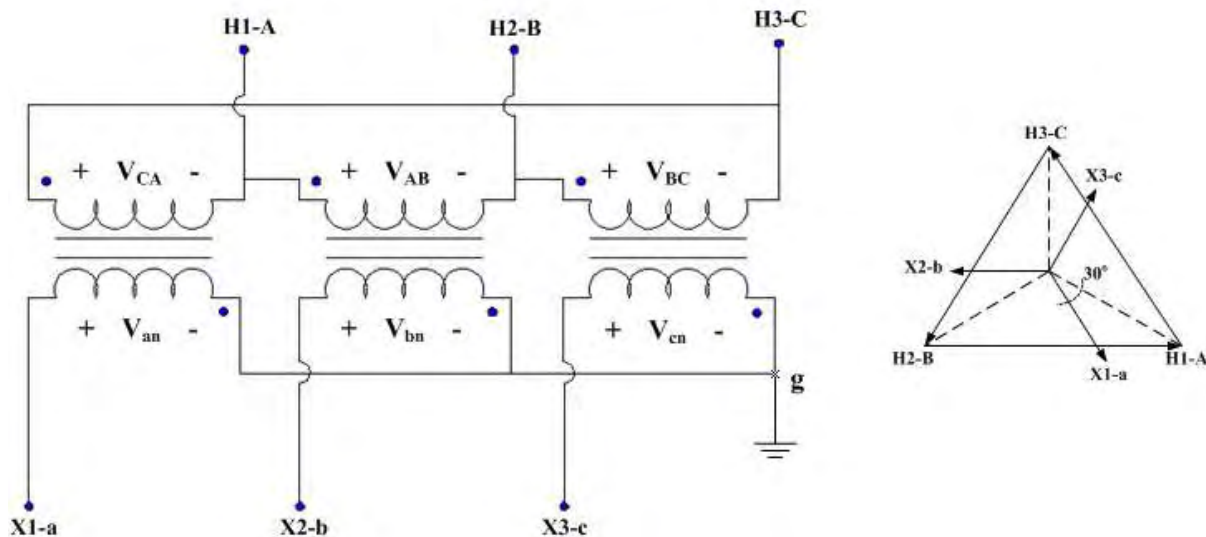


Figure 3. 9: Standard Delta/Grounded-wye connection with voltages

The transformer’s data for the IEEE 13 nodes test feeder is shown in Table 3.7. In order to demonstrate the DIGSILENT transformer models validity, it is employed the the IEEE 4 node test feeder, which is described in the following sections.

Table 3. 7: IEEE 13 node test feeder Transformer’s data [39]

	kVA	kV-High	kV-Low	R-%	X-%
<b>Substation</b>	5,000	115- $\Delta$	4.16-Gr-Y	1	8
<b>XFM-1</b>	500	4.16-Gr-Y	0.48-Gr-Y	1.1	2

### 3.5 Voltage Regulator Model

Balanced three-phase power flow programs are used to calculate the voltage profile on the distribution circuit to determine whether the DG units are exceeding voltage limits. When that occurs, there is concern about the accuracy of the resulting service voltages at individual single-phase loads on single-phase laterals, because only the three-phase portion of the circuit is modeled. *The American National Standards Institute (ANSI) Std. C84.1* voltage ranges can be satisfied based on a three-phase balanced load/impedance analysis, but the limits for single-phase loads can be exceeded.

The voltage regulation of the distribution system is a key operating objective. As the loads on the feeders vary, there must be some means of regulating the voltage so that every customer voltage remains within an acceptable level. Common methods for regulating the voltage are the application of *step type voltage regulators*, *load tap changing transformers (LTC)*, and *shunt capacitors*. This is a significant concern for a electric utility, because responsibility issues arise when customer's equipment is damaged due to a result of either high or low voltage on the circuit. Therefore, the correct transformer modeling is critical to evaluate changes on the distribution feeder voltage profile. *ANSI Std. C84.1* specifies the preferred voltage levels for electric power systems as shown in Table 3.8.

**Table 3.8:** ANSI C84.1 Service voltage ranges for a normal 3-wire 120/240 volts service to a user. Adapted from [23]

		Lower Limit	Upper Limit
<b>Service Voltage</b> <b>120-600 V</b>	<b>Range A</b>	114 V	126 V
	<b>Range B</b>	110 V	127 V
<b>Service Voltage</b> <b>&gt;600 V</b>	<b>Range A</b>	117 V	126 V
	<b>Range B</b>	114 V	127 V

The ANSI Standard give the distribution engineer a range of normal steady-state voltages (Range A) and a range of emergency steady-state voltages (Range B) that must be supplied to all users. In addition to the acceptable voltage magnitudes ranges, the ANSI standard recommends that the electric supply systems should be designed and operated to limit the maximum voltage unbalance to 3% when measured at the electric utility revenue meter under a no-load condition. Voltage unbalance is defined as [49]:

$$V_{unbalance} = \frac{\text{Max. deviation from average voltage}}{\text{Average voltage}} \cdot 100\% \quad (3.17)$$

A *Step-voltage Regulator* consists of an autotransformer and a load tap changing mechanism. The position of the tap is determined by a control circuit (*line drop compensator*). A common regulator range is  $\pm 10\%$  with 32 steps divided into 16 steps up and 16 steps down, 5/8% change per step or 0.75-V change per step, on a 120-V base. The step regulators can be connected in a *Type A* or a *Type B* connection according to the *ANSI/IEEE C57.15-1986* standard [50]. Type B is the more common connection used by utilities for step-voltage regulators, its configuration is shown in Figure 3.10. It is important to note that in Type B connection the primary circuit of the system is connected, via taps, to the series winding of the regulator, while in Type A is connected to the load side.

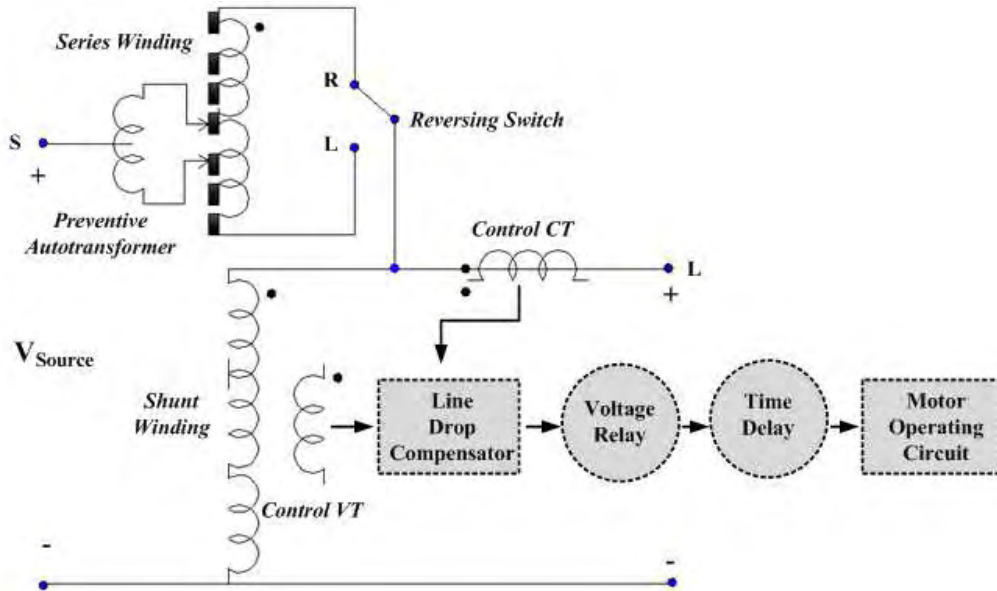


**Figure 3. 10:** Type B step-voltage regulator and control circuit. Adapted from [49]

The only difference between the voltage and current equations for the Type B regulator in the raise and lower positions is the sign of the turns ratio ( $N_2/N_1$ ). In Equation 3.18 the minus sign is when the regulator is in the raise position and the plus sign for the lower position [51].

$$V_L = \frac{1}{a_R} \cdot V_S$$

$$I_L = a_R \cdot I_S \quad (3.18)$$

Where:  $a_R = 1 \mp \frac{N_2}{N_1}$

Equation 3.18 can be modified to give the effective regulator ratio as a function of the tap position. Each tap changes the voltage by 5/8% or 0.00625 per-unit. Therefore, the effective regulator ratio can be given by Equation X.19 as follows:

$$a_R = 1 \pm 0.00625 \cdot \text{Tap} \quad (3.19)$$

W. H. Kersting in [3] apply a set of generalized matrix equations to develop three-phase models of step-voltage regulators. These matrices are very similar to the equation used in transmission line analysis when evaluating for *Pi Models* and *Large Transmission Lines* [41]. In this case, the *abcd* parameters are 3 x 3 matrices rather than single variables.

$$\begin{bmatrix} [V_S]_{abc} \\ [I_S]_{abc} \end{bmatrix} = \begin{bmatrix} [a] & [b] \\ [c] & [d] \end{bmatrix} \begin{bmatrix} [V_L]_{abc} \\ [I_L]_{abc} \end{bmatrix} \quad (3.20)$$

For a three-phase wye-connected step-voltage regulator, such as the test feeder under consideration, neglecting the series impedance and shunt admittance, the generalized matrices are defined as:

$$[a] = \begin{bmatrix} a_{R\_a} & 0 & 0 \\ 0 & a_{R\_b} & 0 \\ 0 & 0 & a_{R\_c} \end{bmatrix} \quad (3.21)$$

$$[b] = \begin{bmatrix} 0 & 0 & 0 \\ 0 & 0 & 0 \\ 0 & 0 & 0 \end{bmatrix} \quad (3.22)$$

$$[c] = \begin{bmatrix} 0 & 0 & 0 \\ 0 & 0 & 0 \\ 0 & 0 & 0 \end{bmatrix} \quad (3.23)$$

$$[d] = \begin{bmatrix} \frac{1}{a_{R\_a}} & 0 & 0 \\ 0 & \frac{1}{a_{R\_b}} & 0 \\ 0 & 0 & \frac{1}{a_{R\_c}} \end{bmatrix} \quad (3.24)$$

The effective turn ratios ( $a_{R_a}$ ,  $a_{R_b}$ , and  $a_{R_c}$ ), can take different values when three single-phase regulators are connected in wye. In DigSILENT it is also possible to have a three-phase regulator where the voltage and current are measured in only one phase, and then all three phases are changed by the same number of taps. In Equations 3.21 and 3.24, the effective turns ratio for each regulator must satisfy:

$$0.9 \leq a_{R_{abc}} \leq 1.1 \text{ in } 32 \text{ steps of } 0.625\% \text{ per step (on } 120 - V \text{ base)}$$

The tap changer controls are adjusted to control the voltage with line-drop compensation. The goal of the compensation circuit is such that the voltage across the compensator voltage relay will be a scale model of the actual voltage at the regulation point, see Figure 3.11. There are four settings that are required for the compensator circuit [52].

- *Set Point Voltage*: The voltage required at the load on a 120-V base.
- *Voltage Bandwidth*: The voltage variation from the set point voltage at the load. When the difference exceeds the bandwidth, a tap change is initiated. As a rule of thumb, the minimum bandwidth should be 2 times the step size (1.25% for 5/8%).
- *Time Delay*: Length of time that a raise or lower operation is called for before the actual execution of the command. This prevents taps changing during a transient or short time change in current.
- *Line Drop Compensator*: The compensator for the voltage drop in the circuit between the regulator and the load. The  $R_{set}$  and  $X_{set}$  values of the line are set to determine the voltage drop in the line.

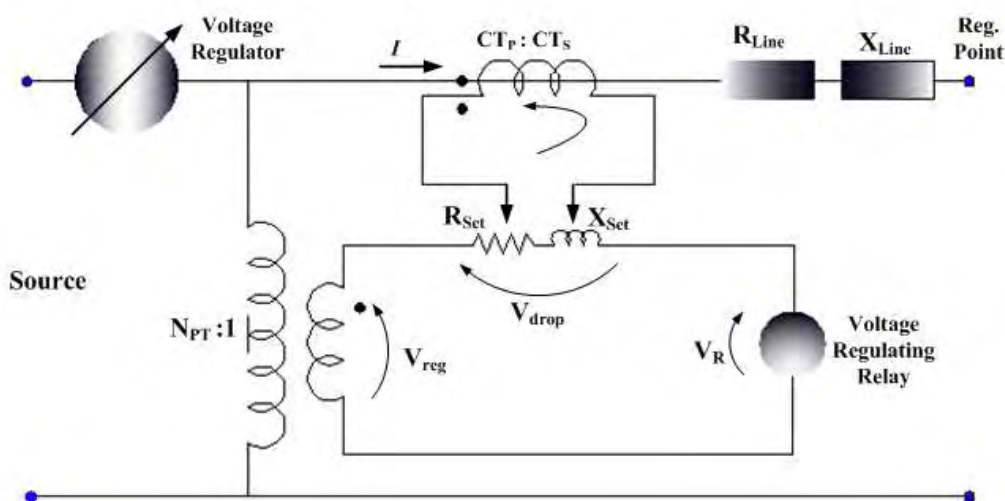


**Figure 3. 11:** Line Drop Compensator Circuit

In order to make the per-unit voltage of the compensator voltage relay equal to the per-unit voltage at the regulation point, the per-unit  $Rset$  and  $Xset$  settings must equal the per-unit equivalent impedance from the regulator output to the regulation point. The line-to-neutral voltage ( $V_{LN}$ ) of the distribution feeder must be chosen as the base line voltage, and the primary rating ( $CT_P$ ) of the current transformer as the base line current. The remaining parameters are determined with the Equations from Table 3.9.

**Table 3. 9:** Line drop compensator parameters [49] [51]

<b>Compensator parameter</b>	<b>Equation</b>
<i>Line base impedance</i>	$Zbase_{Line} = \frac{V_{LN}}{CT_P}$
<i>Compensator base voltage</i>	$Vbase_{comp} = \frac{V_{LN}}{N_{PT}}$
<i>Compensator base current</i>	$Ibase_{comp} = CT_S$
<i>Compensator base impedance</i>	$Zbase_{comp} = \frac{Vbase_{comp}}{Ibase_{comp}}$
<i>Per-unit line impedance</i>	$Zline_{pu} = \frac{Zline}{Zbase_{line}}$
<i>Compensator impedance in ohms</i>	$Zcomp_{ohms} = Zline_{pu} \cdot Zbase_{comp}$
<i>Compensator impedance in volts</i>	$Zcomp_{volts} = Zcomp_{ohms} \cdot CT_S$

After a simple inspection from the Equations in Table 3.9, the compensator  $R$  and  $X$  settings in volts are determined by multiplying the compensator  $R$  and  $X$  in ohms times the rated secondary current in amps ( $CT_S$ ) of the current transformer, and finally leading to Equation 3.25.

$$Z_{volts} = Z_{line} \cdot \frac{CT_P}{N_{PT}} \quad (3.25)$$

The knowledge of the equivalent line impedance in ohms from the generator to the load center is the only parameter needed to determine the required value for the compensator settings. Usually, the load center is located down the primary main feeder after several laterals located upstream. Hence, the current measured by the CT of the regulator is not the current that flows all the way from the regulator to the load center. The only way to determine the equivalent line impedance value is to run a power-flow program of the feeder without the regulator operating.

When the regulation point is identified, and later the results obtained from the power-flow program, the equivalent impedance can be computed as:

$$R_{Line\Omega i} + jX_{Line\Omega i} = \frac{V_{Regulator\_i} - V_{Load\_Center\_i}}{I_{Line\_i}} \Omega \quad (26)$$

For  $i = a, b, c$

Where,

$V_{Regulator}$  = Actual line-to-neutral voltage at the regulator

$V_{Load\_Center}$  = Actual line-to-neutral voltage at the regulation point.

$I_{Line}$  = Actual line current leaving the regulator

In Equation 3.26 the voltages must be specified in system volts and the current in system amperes. Table 3.10 shows the step-voltage regulator data for the IEEE 13 nodes test feeder.

**Table 3. 10:** Step voltage regulator data [39]

Regulator ID	1		
Line Segment	650-632		
Location	650		
Phases	A-B-C		
Connection	3-Phase, LG		
Monitoring Phase	A-B-C		
Bandwidth	2.0 volts		
PT Ratio	20		
Primary CT Rating	700		
Compensator Settings	Ph-A	Ph-B	Ph-C
R-Setting	3	3	3
X-Setting	9	9	9
Voltage Level	122	122	122

### 3.6 IEEE 13 Node Test Feeder Unbalanced Power-Flow

Power-flow studies are very important in planning and designing the future expansion of distribution systems, also in determining the best operation of existing systems. The principal information obtained from a power-flow analysis is the magnitude and phase angle of the voltage at each node and the real and reactive power flowing in each line. The power-flow analysis of a distribution feeder is similar to that of an interconnected transmission system. Usually, what it is known prior to the analysis is the three-phase voltages at the substation and the complex power of all the loads and the load model.

Because a distribution feeder is radial, iterative techniques commonly used in transmission network power-flow studies are not used because of poor convergence characteristics. Several methodologies have been proposed to solve the power-flow problem in distribution systems, and the Forward/Backward Sweep (FBS) method has been preferred in many research studies due to its robustness and simplicity of implementation. However, FBS presents some limitations when control devices are present in the system and also to solve for non-radial (meshed) distribution systems [53].

In Power Factory the nodal equations used to represent the analyzed networks are implemented using two different formulations:

- Newton Raphson ( Current Equations)
- Newton Raphson (Power Equations, Classical)

In both formulations, the resulting non-linear equation systems must be solved by an iterative method. Power Factory uses the Newton Raphson as its non-linear equation solver. Distribution systems, especially unbalanced networks, usually converge better using the “*Current Equations*” formulation. The DIgSILENT Current Equation formulation is derived from the Three-Phase Current Injection Method (TCIM) [54] [55]. According to the TCIM method the three-phase current mismatches for a given bus  $k$  are:

$$\Delta I_k^s = \frac{(P_k^{sch})^s - j(Q_k^{sch})^s}{(E_k^s)^*} - \sum_{i \in \Omega_k} \sum_{t \in \alpha_p} Y_{ki}^{st} E_i^t \quad (3.26)$$

Where,

$$s, t \in \alpha_p$$

$$\alpha_p = \{a, b, c\}$$

$$k = \{1, \dots, n\},$$

$n$  is the total number of buses.

$\Omega_k$  – set of buses directly connected to bus  $k$ .

$P_k^{sch}, Q_k^{sch}$  – scheduled active and reactive powers at bus  $k$  for a given phase  $s$ .

The approach adopted in TCIM consists in rewriting (3.26) in terms of the real and imaginary parts using rectangular coordinates. The equations are then linearized and Newton’s method can be applied as in (3.27). The off-diagonal terms in the Jacobian matrix are equal to the corresponding elements of the nodal admittance matrix and thus remain constant throughout

the iterative procedure. The diagonal terms will depend on the load model used, and should be updated at every iteration.

$$\begin{bmatrix} \Delta I_{Im1}^{abc} \\ \Delta I_{Re1}^{abc} \\ \Delta I_{Im2}^{abc} \\ \Delta I_{Re2}^{abc} \\ \vdots \\ \Delta I_{Imn}^{abc} \\ \Delta I_{Re n}^{abc} \end{bmatrix} = - \begin{bmatrix} J_{11}^{abc} & J_{12}^{abc} & \dots & J_{1n}^{abc} \\ J_{21}^{abc} & J_{22}^{abc} & \dots & J_{2n}^{abc} \\ \vdots & \vdots & \ddots & \vdots \\ J_{n1}^{abc} & J_{n2}^{abc} & & J_{nn}^{abc} \end{bmatrix} \begin{bmatrix} \Delta V_{Re1}^{abc} \\ \Delta V_{Im1}^{abc} \\ \Delta V_{Re2}^{abc} \\ \Delta I_{Im2}^{abc} \\ \vdots \\ \Delta V_{Re n}^{abc} \\ \Delta V_{Im n}^{abc} \end{bmatrix} \quad (3.27)$$

Figure 3.12 shows the IEEE 13 node test feeder modeled in DIgSILENT Power Factory. The transformers between N-650 and RG-60 represent the *Step Voltage Regulator* model for each phase, while the upstream transformer represent the *Main Distribution Substation* (115/4.16 kV, 5 MVA).

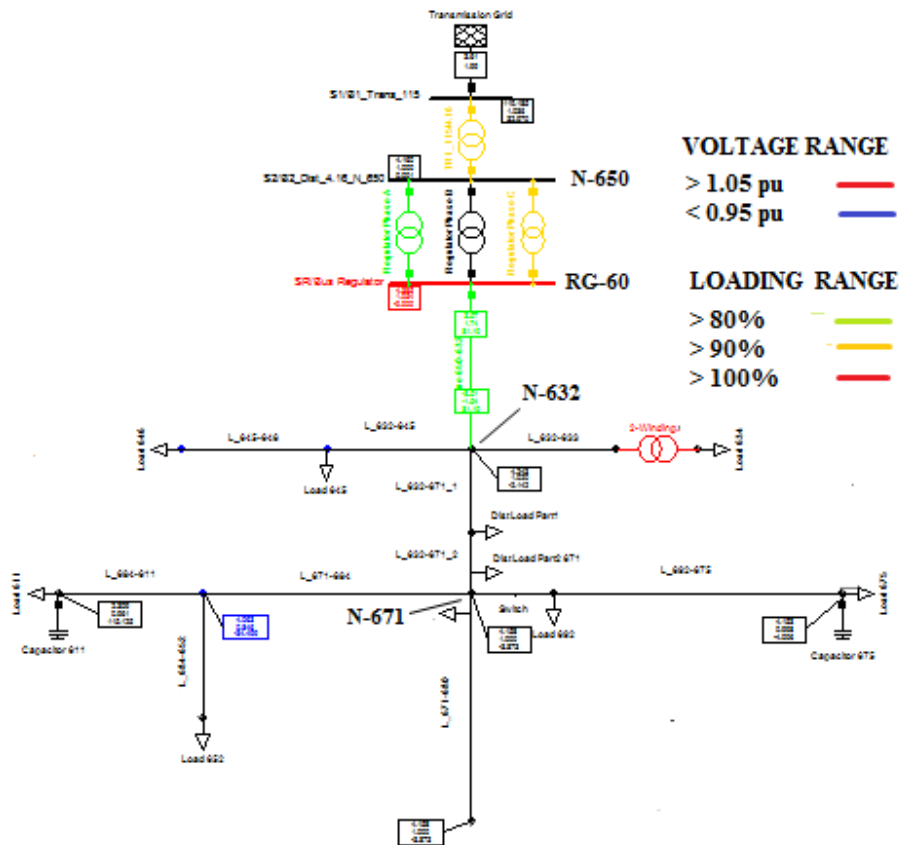


Figure 3. 12: IEEE 13 node test feeder online diagram from DIgSILENT workspace.

The unbalanced power flow results from DIgSILENT for the IEEE 13 node test feeder are shown in Table 3.11, which establishes a comparison between the IEEE and the model developed taking into account voltage magnitudes and phase-angles. The nodes N-650, RG-60, N-632, and N-671 have been selected to show the unbalanced power flow results because they constitute the main feeder of the distribution system under consideration, the other ones are single-phase and two-phase laterals derived from the primary three-phase segment. A brief review of Table 3.11 shows that the voltage magnitude at the secondary side of the step type voltage regulator (RG-60) is higher than its primary side (N-650). Another relevant point is that there is not phase shift between these nodes because of the *G-Wye/G-Wye* connection of the single-phase regulators.

In the analysis of an unbalanced three-phase feeder the real power loss in a device should not be computed by using the phase current squared times the phase resistance. In a balanced system that works, however, in an unbalanced system, the real power losses of a line segment must be computed as the difference (by phase) of the input power in a line segment minus the output power of the line segment. It is possible to have a negative power loss on a phase that is lightly loaded compared to the other two phases. Computing power loss as the phase current squared times the phase resistance does not give the actual real power loss in the phases.

**Table 3. 11:** Unbalanced Power Flow results for the IEEE 13 node test feeder

	IEEE		DIgSILENT	
	Mag. (p.u.)	Angle (degrees)	Mag.(p.u.)	Angle (degrees)
<b>N-650</b>				
$V_{AN}$	1.0000	0.00	0.9926	0.21
$V_{BN}$	1.0000	-120.00	1.0068	-119.73
$V_{CN}$	1.0000	120.00	1.0007	119.53
<b>RG-60</b>				
$V_{AN}$	1.0625	0.00	1.0608	0.21
$V_{BN}$	1.0500	-120.00	1.0446	-119.73
$V_{CN}$	1.0687	120.00	1.0570	119.53
<b>N-632</b>				
$V_{AN}$	1.0210	-2.49	1.0194	-2.25
$V_{BN}$	1.0420	-121.72	1.0355	-121.46
$V_{CN}$	1.0174	117.83	1.0054	117.27
<b>N-671</b>				
$V_{AN}$	0.9900	-5.30	0.9884	-5.02
$V_{BN}$	1.0529	-122.34	1.0455	-122.09
$V_{CN}$	0.9778	116.02	0.9656	115.37

### 3.7 IEEE 4 Node Test Feeder Model

This particular system is employed in order to verify the transformer model validity in DIgSILENT. The primary purpose of this test feeder is to provide a simple system for the testing of all possible three-phase transformer connections, which presents the following characteristics:

- Two line segments with a three-phase transformer bank connected between the two segments.
- Data is specified for *closed* three-phase transformer connections and for two transformer *open* connections.
- Transformer data is specified for step-up and step-down testing. The primary voltage is always 12.47 kV while the secondary voltage can be either 4.16 kV or 24.9 kV.
- Data is specified for balanced and unbalanced loading at the most remote node.

The oneline diagram of the feeder is shown in Figure 3.13 from DIgSILENT workspace. Both the primary line (Node1-Node2) and the secondary line (Node3-Node4) were constructed using the pole configuration *ID-500* shown in Figure 2.4, and phasing *ABCN* from left to right. The conductor data is as follows [56]:

1. Phase Conductor: 336,400 26/7  
GMR = 0.0244ft      Resistance = 0.306 Ω/mile      Diameter = 0.721 inch
2. Neutral Conductor: 4/0 6/1 ACSR  
GMR = 0.00814 ft      Resistance = 0.592 Ω/mile      Diameter = 0.583 inch

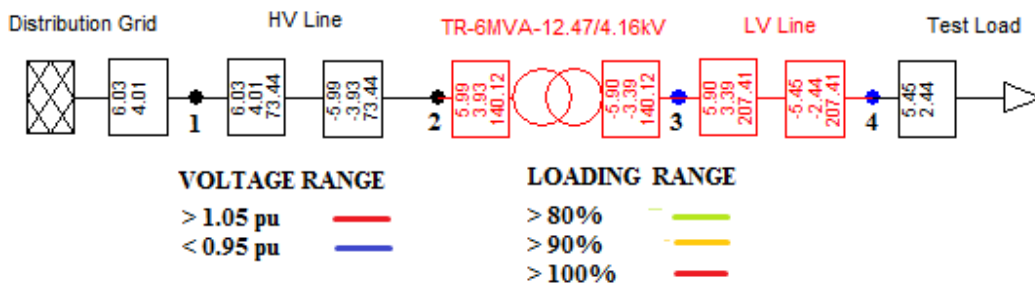


Figure 3. 13: IEEE 4 Node Test Feeder Online Diagram

Although this test feeder can be simulated for single-phase transformer banks under balanced and unbalanced conditions is preferred to evaluate the system considering the second one, due to the original configuration of the IEEE 13 node test system. Hence, the *Grounded-Y/Delta Step-Down* connection with unbalanced loading has been chosen as demonstration.

The three-phase transformer data for a Step-Down connection is shown in Table 3.12. Loads at node 4 are connected in closed delta for the transformer configuration selected; the corresponding data is shown in Table 3.13.

**Table 3. 12:** Three-Phase Transformer Data [56]

Connection	kVA	kVLL-High	kVLL-Low	R-%	X-%
Step-Down	6,000	12.47	4.16	1.0	6.0

**Table 3. 13:** Closed Connection Load Data [56]

Phase-A		Phase-B		Phase-C	
kW	PF	kW	PF	kW	PF
1275	0.85 lag	1800	0.90 lag	2375	0.95 lag

**Table 3. 14:** Unbalanced load flow results for the IEEE 4 node test feeder with *Grounded-Y/Delta Step-Down* Transformer Bank.

	IEEE		DIgSILENT	
	Mag. (kV)	Angle (degrees)	Mag. (kV)	Angle (degrees)
<b>Node-2</b>				
$V_{AN}$	7113	-0.20	7112.80	-0.20
$V_{BN}$	7144	-120.40	7143.82	-120.42
$V_{CN}$	7111	119.50	7108.63	119.53
<b>Node-3</b>				
$V_{AB}$	3896	-2.80	3903.79	-6.22
$V_{BC}$	3972	-123.80	4098.09	-121.18
$V_{CA}$	3875	115.70	3748.26	116.33
<b>Node-4</b>				
$V_{AB}$	3425	-5.80	3297.58	-11.13
$V_{BC}$	3646	-130.30	3762.57	-125.24
$V_{CA}$	3298	108.60	3308.81	108.40
<b>Line 1-2</b>				
$I_{A-L}$	308.50	-41.50	308.73	-41.43
$I_{B-L}$	314.60	-145.50	314.63	-145.44
$I_{C-L}$	389.00	85.90	389.23	85.91
<b>Line 3-4</b>				
$I_{A-L}$	1083.80	-71.00	1084.41	-71.03
$I_{B-L}$	849.90	177.00	850.23	176.98
$I_{C-L}$	1098.70	63.10	1099.29	63.15

An unbalanced power flow was simulated in DIgSILENT Power Factory for the proposed transformer model (*G-Wye/Delta*). Table 3.14 shows the results at nodes 1 to 4 for voltage magnitudes and angles, also the line currents for overhead segments 1-2 and 3-4. The major difference between the IEEE results and DIgSILENT is highlighted, which represent a deviation of 3.74% respective the IEEE measurements.

### 3.8 Overcurrent Protection Model

Overcurrent protection or short-circuit protection is very important on any electrical power system. Circuit breakers and reclosers, expulsion fuses and current-limiting fuses are some of the protective devices employed to interrupt fault current, which is a vital function. The required characteristics necessary for a protective equipment to perform its function properly are [57]:

1. *Sensitivity*: Applies to the ability of the relay to operate reliably under the actual condition that produces the minimum operating tendency. For example, a time-overcurrent relay must operate under the minimum fault current condition expected. The maximum fault current condition occurs when the largest number of generators is in service, which usually occurs at peak load. The fault current available at any point in the network depends on the Thevenin equivalent impedance seen looking into the network from the fault point. Note: On many distribution systems, the fault-current magnitude does not differ very much for minimum and maximum generation conditions because most of the system impedance is in the transformer and lines rather than the generators [58].
2. *Selectivity*: Is the ability of the relay to differentiate between those conditions for which immediate action is required and those for which no action of a time-delayed operation is required.
3. *Speed*: Is the ability of the relay to operate in the required time period.
4. *Reliability*: Refers to the ability of the relay system to perform correctly. The proper application of protective relaying equipment involves the correct choice not only of relaying equipment but also of the associated apparatus.

The overcurrent relay, as the name implies, operates or picks up when its current exceeds a predetermined value. There are two basic forms of the overcurrent relays: the instantaneous type and the time-delay type. It has been noted that these relays can be designed with a wide variety of time-current characteristics, such that coordination between the relays and other devices is practical. In terms of the logical operations of an instantaneous overcurrent relay, the following stages are identified in DIGSILENT relay models (see Figure 3.14):

1. A current transformer slot (CT Model), which outputs are the real and imaginary parts of the three-phase currents ( $I_{rA}$ ,  $I_{iA}$ ,  $I_{rB}$ , etc.) and the real and imaginary parts of the zero sequence current ( $I_{0x3r}$ ,  $I_{0x3i}$ ).
2. A measurement unit slot, which output is  $I_{max}$ , which is the maximum of the three-phase currents.
3. A slot for a time-overcurrent relay unit (TOC Unit) and one for an instantaneous overcurrent relay unit (IOC Unit), with the tripping signals as outputs.
4. A logic unit slot, which combines the tripping signals in an AND/OR expression to produce a single tripping signal.

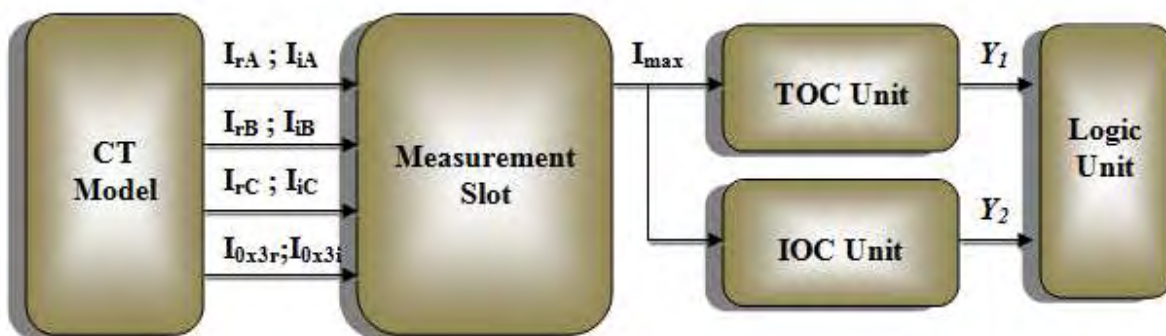


**Figure 3. 14:** Composite Frame of a Time-Overcurrent Relay. Adapted from [54]

The time-current characteristics are based on the historically dominant manufactures of relays. Westinghouse relays have a CO family of relays, and the General Electric relays are IAC (see Table 3.15). Most relays (digital and electromechanical) follow the characteristics of the GE or Westinghouse relays. For distribution overcurrent protection, the extremely inverse relays are most often used (CO-11 or IAC-77) [59] [60].

The time-current curves for induction relays can be approximated by the Equation X.28, which is presented in [61] (*IEEE Std.C37.112-1996*) as an attempt to make relay characteristics consistent. The constants  $A$ ,  $B$ , and  $p$  for the standardized inverse relay characteristics are shown in Table X.16, while the corresponding graphs for extremely inverse relays are shown in Figure X.15.

$$t(I) = TDS \cdot \left( \frac{A}{M^p - 1} + B \right) \quad (28)$$

Where,

$t$  = trip time, seconds

$M$  = multiple of pick up current ( $M > 1$ )

$TDS$  = time dial setting

$A, B, p$  = curve shaping constants

**Table 3. 15:** Relay Designations

	Westinghouse/ABB Designation	General Electric Designation
<b>Moderately inverse</b>	CO-7	
<b>Inverse Time</b>	CO-8	IAC-51
<b>Very Inverse</b>	CO-9	IAC-53
<b>Extremely inverse</b>	CO-11	IAC-77

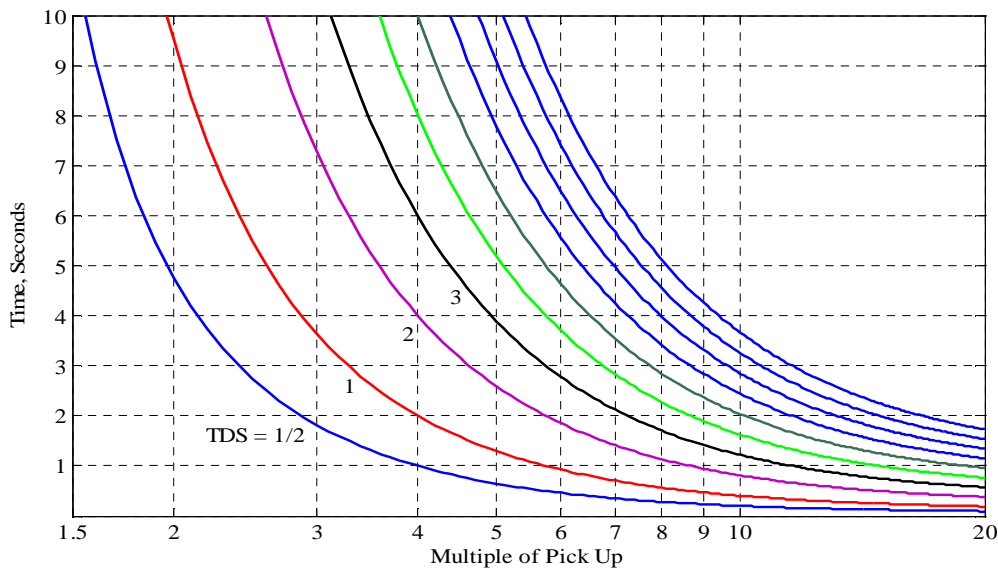


**Figure 3. 15:** Extremely Inverse Relay curves following the IEEE standardized characteristics

Protective relays provide the brains to sense an abnormal condition, but as low-energy devices, because they are not able to open and isolate the problem area of the power system. Instead, circuit breakers and various types of circuit interrupters are used for this and provide the muscle for fault isolation. Hence, a protective relay without a circuit breaker has no value except possibly for alarm. Similarly, a circuit breaker without relays has minimum value, and only can be employed for manually energizing or de-energizing a circuit or equipment.

**Table 3. 16:** IEEE Standardized Relay Curve Equations Constants [61]

	<b>A</b>	<b>B</b>	<b>p</b>
<b>Moderately inverse</b>	0.0515	0.114	0.02
<b>Very inverse</b>	19.61	0.491	2.0
<b>Extremely inverse</b>	28.2	0.1217	2.0

The relays are connected to the strong current and high-voltage of the power system through special matching transformers called: “Current Transformers” (CT) and “Voltage Transformers” (VT), which is the first block in Figure 3.14. The primary currents of CT can reach tens of thousands amperes. Standard values for secondary currents are 5 or 1 A, and it is for these current values that most relays in the world are constructed today. In circuit schematics and diagrams the combination of CTs, relays, and breakers are represented as shown in Figure 3.16. This diagram shows a typical ac oneline schematic and a DC trip circuit.

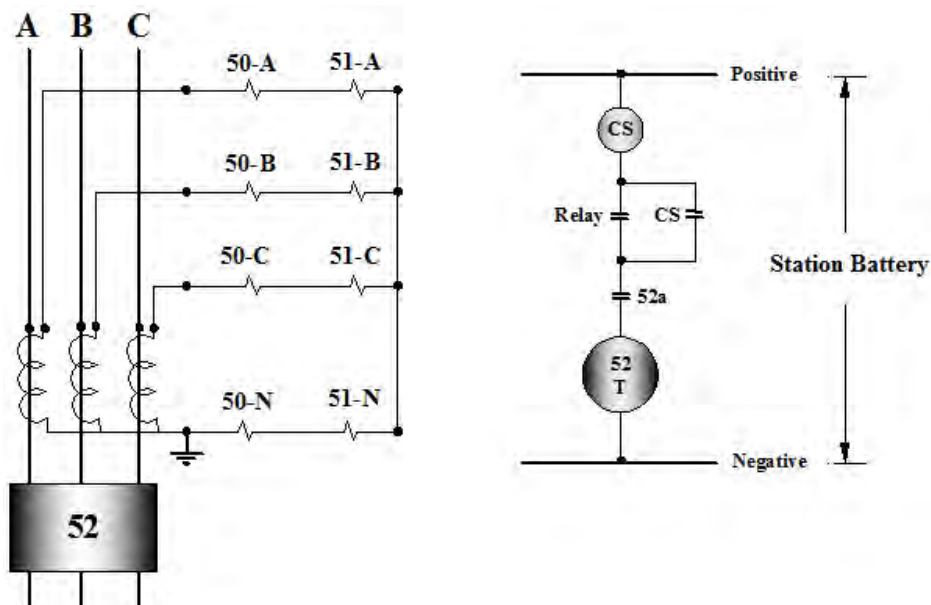


**Figure 3. 16:** Typical ac connections of a protective relay with its DC trip circuit

The circuit breaker on Figure 3.16 is designated as device 52 following the ANSI/IEEE device number system (*IEEE Std C37.2-2008*), in the same way the device numbers 50 and 51 refers to the instantaneous and time-delay overcurrent relays respectively [62]. In the DC diagram the contacts are shown in their deenergized position. Thus, when the circuit breaker is closed and in service, its 52a contact is closed. When a system fault activates the protective relay, its output contacts close to energize the circuit breaker trip coil 52T, which open the breaker main contacts and deenergize the connected power circuit.

The electromechanical relay contacts basically are not design to interrupt the circuit breaker trip coil current, son an auxiliary dc-operated unit called CS (Contactor Switch) was employed to seal-in (or bypass) the protective relay contacts. When the circuit breaker opens, the 52a contacts will open to deenergize the trip coil 52T.

All devices (including circuit breakers, fuses, and reclosers) interrupt fault current during a zero-crossing. To do this, the interrupter creates an arc. In a fuse, an arc is created when the fuse element melts, and in a circuit breaker or recloser, an arc is created when the contacts mechanically separate. An arc conducts by ionizing gasses, which leads to a relatively low-impedance path. After the arc is created, the trick is to increase the dielectric strength across the arc so that the arc clears at a current zero. During this period when the current is reversing, the arc is not conducting and is starting to de-ionize, and the circuit is interrupted, at least temporarily. Just after the arc is interrupted, the voltage across the now-interrupted arc path builds up, which it is known as *Transient Recovery Voltage*. Therefore, the successful interruption depends upon controlling and finally extinguishing the arc. Usually, the interrupting medium in circuit breakers can be any of vacuum, oil, air, or SF<sub>6</sub> [63].

Although this section has been focused on overcorrect protection relays and circuit breakers, the integration of *Power Fuses* and *Distribution Cutouts*, as classified in the IEEE/ANSI Std. C37.40-2003 [64], are taken into consideration for the overcurrent protection of lateral branches and transformers. The addition of a recloser, or even a sectionalizer, on every lateral would be costly and unnecessary.

In order to achieve a successful operation of the protective scheme, a coordination study must be carried out. The next step-by-step ordering of tasks provides the logical procedure to follow:

1. Establish tentative locations of sectionalizing devices, see Figure 3.17.
2. Calculate maximum and minimum values of fault currents at each of the tentative sectionalizing points, and at the end of the main, branch, and lateral circuits. Calculate line-to-ground and three-phase currents.
3. Coordinate the sectionalizing devices from the substation out, or from the ends of the circuit back to the substation.
4. Check the selected protective devices for current-carrying capacity, interrupting capability, and minimum pickup rating.

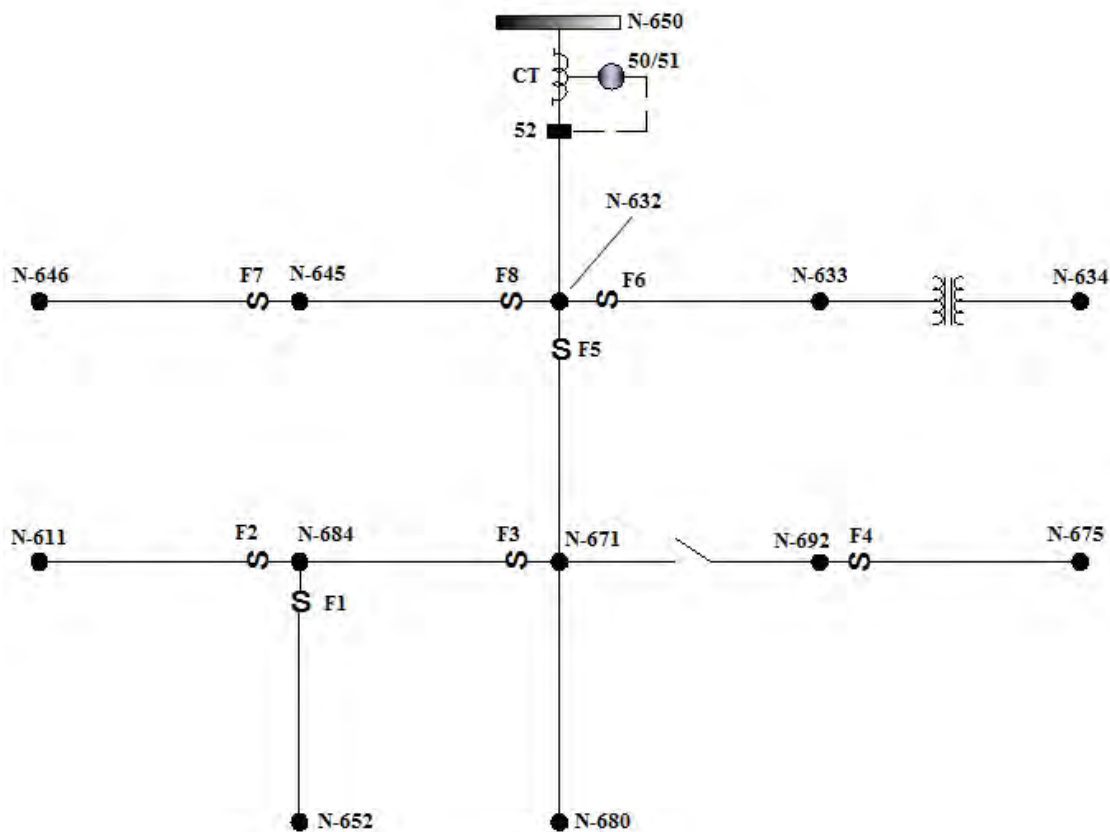
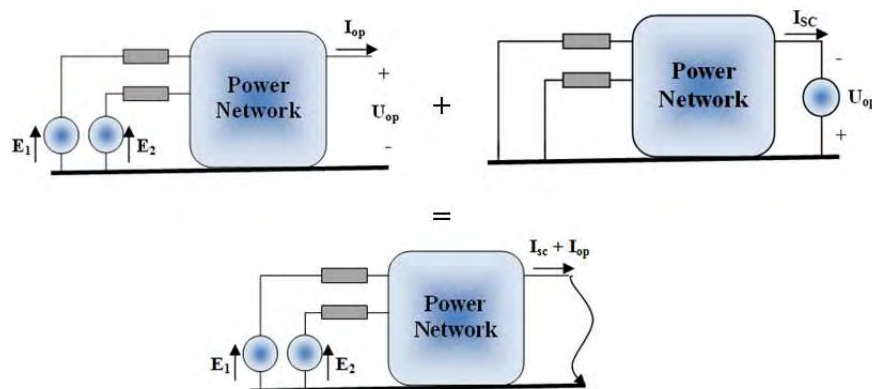


Figure 3. 17: Tentative location of overcurrent protection on the IEEE 13 Node Test Feeder

The computation of short-circuit currents for unbalanced faults in a normally balanced three-phase system has traditionally been accomplished by the application of symmetrical components. However, this method is not well suited to a distribution feeder that is inherently unbalanced. The unequal mutual coupling between the phases leads to mutual coupling between sequence networks. When this happens there is no advantage to using symmetrical components [65].

One of the main application of short-circuit calculations is to check the rating of network equipment at the planning stage. In this case, the planner is interested in knowing the expected maximum currents (for the rating of the components) and the minimum currents (to ensure that the protection scheme will work). Short-circuit calculations at the planning stage commonly use calculation methods that required less network modeling, i.e. that do not require load information, and will apply extreme estimations. Examples of these methods include the *ANSI/IEEE Std. 1411993* and the *IEC 60909* [66] [67]. For short-circuit calculations in a system operation environment the exact network operating conditions are well known (e.g. previous unbalanced load flow), and the *Superposition Method* can be applied, which is in terms of system modeling an accurate method.

In DIGSILENT Power Factory different calculation methods are available (i.e. *ANSI/IEEE*, *VDE*, and the *Complete Method* based on the superposition model). For the aim of this work the complete method will be applied in the short circuit calculations. Hence, the short-circuit currents are determined by overlaying a healthy load-flow condition before short-circuit inception with a condition where all voltage supplies are set to zero and the negative operating voltage is connected at the fault location [68]. The procedure is shown in Figure 3.18.



**Figure 3. 18:** Principle of the Superposition Method. Adapted from [68]

From the complete method calculation the following parameters are determined:

1. **Peak Short-Circuit Current,  $i_p$** : The largest possible momentary value of the short circuit occurring.
2. **Initial Symmetrical Short-Circuit Current,  $I_{kss}$  ( $I_k''$ )**: This is the effective value of the symmetrical short circuit current at the moment at which the short circuit arises, when the short circuit impedance has its value from the time zero.
3. **Steady State Short-Circuit Current,  $I_k$** : Effective value of the initial symmetrical short circuit current remaining after the decay of all transient phenomena.

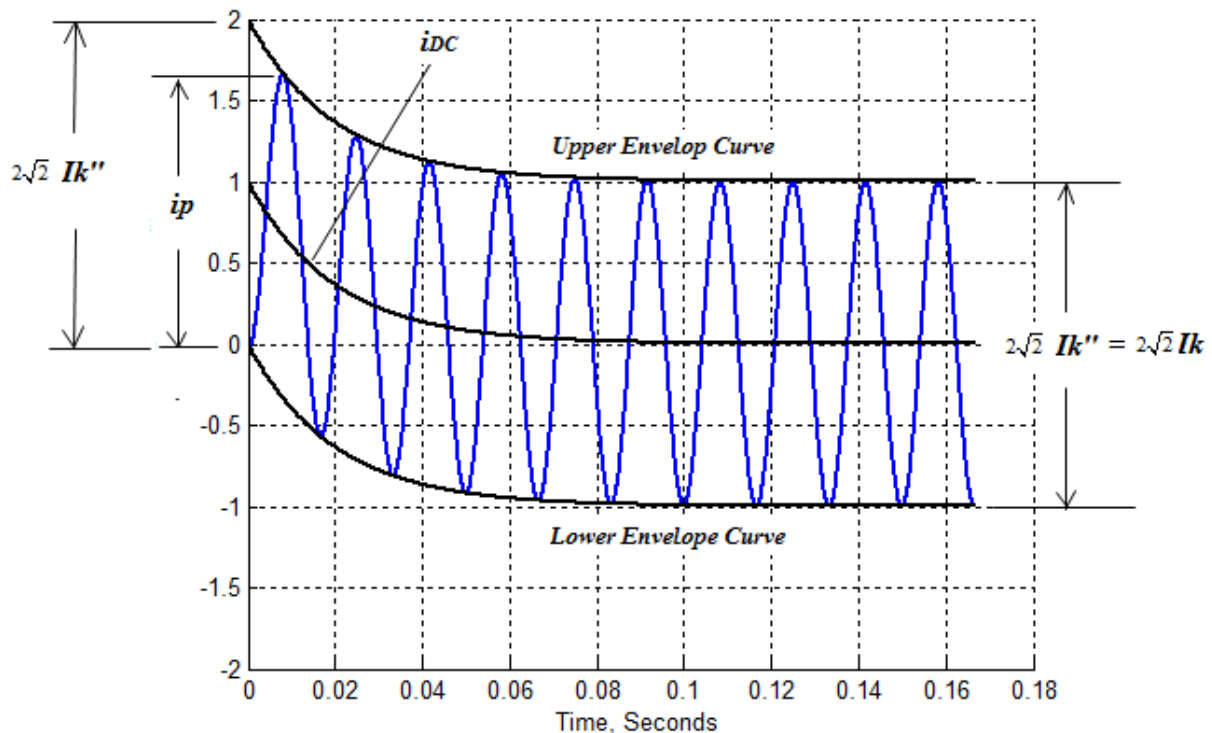


**Figure 3. 19:** Behavior of the Short-Circuit Current far from the Generator

Figure 3.19 shows the behavior of the short-circuit current far from the generator station (this assumption is valid for the IEEE 13 Node Test Feeder). In a synchronous machine the flux across the air gap is not the same at the instant the short circuit occurs as it is a few cycles later. The change of flux is determined by the combined action of the field, the armature, and the damper windings or iron parts of the rotor. After a fault occurs, the sub-transient, transient, and steady-state periods are characterized by the sub-transient reactance ( $X_d''$ ), the transient reactance ( $X_d'$ ), and the steady-state reactance ( $X_d$ ), respectively. This reactance has increasing values, so that the corresponding components of the short circuit current have decreasing values.

Before the implementation of a short circuit analysis it is recommended to determine the continuous full load current in every line segment. Table 3.17 summarizes the current magnitudes per phase for the IEEE 13 Node Test Feeder from an unbalanced power flow. The zero values in some phases indicate the lack of that phase for the line segment considered, e.g. L\_671-684 is a two-phase line segment with phases A and C, while L\_684-652 is a single-phase line segment. The line L\_671-680 has all its current magnitudes equal to zero because there is no load connected.

**Table 3. 17:** Full load current magnitudes per phase for the IEEE 13 Node Test Feeder

<b>Line</b>	<b><math>I_{\phi A}</math> (kA)</b>	<b><math>I_{\phi B}</math> (kA)</b>	<b><math>I_{\phi C}</math> (kA)</b>	<b>Max</b>
<b>L_650-632</b>	0.55745	0.41978	0.59269	0.59269
<b>L_692-675</b>	0.20206	0.06756	0.12707	0.20206
<b>L_684-652</b>	0.06319	0.00000	0.00000	0.06319
<b>L_684-611</b>	0.00000	0.00000	0.07110	0.07110
<b>L_671-684</b>	0.06319	0.00000	0.07110	0.07110
<b>L_671-680</b>	0.00000	0.00000	0.00000	0.00000
<b>L_645-646</b>	0.00000	0.06460	0.06460	0.06460
<b>L_632-671_2</b>	0.47145	0.19920	0.44407	0.47145
<b>L_632-671_1</b>	0.47683	0.21869	0.48078	0.48078
<b>L_632-645</b>	0.00000	0.14301	0.06460	0.14301
<b>L_632-633</b>	0.08185	0.06218	0.06383	0.08185

An unbalanced three-phase short-circuit analysis is carried out for the test feeder under study. Since there are some single-phase and two-phase laterals it is not possible to determine three-phase currents for all the nodes. Figure 3.20 shows the location of the possible three-phase fault analysis. It is important to note that the original IEEE test system does not provide a short circuit calculation, and this fact is pointed out by Dugan, R. and Kersting, W.H. in several IEEE papers. Table 3.18 summarizes the current magnitudes for each three-phase fault.

The three-phase short circuit current at node N\_650 (see Table 3.18) it seems to be symmetrical, but this point is the upper node of the radial feeder, i.e. is the only node connected to the transmission system. As the distance from this point increases also increases the unbalance between the fault currents, and gradually reduce its magnitude. For distribution feeders, it is a common practice to add incremental impedances to the Thevenin equivalent at the main substation, i.e., looking into the transmission system, e.g. node N\_650.

If the distribution substation is supplied from a very large system, then  $Z_{th}$  will be small. A common assumption, when no exact data are available, is to set  $Z_{th} \approx 0$ , which equivalent to an infinitely large system. This assumption has been made for this study.

**Table 3. 18:** Unbalanced Three-phase fault currents for the IEEE 13 Node test feeder

Node	$i_{pA}$ (kA)	$i_{pB}$ (kA)	$i_{pC}$ (kA)	$I_k''_A$ (kA)	$I_k''_B$ (kA)	$I_k''_C$ (kA)
N_650	21.1755	21.1755	21.1755	8.8643	8.8643	8.8643
RG-60	19.8134	20.4101	19.9299	8.2940	8.5439	8.3428
N_632	10.6920	10.5845	10.0911	4.9241	4.8746	4.6473
N_633	8.6131	8.4632	8.0631	4.2428	4.1689	3.9718
N_634	23.8900	24.0439	23.2584	13.2454	13.3307	12.8952
N_671	7.3253	7.1658	6.6544	3.4827	3.4068	3.1637
N_675	6.5081	6.5193	6.0496	3.2056	3.2111	2.9797
N_680	6.2485	6.1592	5.6223	2.9959	2.9530	2.6956
N_692	7.3253	7.1658	6.6544	3.4827	3.4068	3.1637

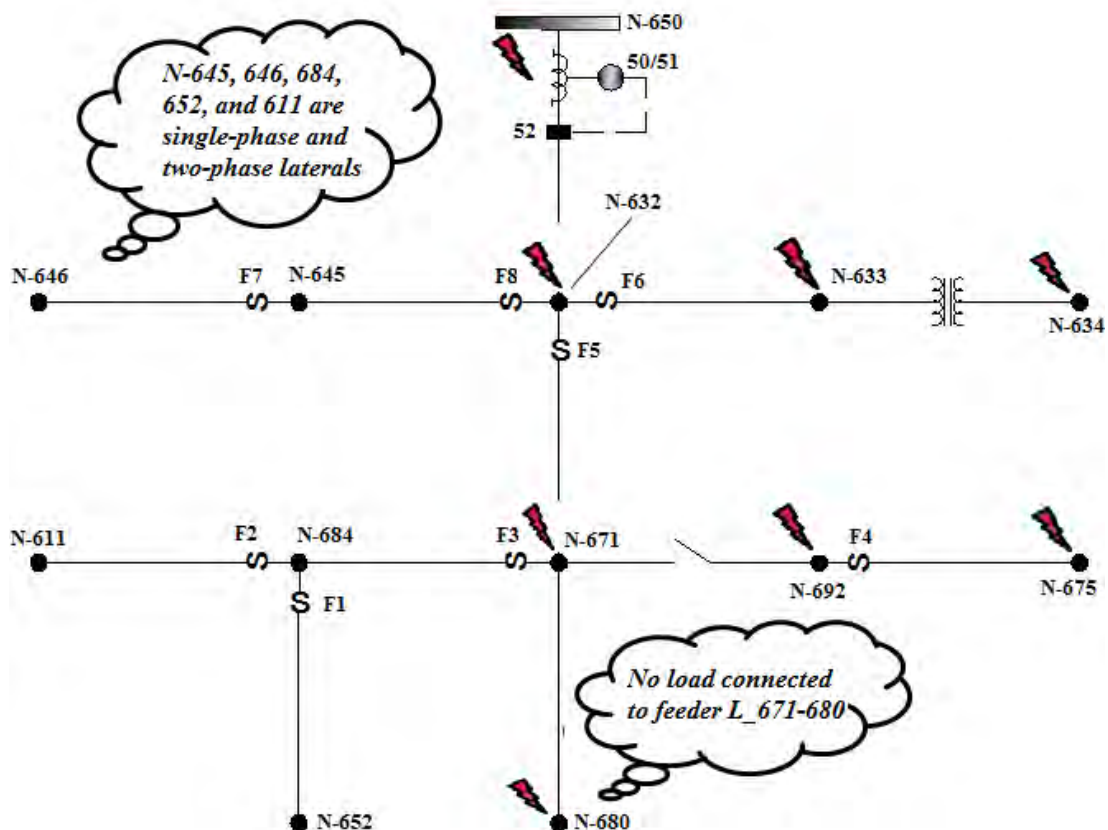


**Figure 3. 20:** Location of Three-Phase Short Circuit Calculations

Figure 3.21 shows an EMT simulation developed in DigSILENT workspace for the three-phase short circuit at node RG\_60 (secondary side of the step voltage regulator). The peak-current magnitude is approximately 20 kA, and the effective steady-state current will be below 10 kA, which coincide with the initial short-circuit current value ( $I_k''$ ) because the fault is assumed to be far from the generator.

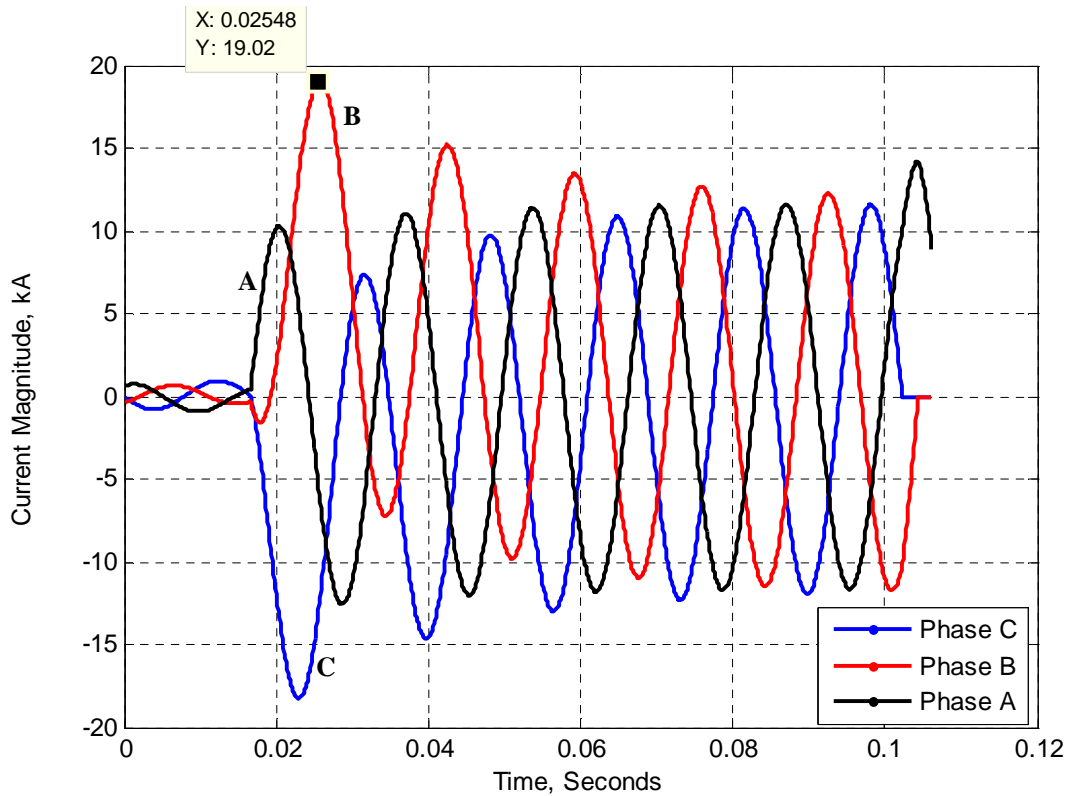


**Figure 3. 21:** Electromagnetic Transient behavior of a three-phase fault at node RG-60

In order to assure a good sensitivity of the overcurrent protection scheme a single-phase-to-ground fault analysis is carried out. Usually, the Line-to-Line (LL) fault is the smallest, and for zero fault resistance ( $Z_F$ ) it is always 0.866 of the three-phase fault, but this relation does not hold as  $Z_F$  increases. The fault impedance  $Z_F$  is often taken to be 1 to 40 ohms of resistance for minimum faults and zero for maximum fault conditions [58]. The aim of this section is to set the coordination for overcurrent protection devices. Hence, three-phase and single-phase-to-ground faults will be determined for  $Z_F = 0$  to find maximum fault currents. The minimum fault current will be at least 2 pu the full load current (rule of thumb).

The results from single-phase-to-ground fault calculation are shown in Table 3.19. The single-phase-to-ground fault current has bigger magnitudes than three-phase fault currents in the same locations (see nodes N\_650 and RG\_60 at Tables 3.18 and 3.19). This is true for faults close to the main substation (i.e.  $Z_{line} = 0$ ) and  $Z_F = 0$ . The empty cells in Table 3.19 mean that the corresponding phase is not available, e.g., only phase C is available at N\_611, so that the single-phase-to-ground fault is calculated for that phase.

**Table 3. 19:** Single-phase-to-ground fault currents for the IEEE 13 node test feeder

<b>Name</b>	$i_{pA}$ (kA)	$i_{pB}$ (kA)	$i_{pC}$ (kA)	$I_k''_A$ (kA)	$I_k''_B$ (kA)	$I_k''_C$ (kA)
<b>N_650</b>	26.6272	0.0000	0.0000	11.1464	0.0000	0.0000
<b>RG_60</b>	24.9143	0.0000	0.0000	10.4293	0.0000	0.0000
<b>N_611</b>			3.7595			2.0053
<b>N_632</b>	8.8152	0.0000	0.0000	4.0598	0.0000	0.0000
<b>N_633</b>	6.8286	0.0000	0.0000	3.3637	0.0000	0.0000
<b>N_634</b>	22.2876	0.0000	0.0000	12.3570	0.0000	0.0000
<b>N_645</b>		0.0000	6.0201		0.0000	3.1378
<b>N_646</b>		0.0000	5.0606		0.0000	2.7704
<b>N_652</b>	4.0375			2.1656		
<b>N_671</b>	5.2853	0.0000	0.0000	2.5128	0.0000	0.0000
<b>N_675</b>	4.6437	0.0000	0.0000	2.2873	0.0000	0.0000
<b>N_680</b>	4.3125	0.0000	0.0000	2.0676	0.0000	0.0000
<b>N_684</b>	4.5214		0.0000	2.2777		0.0000
<b>N_692</b>	5.2853	0.0000	0.0000	2.5128	0.0000	0.0000

Although the peak-current is calculated, its value is only applied to determine the device ratings. The steady-state short circuit current will be employed to coordinate the overcurrent protection ( $I_k'' = I_k$ ) because the relay and fuses must withstand the transient induced by switching operations, and transformer inrush currents. Thus, the minimum and maximum fault currents are determined from Tables 3.18 to 3.19. However, to set the proper sizing and coordination between the downstream devices (fuses) the maximum continuous current must be taken into consideration. Since the IEEE 13 Node test feeder is composed of unbalanced single-phase, two-phase and three-phase laterals, the phase with the higher current is selected to calculate the fuse rating. Often utility operators choose the fuse size taking into account balanced system operation, and then line segments are commonly subject to open-phase conductor and high-impedance faults. Some faults will always remain undetectable (high impedance faults). The trick is to try to clear all high-current faults without being too conservative.

Table 3.20 shows the maximum continuous current and indicates the corresponding phase (A, B or C), also the maximum fault current and the type of fault (1PH-G or 3PH). Later, the coordination between downstream fuses and overcurrent relays will be carried out, but both devices present different physical behavior when clearing a fault. The coordination procedure is as follows, see Figure X.17:

1. Coordinate F1&F2 with F3, and F7 with F8
2. Coordinate F3&F4 with F5
3. Coordinate F6&F8 with TOC-50/51

**Table 3. 20:** Maximum continuous and fault current magnitudes for the device location

Device	Maximum continuous Current		Maximum Fault	
	Line Segment/Phase	Mag. (kA)	Location/Type	Mag. (kA)
<b>F1</b>	<b>L_684-652/A</b>	0.06319	<b>N_684/1PH-G</b>	2.2777
<b>F2</b>	<b>L_684-611/C</b>	0.07110	<b>N_684/1PH-G</b>	2.2777
<b>F3</b>	<b>L_671-684/C</b>	0.07110	<b>N_671/3PH-G</b>	3.4827
<b>F4</b>	<b>L_692-675/A</b>	0.20206	<b>N_692/3PH-G</b>	3.4827
<b>F5</b>	<b>L_632-671/C</b>	0.48078	<b>N_632/3PH-G</b>	4.9241
<b>F6</b>	<b>L_632-633/A</b>	0.08185	<b>N_632/3PH-G</b>	4.9241
<b>F7</b>	<b>L_645-646/B</b>	0.06460	<b>N_645/1PH-G</b>	3.1378
<b>F8</b>	<b>L_632-645/B</b>	0.14301	<b>N_632/3PH-G</b>	4.9241
<b>50/51</b>	<b>L_650-632/C</b>	0.59269	<b>N_650/1PH-G</b>	11.1464

When coordinating two fuses, the downstream fuse (referred to as the *Protecting Fuse*) should operate before the upstream fuse (the *Protected Fuse*). To achieve this goal, it is assured that the total clear time of the protecting fuse is less than the damage time of the protected fuse. The damage time is 75% of the minimum melt time. The minimum-melt time is 90% of the average melt time to account for manufacturing tolerances. The total clearing time is the average melting time plus the arcing time plus manufacturing tolerances.

Power fuses are available for both indoor and outdoor, and in expulsion or current limiting types. The choice depends on the location and ratings available. One class of power fuses are identified by the letter “E” to signify that their TC characteristics belong to the requirements given in Table 3.21 [69], which is the type of fuse considered for the coordination process. The E rated fuse is 100% current fuse; that is, the rating must be equal to or greater than the maximum continuous load current.

DIgSILENT provides a full data base with several commercial devices and its TC characteristics. Some of the companies are ABB/Westinghouse, General Electric, Gould-Shawmut, and S&C, so that it was not considered ideal devices in the protection modeling. For fuse models it was selected S&C power fuses (SMU-40 indoor and outdoor distribution) [70]. Figure 3.22 shows the TCC coordination for the selected fuse based on Table 3.20. The TCC for the moderately inverse overcurrent relay was modeled following the guidelines established by the *IEEE Std.C37.112-1996* [61].

**Table 3. 21:** Melting Time-Current characteristics of E Rated Links [69]

Line Current Reading	Melting Time	Continuous Current
100 amperes and below	300 sec	200-400%
Above 100 amperes	600 sec	220-264%

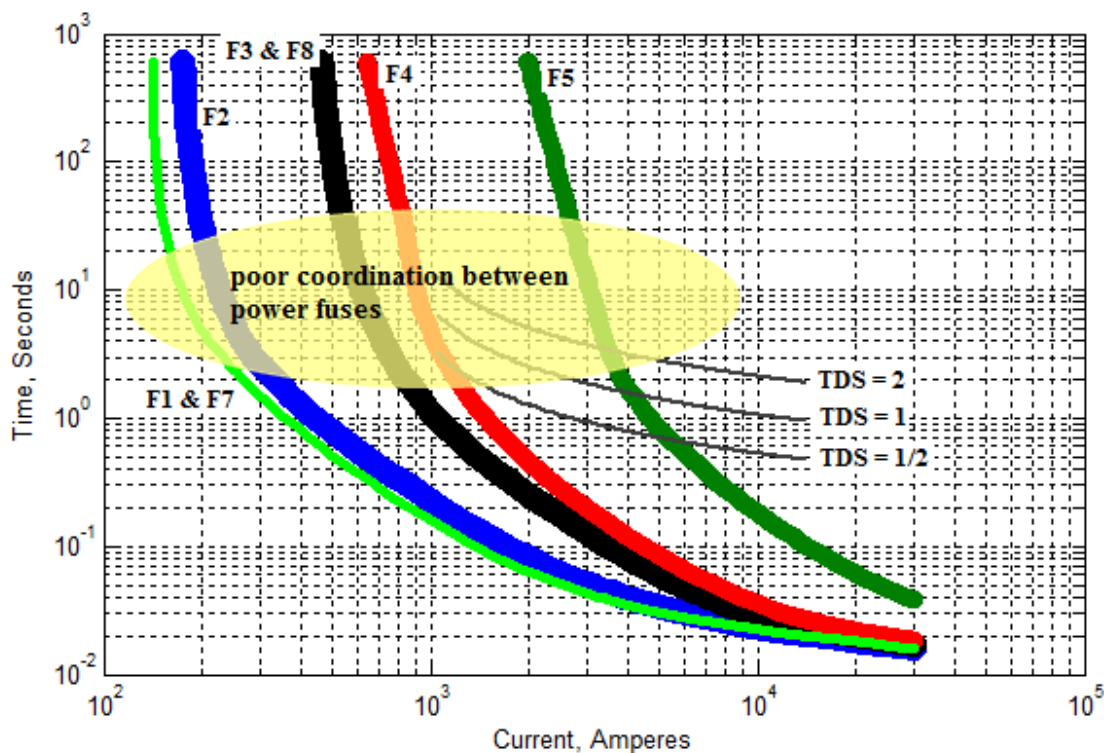


**Figure 3. 22:** TCC Coordination for S&C SMU-40 fuses and ABB/Westinghouse CO-7 Moderately Inverse Overcurrent Relay

The power fuses are very good at clearing high-current faults (good coordination characteristic), but they have a much harder time with low-current faults or overloads, and it is shown in Figure 3.22 as a poor coordination area. The overcurrent relay at N\_650 must provide backup to these fuses for high-impedance faults, but without sacrifice the high-current fault

coordination between fuses. Hence, the selection of the *Time Dial Setting* (TDS) is according to the fuse protection scheme implemented (*Fuse Blowing* or *Fuse Saving*). The coordination between downstream fuses and the overcurrent relay was done taking into consideration fuse blowing.

Fuse saving is a protection scheme where a circuit breaker or recloser is used to operate before a lateral fuse. Fuse saving is usually implemented with an instantaneous relay (50) on a breaker or recloser. The main disadvantage of fuse saving is that all customers on the circuit see a momentary interruption for lateral faults. Because of this, many utilities are switching to a fuse blowing scheme. Table 3.22 summarizes the rating of each fuse, while Table 3.23 shows the maximum rating capabilities. From Figure 3.21 the EMT transient simulation shows that the maximum peak-current at RG\_60 is less than 20 kA, which is under the device maximum (SMU-40) for a 60 Hz system, see Table 3.23.

**Table 3. 22:** Device Rating for F1 to F8, E Rated [70]

S&C Power Fuses – Type SMU-40 (4.8 kV) – Standard Speed Ambient Temperature 30°								
	<b>F1</b>	<b>F2</b>	<b>F3</b>	<b>F4</b>	<b>F5</b>	<b>F6</b>	<b>F7</b>	<b>F8</b>
<b>Amp. Rating</b>	65E	80E	175E	250E	2-400E	80E	65E	175E
<b>Pre-Load (A)</b>	63	71	71	203	481	80	65	143

**Table 3. 23:** Maximum Rating Capabilities for SMC-40 Fuse [70]

<b>Fuse Type</b>	<b>kV</b>		<b>Amperes, RMS, Symmetrical</b>			
	<b>Nominal</b>	<b>Maximum</b>	<b>BIL</b>	<b>Maximum</b>	<b>Interrupting</b>	
					<b>60 Hz</b>	<b>50 Hz</b>
<b>SMD-40</b>	4.8	5.5	95	400E	25000	20000

### 3.9 PWM Converter Model

Distributed Energy Resource (DER) units, in terms of their interface with a power system, are divided into two groups. The first group includes conventional or rotary units that are interfaced to the grid through rotating machines. The second group consists of electronically coupled units that utilize power electronic converters to provide the coupling media with the host system. The control concepts, strategies, and characteristics of power electronic converters are significantly different than those of the conventional rotating machines. The input power to the interface converter from the source side can be ac at fixed or variable frequency or DC. Only DC sources are considered in this work, e.g. photovoltaic panels, fuel cells, battery storage.

DC-to-AC converters are known as *inverters*. The function of an inverter is to change a dc input voltage to a symmetrical AC output voltage of desired magnitude and frequency. A variable output voltage can be obtained by varying the input DC voltage and maintaining the gain of the inverter constant. On the other hand, if the DC input voltage is fixed and it is not controllable, a variable output voltage can be obtained by varying the gain of the inverter, which is normally accomplished by pulse-width-modulation (PWM) control within the inverter. The output voltage waveforms of ideal inverters should be sinusoidal. However, the waveforms of practical inverters are nonsinusoidal and contain certain harmonics. With the availability of high-speed power semiconductor devices, the harmonic contents of output voltage can be minimized or reduced significantly by switching techniques [71].

Inverters can be classified into A) Single-phase inverters and B) Three-phase inverters. Each type can use controlled turn-on and turn-off devices, such as BJTs, IGBTs, power MOSFETs. A feedback diode is always connected across the device to have free reverse current flow. An inverter is called a Voltage Source Inverter (VSI) if the input voltage remains constant and Current Source Inverter (CSI) if the input current is maintained constant. One important characteristic of a VSI is that the AC fabricated voltage wave is not affected by the load parameters [72]. The PWM converter model of DIgSILENT represents a self-commutated VSI, and supports sinusoidal and rectangular modulation. In the sinusoidal PWM (SPWM) technique the width of each pulse is varied in proportion to the amplitude of a sine wave evaluated at the center of the same pulse, see Figure 3.23.

The frequency of reference signal (sinusoidal signal),  $f_r$ , determines the inverter output frequency,  $f_o$ , and its peak amplitude,  $A_r$ , controls the *Modulation Index* ( $Pm$ ). If  $A_c$  is the amplitude of the carrier signal, then  $Pm$  is defined as the ratio of  $A_r$  to  $A_c$ .

$$Pm = \frac{A_r}{A_c} \quad (29)$$

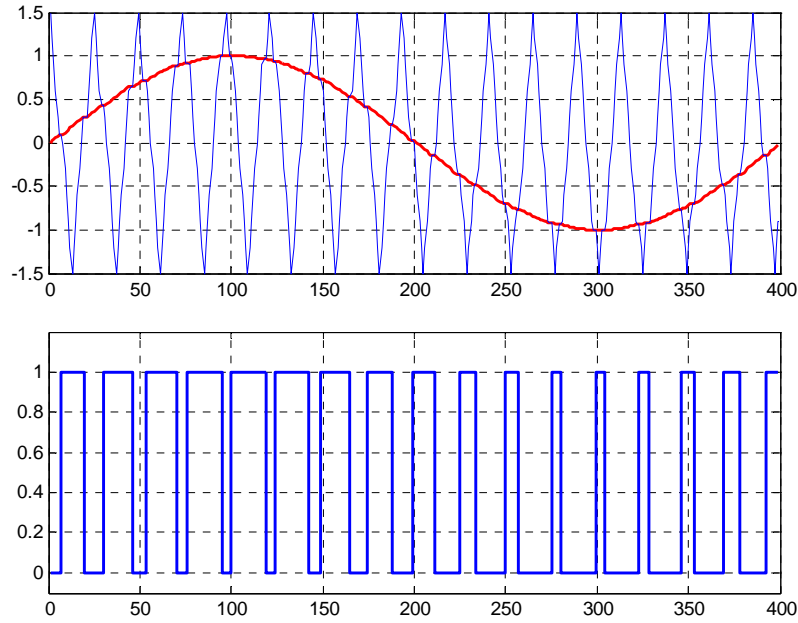


**Figure 3. 23:** Sinusoidal pulse-width modulation

The  $Pm$  value of the example in Figure 3.23 is approximately 0.67. For values of  $|Pm| < 1$ , the following equations can be applied:

$$\begin{aligned} U_{ACr} &= K_0 Pm_r U_{DC} \\ U_{ACi} &= K_0 Pm_i U_{DC} \end{aligned} \quad (30)$$

The fundamental frequency equations are completed by the active-power conservation between AC and DC side:

$$P_{AC} = \text{Re}(\bar{U}_{AC} \bar{I}_{AC}^*) = U_{DC} I_{DC} = P_{DC} \quad (31)$$

Equation 3.31 assumes an ideal, loss-less PWM converter. The variables in (3.30) are defined as follows:

$U_{ACr}$ : Real part of AC-voltage (RMS-value)

$U_{ACi}$ : Imaginary part of AC-voltage (RMS-value)

$K_0$ : Constant depending on the modulation method

$Pmr$ : Real part of the modulation index

$P_{mi}$ : Imaginary part of the modulation index

$U_{DC}$ : DC-voltage

For a SPWM power electronic converter, the  $K_0$  factor is:

$$K_0 = \frac{\sqrt{3}}{2\sqrt{2}}$$

If the coupling converter is a VSI, a current-controlled strategy can be used to determine the reference voltage waveforms for the PWM of the VSI. The reference signals are also synchronized to the power system frequency by tracking the Point of Common Coupling (PCC) voltage waveform. The control strategy can be implemented in a synchronous “ $dq0$ ” frame that specifies the direct ( $d$ -axis) and quadrature ( $q$ -axis) components of the converter output currents corresponding to the real and reactive output power components. Figure 3.24 shows a representation of a “ $dq0$ ” current controller. For the aim of this work the DG is designed to operate as a constant power source by setting the controller’s active and reactive reference values to fixed values. The reactive power reference value is set to zero, thus simulating a unity power factor DG operation [73].

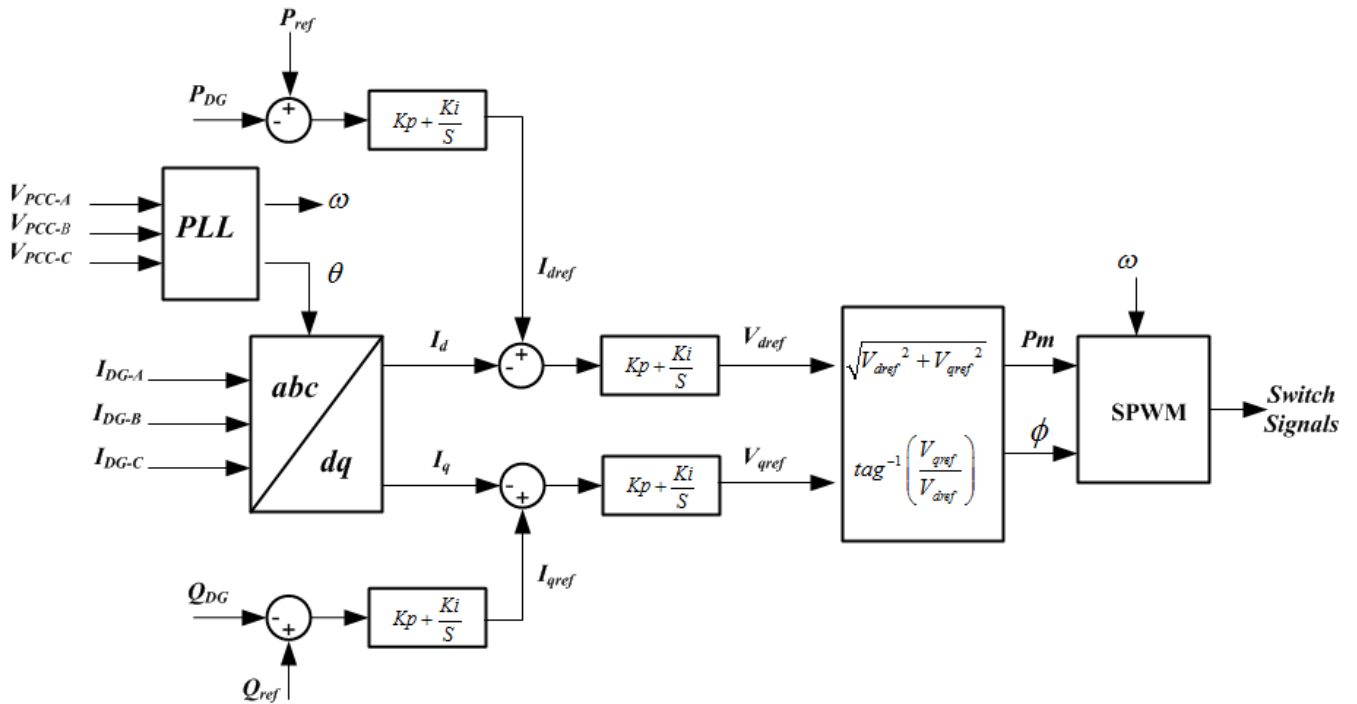


**Figure 3. 24:** DG Interface Control operated as a constant power source with unity power factor operation [77].

## CHAPTER 4

# DISTRIBUTED GENERATION UNDER UNBALANCED CONDITIONS

### 4.1 Introduction

The main purpose of this section is to evaluate the impact of single-phase and three-phase DG units over the voltage regulation of unbalanced power systems, taking into consideration the host system loading and power losses. In order to establish the problem under study photovoltaic (PV) generation was selected as the energy source.

Global PV production has been doubling every two years, increasing by an average of 48% each year since 2002, making it the world's fastest growing energy technology. According to [74] the annual percentage gains for 2008 were even more dramatic. Grid-tied solar PV grew by 70 percent in existing capacity to 13 GW. Growing grid-tied solar PV markets emerged in several countries in 2007-2008. Including off-grid applications, total PV existing worldwide in 2008 increased to more than 16 GW. The combination of rapid growth, falling costs, and vast technical potential could make solar energy a serious contender for meeting the future energy needs in the coming decades.

Electrical distribution systems are designed and operated based on the assumption of centralized generation and that power always flows from the distribution substation to end-use customers. With the increasing penetration of residential and commercial PV at the point of end use, PV power generation would not only offset the load, but also could cause reverse power flow through the distribution system. Among the distribution integration issues, voltage regulation issues stand out because they directly correlate to the amount of reverse power flow. Existing interconnection requirements in [11] prohibit inverters from controlling voltage, hence the DG units here considered operate at unity power factor, i.e. the  $Q_{ref}$  value is set to zero. Figure 4.1 shows the single-phase and three-phase PV integration to a three-phase distribution feeder. Although the single-phase integration is presented as individual home projects, it can be office buildings, parking lot structures, or three-phase multi-megawatt arrays supplying power directly to the grid or at substations.

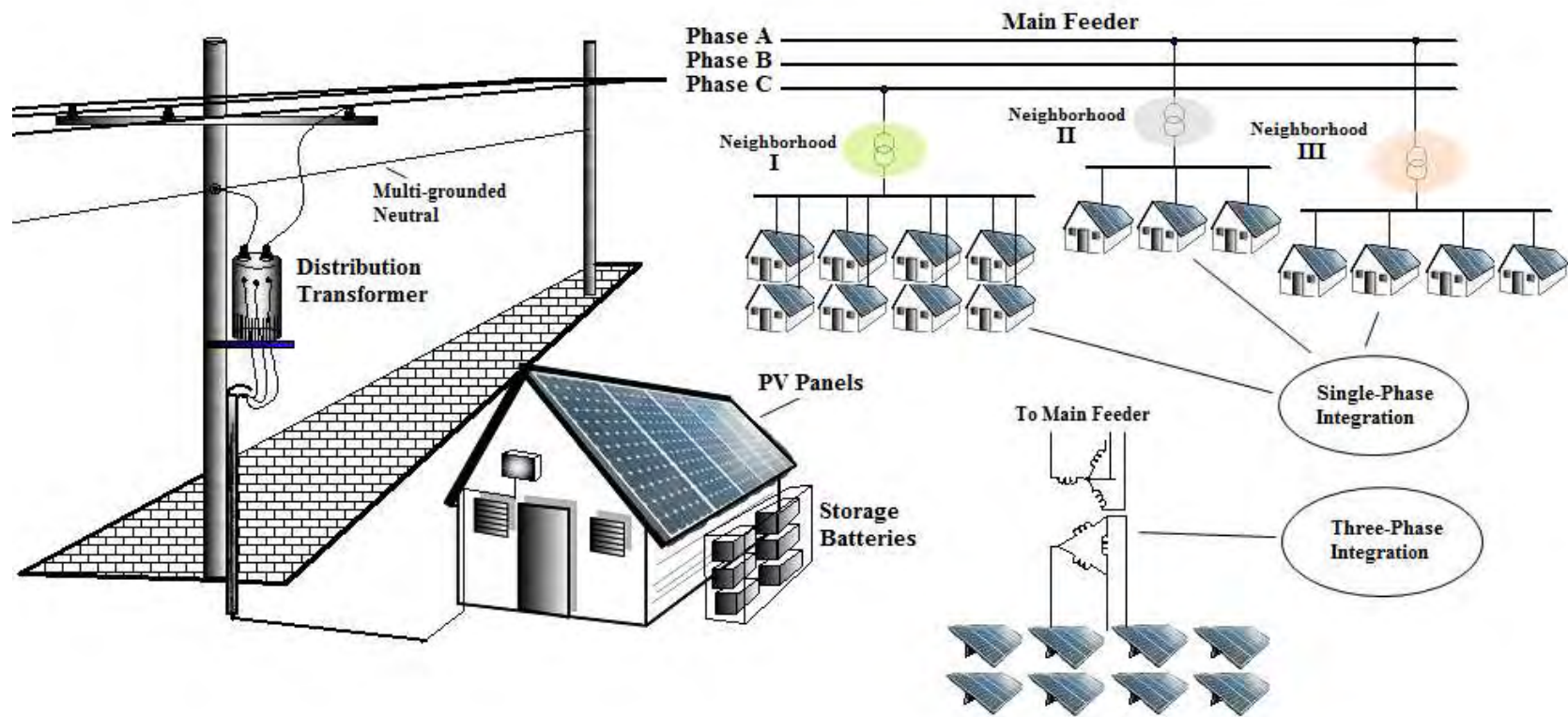


**Figure 4. 1:** Single-phase and Three-Phase DG integration considering individual home projects and multi-megawatt three-phase PV arrays. Adapted from [75].

NOTE: Neighborhood I and III illustrates the single-phase active power injection on phase-A for different locations, while neighborhood I the active power injection on phase-C. Depending on the penetration level, location and type of integration (single-phase or three-phase), photovoltaic DG units will impact the voltage profile of the main feeder in different ways.

In terms of power control, a DG unit is either a dispatchable or a nondispatchable unit. The DG units that use renewable energy sources are often nondispatchable units. To maximize output power of a renewable DG unit, normally a control strategy based on the Maximum Power Point Tracking (MPPT) is used to deliver the maximum power under all viable conditions. Figure 4.2 shows a hybrid electronically coupled DER unit for which the converter system is composed of two parallel DC-DC converters and one DC-AC converter (inverter). Although the PV array provides nondispatchable power, the converter system can be controlled to provide a dispatchable power at the output of the unit.

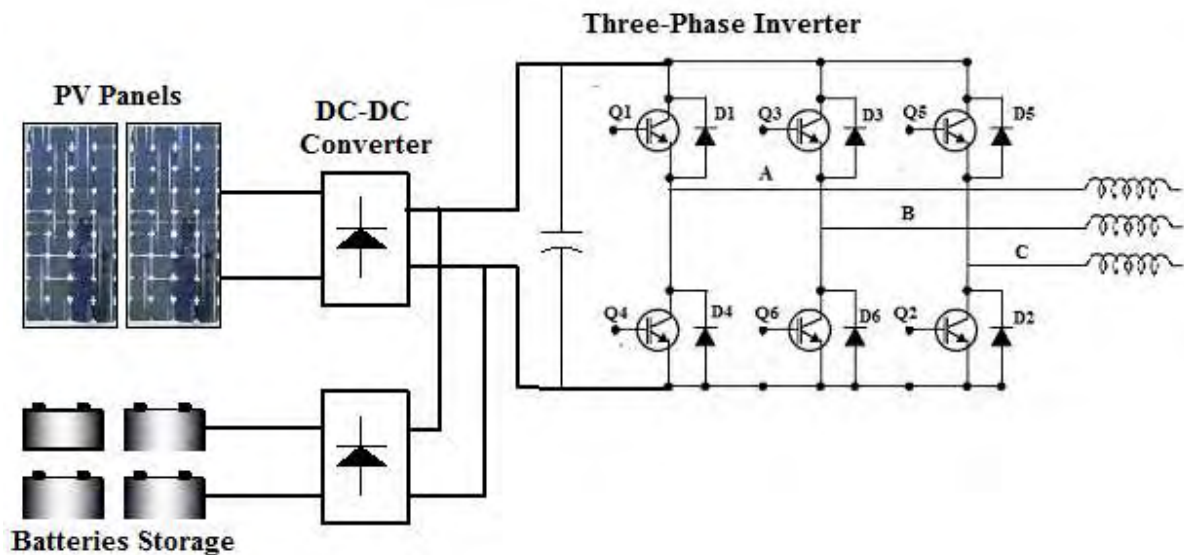


**Figure 4. 2:** Electronically coupled DER unit: Dispatchable DG plus batteries storage

Balanced three-phase power flow programs are used to calculate the voltage profile on the distribution circuit to determine whether the DG units are exceeding voltage limits. When that occurs, there is concern about the accuracy of the resulting service voltages at individual single-phase loads on single-phase laterals, because only the three-phase portion of the circuit is modeled. *The American National Standards Institute (ANSI) Std. C84.1* voltage ranges can be satisfied based on a three-phase balanced load/impedance analysis, but the limits for single-phase loads can be exceeded. Following the *ANSI Std. C84.1* the *IEEE Std. 1547* establishes that the DG shall not cause the Area EPS service voltage at other Local EPS to go outside the requirements of Range A, i.e. the voltage must lie between 126-V and 114-V on a 120-V base.

The voltage regulation of the distribution system is a key operating objective. As the loads on the feeders vary, there must be some means of regulating the voltage so that every customer voltage remains within an acceptable level. Common methods for regulating the voltage are the application of *step type voltage regulators*, *load tap changing transformers (LTC)*, and *shunt capacitors*. The aim of this work is to study the impact of single-phase and three-phase DG integration on the voltage regulation of unbalanced power systems. To realize the proposed analysis the following assumptions are made:

- The DER is a dispatchable unit
- The DER is operated at unity power factor, i.e.  $Q_{ref}$  is set to zero.
- The magnitude of the active power injected by each DG is expressed in terms of the main substation capacity (5 MVA). The percent of power injected has been selected as 5%, 10%, 15% and 20%, which corresponds to 0.25 MW, 0.5 MW, 0.75 MW and 1.0 MW respectively.
- The impact of each DG type will be evaluated on every phase of the main feeder.

The DigSILENT power flow program is capable of modeling both the shunt capacitors and the step voltage regulators. The modeling of the step voltage regulators can be complex. It is critical that the program is able to model the compensator circuit since this provides the control that determines when a tap change is necessary. The compensator model will include the desired voltage held within a specified bandwidth at the “Regulation Point” and the R and X settings [51].

## 4.2 Impact of SVR and Shunt Capacitors on Voltage Regulation

The impact of SVR and shunt capacitors on the voltage regulation of the original IEEE 13 Node test feeder is evaluated. The IEEE 13 Node Test Feeder was originally developed to test the convergence capabilities of different software programs. The feeder is highly unbalanced and is a good test for convergence [76]. For the simulations, the next sequence of steps was developed:

- Case I: It is considered the original system without SVR or shunt capacitors.
- Case II: Integration of the main substation SVR. The SVR consists of three single-phase SVR connected in Wye.
- Case III: Integration of shunt capacitors (original feeder). The original feeder shunt capacitors are located at node N\_675 (Three-phase, balanced 600-kVAr) and node N\_611 (single-phase, phase-C 100-kVAr). The location of each element on the IEEE 13 Node Test Feeder is shown in Figure 4.3.

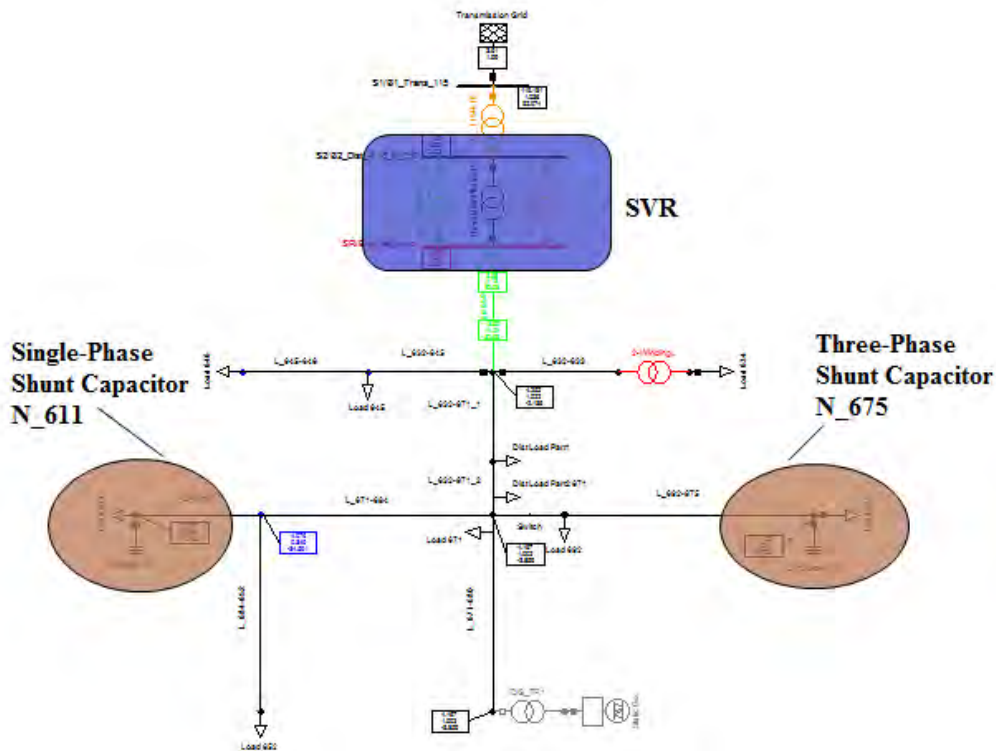


**Figure 4. 3:** SVR and Shunt Capacitors Location on the IEEE 13 Node Test Feeder

The results for the simulations are summarized in Figure 4.5. For a better understanding, consider Figure 4.5 as a matrix of order  $(i, j)$ , where  $i$  represents the rows and  $j$  the columns, then Figure 4.5 (1, 2) represents the voltage profile of phase B for each of the steps mentioned above. From Figure 4.5 (1, 1), which represents the voltage profile of phase A, considering the Case I (No SVR, No Shunt Capacitors), the voltage along the main feeder decays from the regulator node (RG\_60) to the node N\_671, and remains constant up to node N\_680 (Line 671-680 does not have load). The voltage drop through the line segment between the node N\_650 (main substation) and RG\_60 is due to the main transformer and SVR impedances, thus, it seems that there is not voltage drop. This is an expected behavior for the voltage drop of the main feeder in Case I. For Cases II and III (Only SVR, and the addition of shunt capacitors) the SVR raises the voltage magnitude at node RG and from that point decreases to the last node. Without shunt capacitors the current magnitude seen by the regulator is higher because there is not reactive power compensation. Hence, the voltage at the regulator point will be higher, i.e. the regulator increases the tap position in order to maintain the voltage at the regulation point.

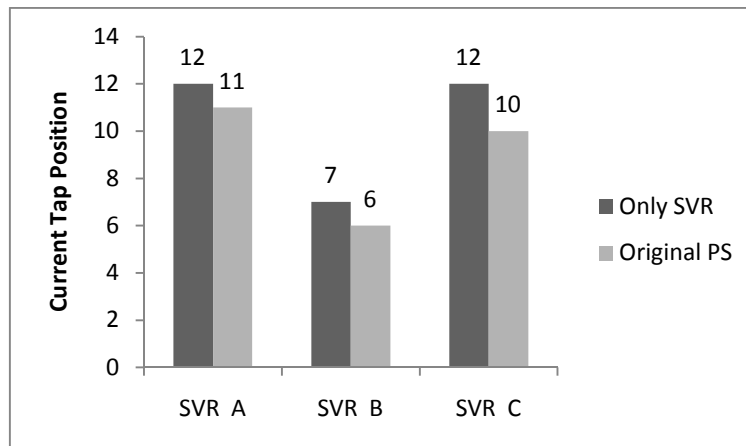


**Figure 4. 4:** Current Tap Position of the SVRs for Cases II and III

Figure 4.4 shows the current tap positions per phase for Cases II and III. For the original power system (addition of shunt capacitors) the tap decreases one position for phases A and B, while decreases two positions for phase C because of the integration of a single-phase shunt capacitor at node N\_611 (phase C). The tap position is directly related to the loading of each phase, which is sensed by the current transformers.

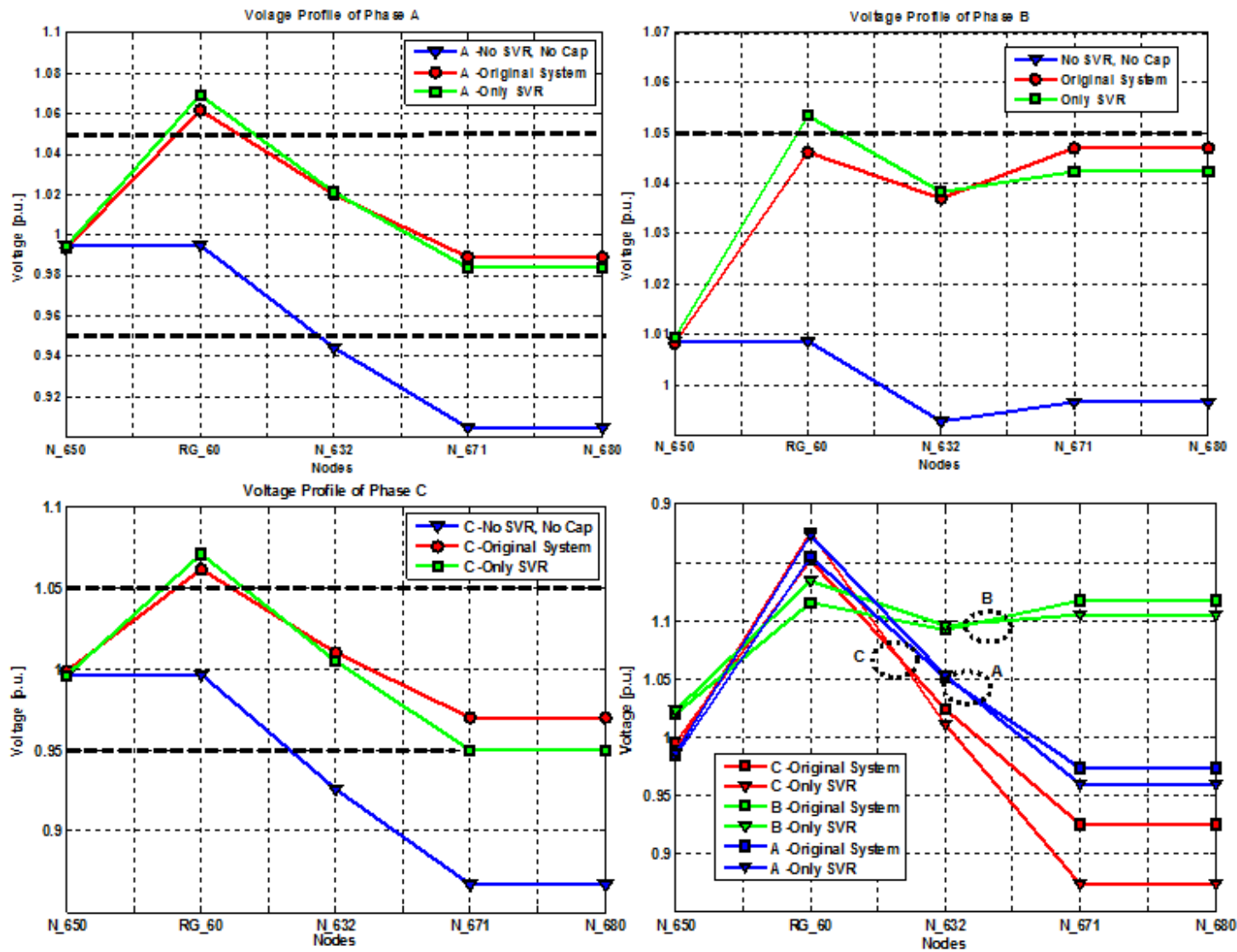


**Figure 4. 5:** Voltage profile of the Main Feeder per phase. (1, 1) phase A; (1, 2) phase B; (2, 1) phase C; and (2, 2) phases A-B-C for Cases II-III

The dotted lines represent the service voltage limits established by the *ANSI standard C84.1*. Phases A and C violate the Range A voltage limits in the Case I from node N\_632 up to Node N\_680, while phase B remains into the specified limits and shows an increase in voltage magnitude from node N\_632. Because of the unbalanced loading and resulting unbalanced line currents, the mutual coupling of the lines become very important. To explain the importance of the system unbalances over this problem consider Figure 4.6, where a four-wire grounded wye three-phase line (main feeder) is shown. The general voltage equations in matrix form for this line are determined by applying KVL and results in Equation 4.1. Implementing Kron reduction technique, the primitive impedance matrix can be reduced to a 3x3 phase matrix, see Equation 3.16. Writing a KVL around the loop formed by line B and the neutral conductor gives the relation between the unbalanced currents and the additional unbalance introduced by the unequal impedances, and solving for  $V'_{bn}$  can be obtained Equation 4.2.

$$\begin{bmatrix} V_{ag} \\ V_{bg} \\ V_{cg} \\ V_{ng} \end{bmatrix} = \begin{bmatrix} V'_{ag} \\ V'_{bg} \\ V'_{cg} \\ V'_{ng} \end{bmatrix} + \begin{bmatrix} Z_{aa} & Z_{ab} & Z_{ac} & Z_{an} \\ Z_{ba} & Z_{bb} & Z_{bc} & Z_{bn} \\ Z_{ca} & Z_{cb} & Z_{cc} & Z_{cn} \\ Z_{na} & Z_{nb} & Z_{nc} & Z_{nn} \end{bmatrix} \begin{bmatrix} I_a \\ I_b \\ I_c \\ I_n \end{bmatrix} \quad (4.1)$$

$$\begin{aligned} V'_{bn} = & V_{bn} - Z_{bb}I_b - Z_{ba}I_a - Z_{bc}I_c - Z_{bn}I_n \\ & + Z_{nn}I_n + Z_{cn}I_c + Z_{bn}I_b + Z_{an}I_a \end{aligned} \quad (4.2)$$

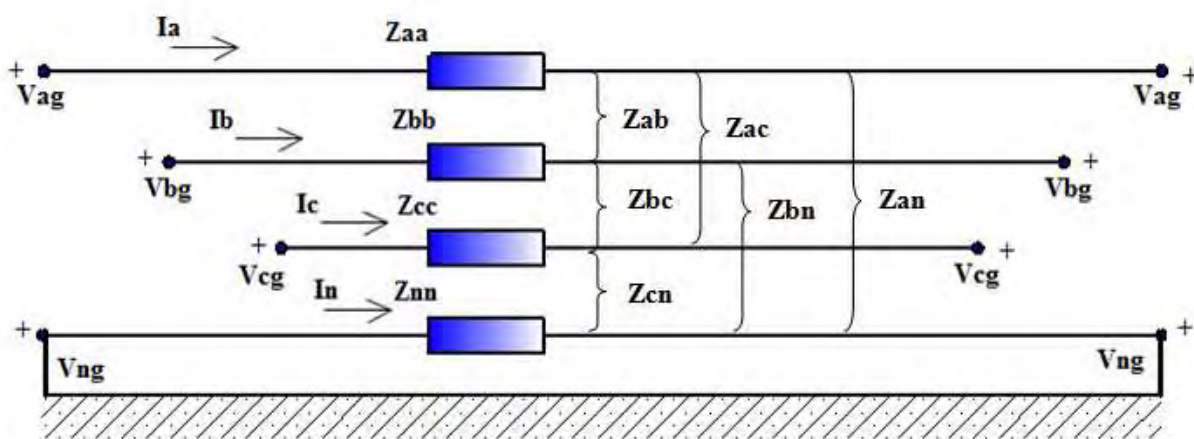


**Figure 4. 6:** Grounded Wye Three-phase Line

When the line currents  $I_a$ ,  $I_b$ , and  $I_c$  return together as  $I_n$  in the neutral conductor of Figure 4.6,  $I_n$  takes the form of Equation 4.3. After the substitution of Equation 4.3 in Equation 4.2, a brief inspection of the resulting equation leads to the possibility of  $V'_{bn} > V_{bn}$  for highly unbalanced conditions, taking into consideration that phase B is lightly loaded respect to phase A or C, see Figure 4.4.

$$I_n = -I_a - I_b - I_c \quad (4.3)$$

For Cases II and III shown in Figure 4.5 the phases A, B, and C seems to have the same crossing point (pivot point), which is the regulation point, but an inspection of Figure 4.5 (2, 2) shows that has different locations per phase. This is a result of using an average value of the equivalent impedance between the regulator and the regulation point, i.e. three single-phase SVR have the same R and X settings. However, the pivot point seems to be located between node N\_632 and node N\_671.

Another relevant issue is shown in Figure 4.7 with respect to the kilowatts losses per phase and the total losses of the system. Although the total losses of the system decreases for Cases II and III (introduction of SVR and shunt capacitors), the phase B presents an unexpected behavior (*negative active power losses*).

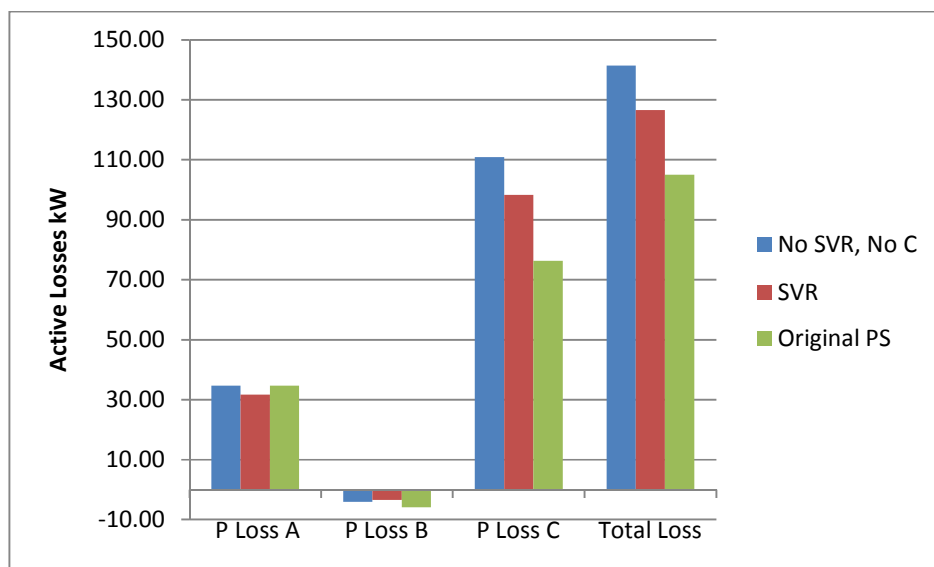


**Figure 4. 7:** Kilowatts losses per phase and Total losses for Cases II and III

W. H. Kersting in [77] specifies that the real power loss of a line segment that has been represented by the phase impedance matrix must be computed for each phase as the difference between the output power and input power, and it is not unusual to have one of the phase power losses to be negative in a line carrying unbalanced currents. Typically the lightly loaded phase will display a negative power loss. Although this appears to be a problem, the total three-phase loss is correctly computed as the sum of the three individual phase power losses even if one of them is negative. The main issue computing the power losses in this way is that the effect of neutral conductor and dirt power losses are included, but that process will give only the power loss in the phase conductors and will ignore the power loss in the neutral and dirt. Thus, in this procedure the value of total losses is correct, but the losses in each phase are incorrect. In Chapter 3 it was presented the equivalent impedance matrix determined by DIGSILENT, which corresponds to the phase impedance matrix  $Z_{ABC}$ .

$$[\hat{z}_{abc}] = \begin{bmatrix} \hat{z}_{aa} & \hat{z}_{ab} & \hat{z}_{ac} \\ \hat{z}_{ba} & \hat{z}_{bb} & \hat{z}_{bc} \\ \hat{z}_{ca} & \hat{z}_{cb} & \hat{z}_{cc} \end{bmatrix} \Omega / mile$$

In order to determine the power losses in the neutral and dirt, the neutral and dirt current must be computed, later the power losses in the individual phases can be computed. DIGSILENT applies the phase impedance matrix into the calculations, so that negative power losses per phase can be presented depending on the feeder unbalance.

### 4.3 Impact of DG Integration on the Original System

Balanced three-phase power flow programs are used to calculate the voltage profile on the distribution circuit to determine whether DG generators are exceeding voltage limits. When that occurs, there is concern as to the accuracy of the resulting service voltages at individual single-phase loads on single-phase laterals, because only the three-phase portion of the circuit is modeled. The ANSI Standard C84.1 voltage limits can be satisfied based on a three-phase balanced load/impedance analysis, but limits for single-phase loads can be exceeded. Therefore, it is critically important to evaluate the effects of DG on the distribution circuit voltage profile to ensure that customers do not receive service voltages (voltages at the customer's billing meter) outside Range A or Range B of the *ANSI C84.1* standard. To evaluate the impact of single-phase and three-phase DG units on voltage regulation consider Figure 4.8.

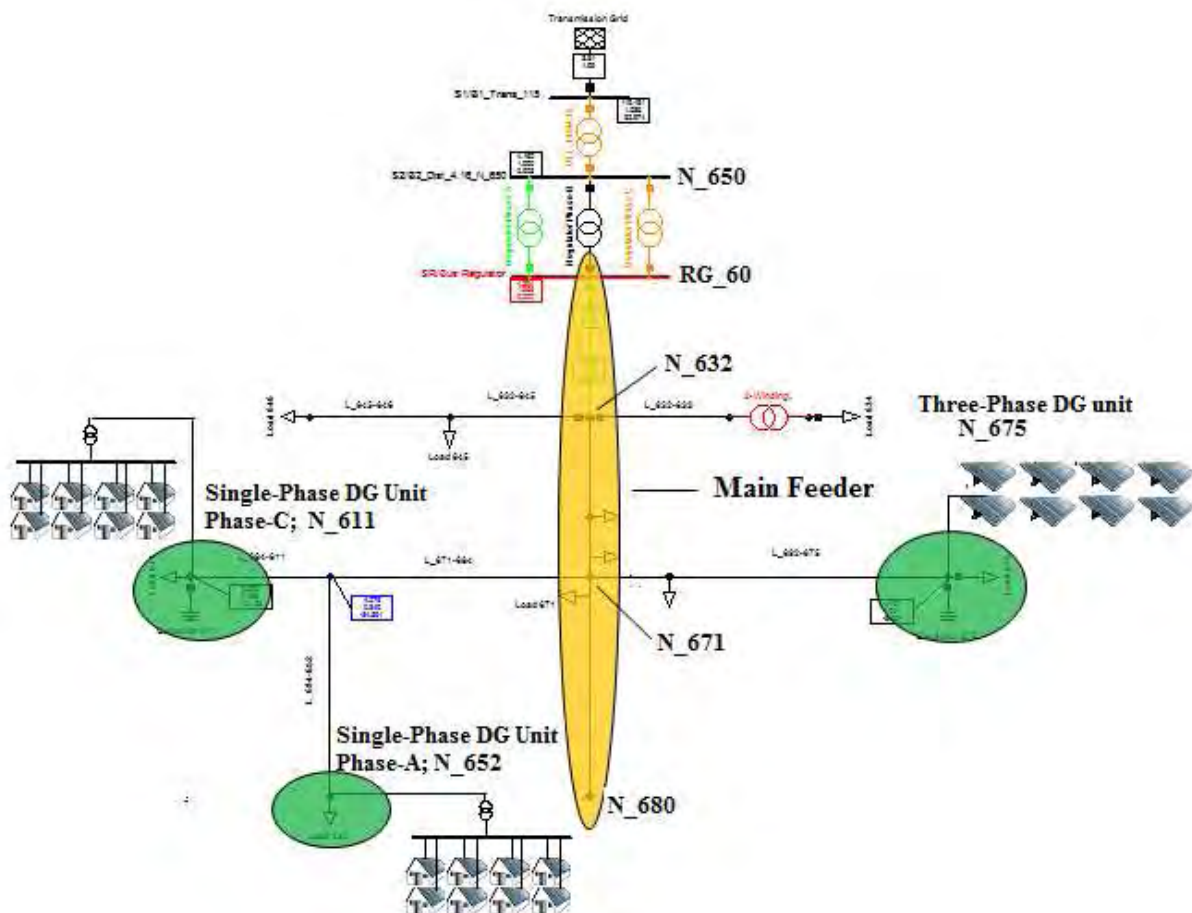


**Figure 4. 8:** Modification of the IEEE 13 Node Test Feeder to Evaluate the Impact of DG on Voltage Regulation

The original IEEE 13 Node Test Feeder has been modified as shown in Figure 4.8 to analyze the impact of single-phase and three-phase DGs on voltage regulation. The main feeder, i.e. Nodes N\_650, RG\_60, N\_632, N\_671, and N\_680, were selected to measure the impact on the voltage profile because it is the only path with the same line configuration. The three-phase DG is connected at Node N\_675, while single-phase DGs are connected at Nodes N\_611 (phase C) and N\_652 (phase A). It is assumed that all DGs are dispatchable at unity power factor, i.e. there will be only injection of active power to the distribution network. The level of power that each DG can inject to the grid is expressed in terms of the main substation capacity (5 MW). The percent of power injected has been selected as 5%, 10%, 15%, and 20%, which corresponds to 0.25 MW, 0.5 MW, 0.75 MW, and 1.0 MW respectively. Each operation condition will evaluate the impact for a full three-phase simulation on the main feeder, e.g. the penetration of 5% of active power on N\_611 (phase-C) will determine the variation in the voltage profile on phase-A, phase-B, and phase-C of the main feeder. The matrix below represents the different operation scenarios, which it is intended to be repeated for 0.25 MW, 0.50 MW, 0.75 MW, and 1.0 MW.

$$\begin{bmatrix} 1 & 0 & 0 \\ 0 & 1 & 0 \\ 0 & 0 & 1 \end{bmatrix} \begin{bmatrix} N611 \\ N652 \\ N675 \end{bmatrix} [V_A \quad V_B \quad V_C]$$

A brief review of the expression above establishes that for a particular level of penetration will be 9 cases to be evaluated, e.g. the integration of 0.5 MW on phase-A (N\_652) will result in three single cases (voltages on phase-A, B, and C), then for the complete operation scenario at four different penetration levels there will be 36 voltage profiles to be analyzed. A balanced three-phase analysis would only consider 12 voltage profiles. This will be done taking into consideration the total system losses and loading. The last one because the conductor loading is expressed as a percentage of the conductor rated current, so that is directly related to the tap position of the SVR at the main substation. The change of the line drop compensator settings it is out the scope of this work, hence, the regulation point remains the same.

In Figure 4.2 each node of the main feeder is identified on the x-axis. The voltage at RG\_60 (secondary side of the voltage regulator) is elevated to improve the voltage profile of the main feeder. The unbalance between phases makes the step voltage regulator to set different tap positions for each phase. The line drop compensator (control system of the regulator) is a scale representation of the line impedance between the regulator and the regulation point; hence, the more loaded phase will create a higher voltage representation on the control system of the step voltage regulator, and then demanding a higher tap. However, the increase or decrease of current in one phase affects the others in a different manner, which depends on the mutual impedance between phases. It can be observed that phase-B is lightly loaded because the voltage at the secondary side on phase-B is higher than the others, which is emphasized with the tap position.

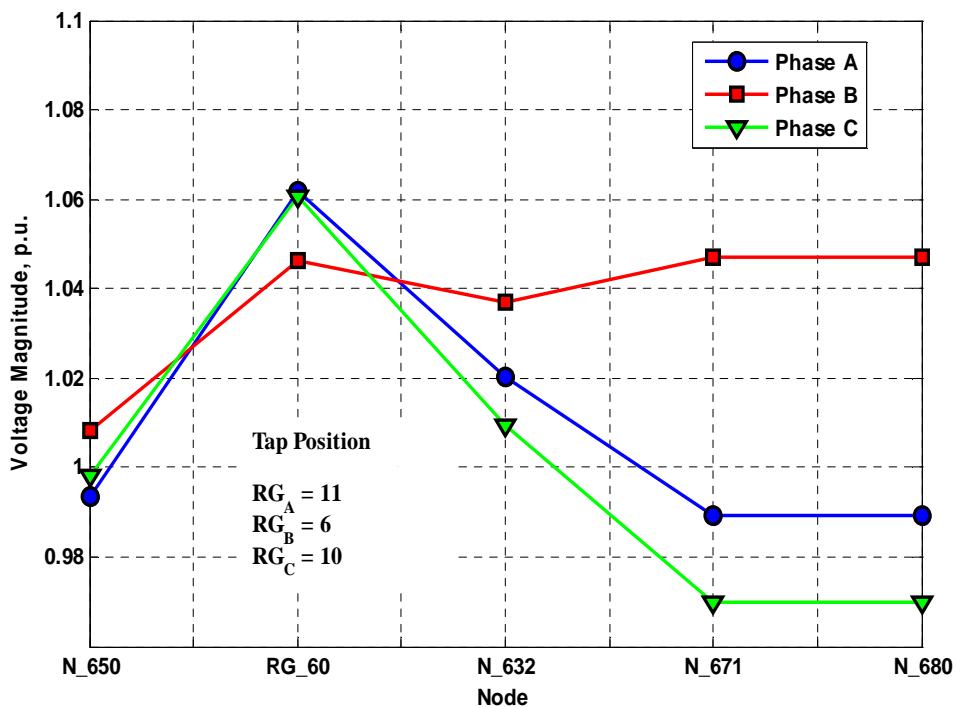


Figure 4. 9: Original Three-phase Voltage Profile of the Main Feeder

#### 4.4 Case Study I: DG Interconnection at Phase A (N\_652)

A single-phase DG unit is interconnected at node N\_652, as shown in Figure 4.8, to evaluate the impact of different penetration levels on the voltage profile of the main feeder, total system losses, and loading. The node N\_652 is located at a single-phase lateral, which has a distance of 1100 ft from the main feeder. The total load is concentrated in that node as specified by the IEEE 13 Node Test Feeder, and all the specified active power for the DG unit will be injected into that point. The results of the simulations are summarized in Figure 4.10.

From Figure 4.10 (1, 1) the voltage profile of the main feeder tends to improve with the injection of active power at node N\_652. The current injection in phase A helps the SVR located at the same phase on the main feeder, hence, the SVR decreases its current tap position to reduce the secondary voltage (node RG\_60) and keep the voltage magnitude constant at the regulation point (N\_632), which is a pivot for the voltage profile of phase A. However, the regulation point for phases B and C cannot be identified that easily for phase A because there is not active power injection into them, so that the SVR will not change its current tap position, as it seems that the phase current remains with the same magnitude. Phase B tends to reduce its voltage magnitude from N\_632 to N\_680, meaning that the DG interconnection at phase A improves the balance of the system. Phase C also presents a voltage profile improvement as the penetration level increases. The change in the voltage profile experimented by phases B and C it is due to the mutual coupling between the phases and a reduction of current flowing through phase A.

The SVR tap positions per phase is shown in Figure 4.10 (2, 2) for different penetration levels at N\_652 and compared with the original power system. The tap position of the SVR is directly related to the current flowing through that phase, hence, with the phase loading. The phase loading is the percentage of the conductor nominal current flowing through the corresponding phase. The phase A changes two and three tap positions depending on the penetration level, while phases B and C only make one tap change. The behavior of the voltage profile of phases B and C is better understood analyzing Figure 4.10 (2, 2), e.g. for the penetration levels of 0.50 MW, 0.75 MW, and 1 MW there is an increase of one tap at phase C, which tends to increase the voltage profile almost with the same slope of the original system because there is not active power compensation into that phase.

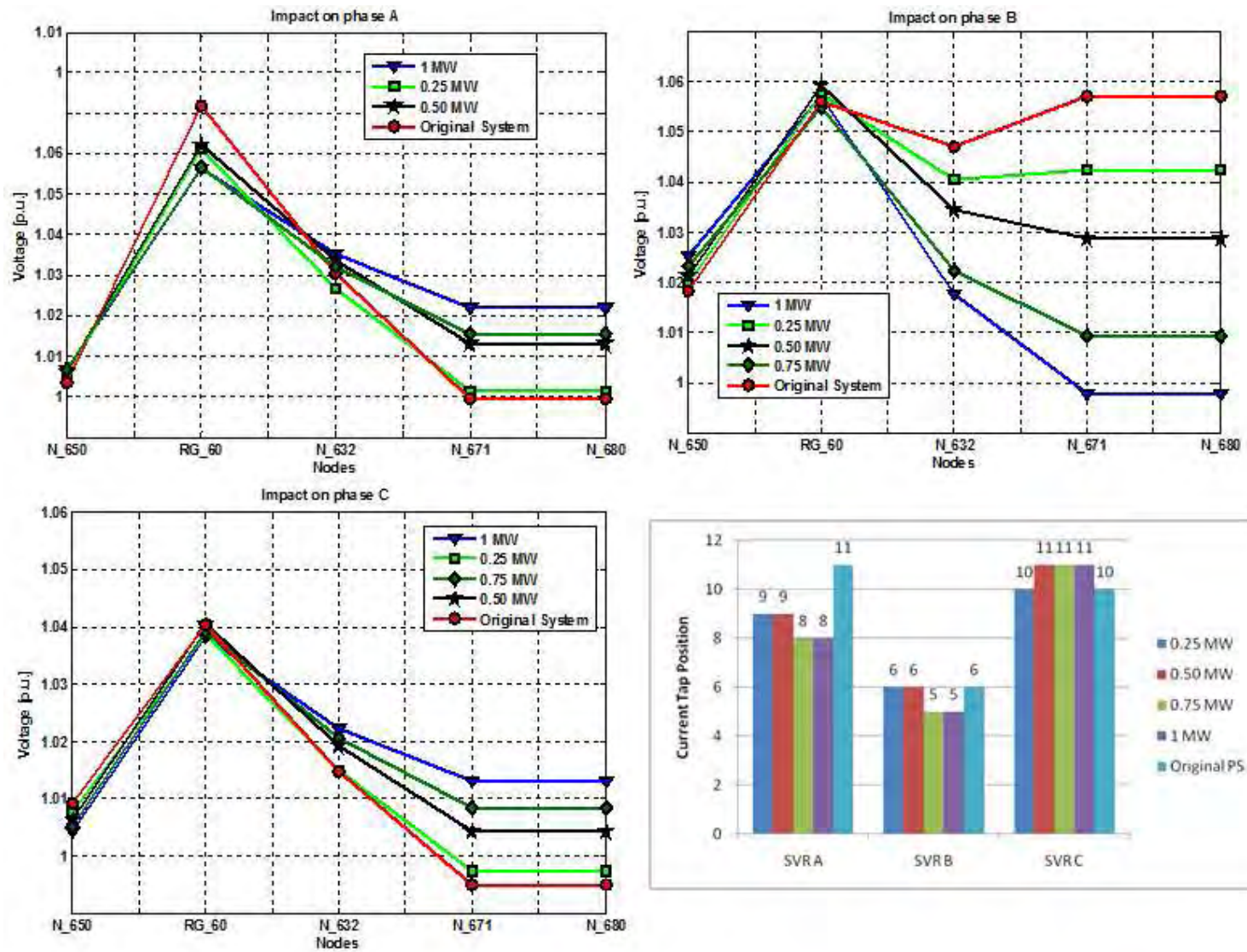
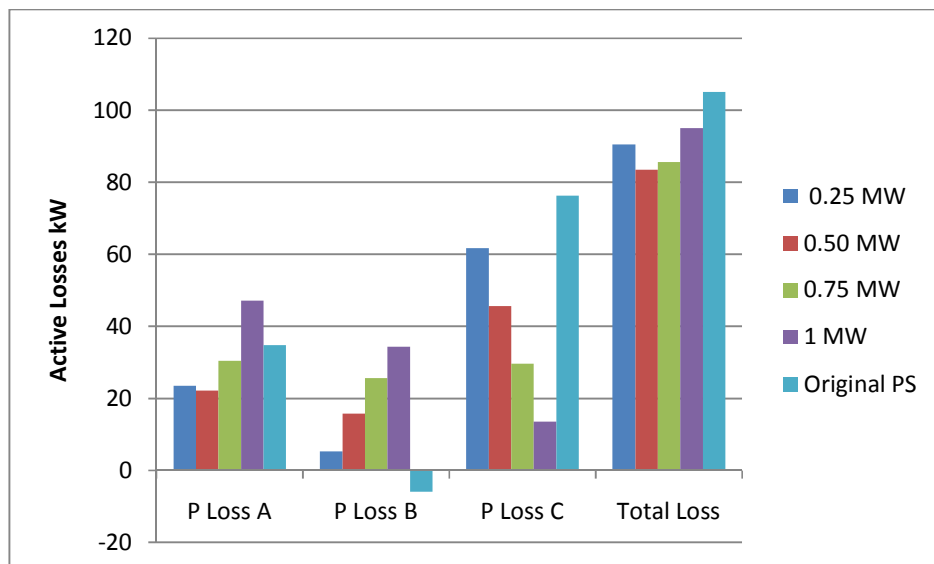


Figure 4.10: Voltage profile of the Main Feeder and SVR Tap Positions for DG Interconnection at Phase A

The total losses of the system in kilowatts are shown in Figure 4.11 for different active power injection at N\_652. In a previous section it was specified that a highly unbalanced power system could present negative power losses in a lightly loaded phase (phase B), also it was pointed out that the calculation of the active power losses per phase considering the phase impedance matrix gives incorrect values, but the calculation of the total three-phase power losses is correct. Therefore, a review of the per phase values obtained for active power losses can be used to determine whether the system is becoming more balanced or not. The active power loss at phase B makes a change from negative to positive with the integration of active power at N\_652, meaning that the system is turning into a balanced feeder. For a penetration level of 0.75 MW and higher the system losses tends to increase. Although this is true, it is not a valid indicator to define a limit of penetration for single-phase DG units.



**Figure 4. 11:** Active power losses of the system for DG interconnection at Phase A

#### 4.5 Case Study II: DG Interconnection at Phase C (N\_611)

The same assumptions made in section 4.4 will be applied to the interconnection of a single-phase DG at N\_611 (phase C). In Figure 4.13 (2, 1) the voltage profile of the main feeder tends to improve with the injection of active power at node N\_611. The current injection in phase C helps the SVR located at the same phase on the main feeder, hence, the SVR decreases its current tap position to reduce the secondary voltage (node RG\_60) and keeps the voltage magnitude constant at the regulation point (N\_632), which is a pivot for the voltage profile of phase C. This was the same behavior for the voltage profile of phase A in section 4.4, taking into consideration corresponding DG interconnection. The phase B tends to increase its voltage magnitude from N\_632 to N\_680, meaning that the system balance becomes more unbalanced. The voltage profile of Phase A also becomes worse instead of improving. Observing Figure 4.12 helps to determine that an increase of the active power injected into phase C leads the system to a higher unbalance. The integration of the DG unit at phase C such as at phase A increase the system losses when the penetration level exceeds 0.50 MW. The voltage dependency of loads was also modeled together with the unbalanced currents and mutual coupling. All these variables make each distribution system a very particular system depending on its configuration, loading, and phasing. Thus, once again, an increase in system losses due to active power injections of 0.5 MW and higher it is not a valid indicator to define a limit of penetration.



Figure 4. 12: Active Power Losses of the System for DG Interconnection at Phase C

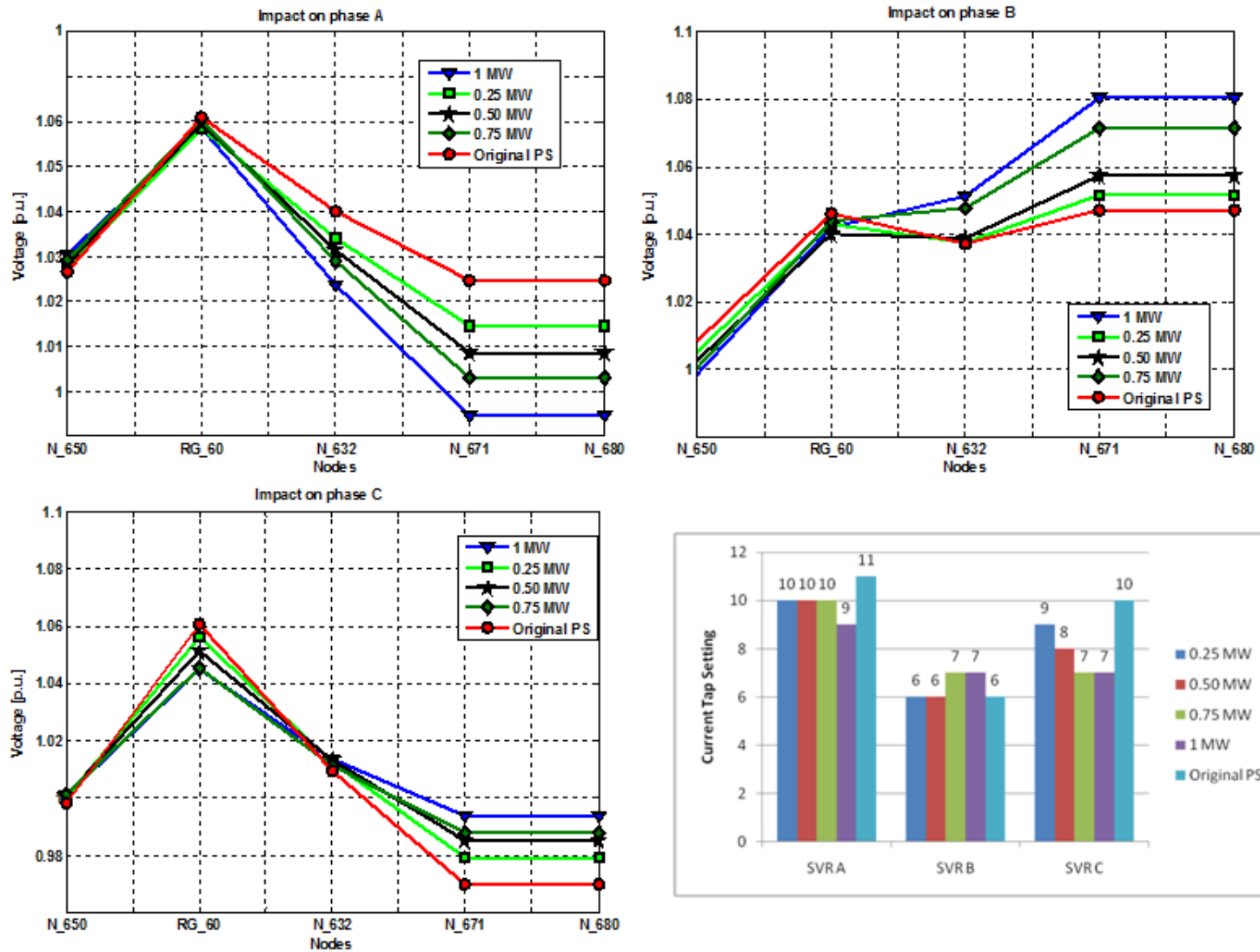


Figure 4.13: Voltage profile of the Main Feeder and SVR Tap Positions for DG Interconnection at Phase C

### 4.6 Case Study III: Three-Phase DG Interconnection

The interconnection of a three-phase DG unit was made at N\_675, which is illustrated in Figure 4.8. The results for the corresponding penetration levels are summarized in Figure 4.15. The complete system presents an improvement for the voltage profile of the main feeder. It is very important to point out that a balance three-phase interconnection injects a percentage per phase of the total active power injected when single-phase interconnection is considered. Another relevant observation is that the change in tap positions for different three-phase penetration levels is more uniform than the single-phase integration. For all the active power injections there was only one tap change. Therefore, the three-phase DG integration is a healthier interconnection than the single-phase one in terms of voltage regulation and total system losses for the particular conditions evaluated. This is determined from Figure 4.14, where the kilowatt losses at phase B tend to be more positive with an increase of three-phase active power injection. Even more important is the reduction of the total system losses by almost 50% with an integration of 1 MW (20% of the main substation capacity). Higher levels of load unbalance produce greater losses while the same demand is maintained at each unbalance scenario. This means that network reconfiguration considering load balancing must be taken into consideration in order to reduce the overall system losses.

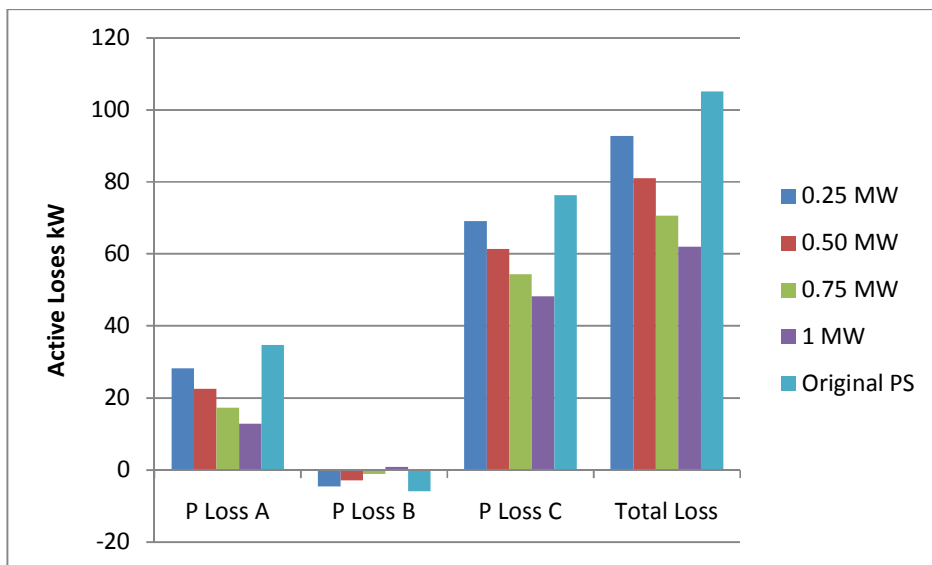


Figure 4. 14: Active Power Losses of the System for Three-phase DG Interconnection

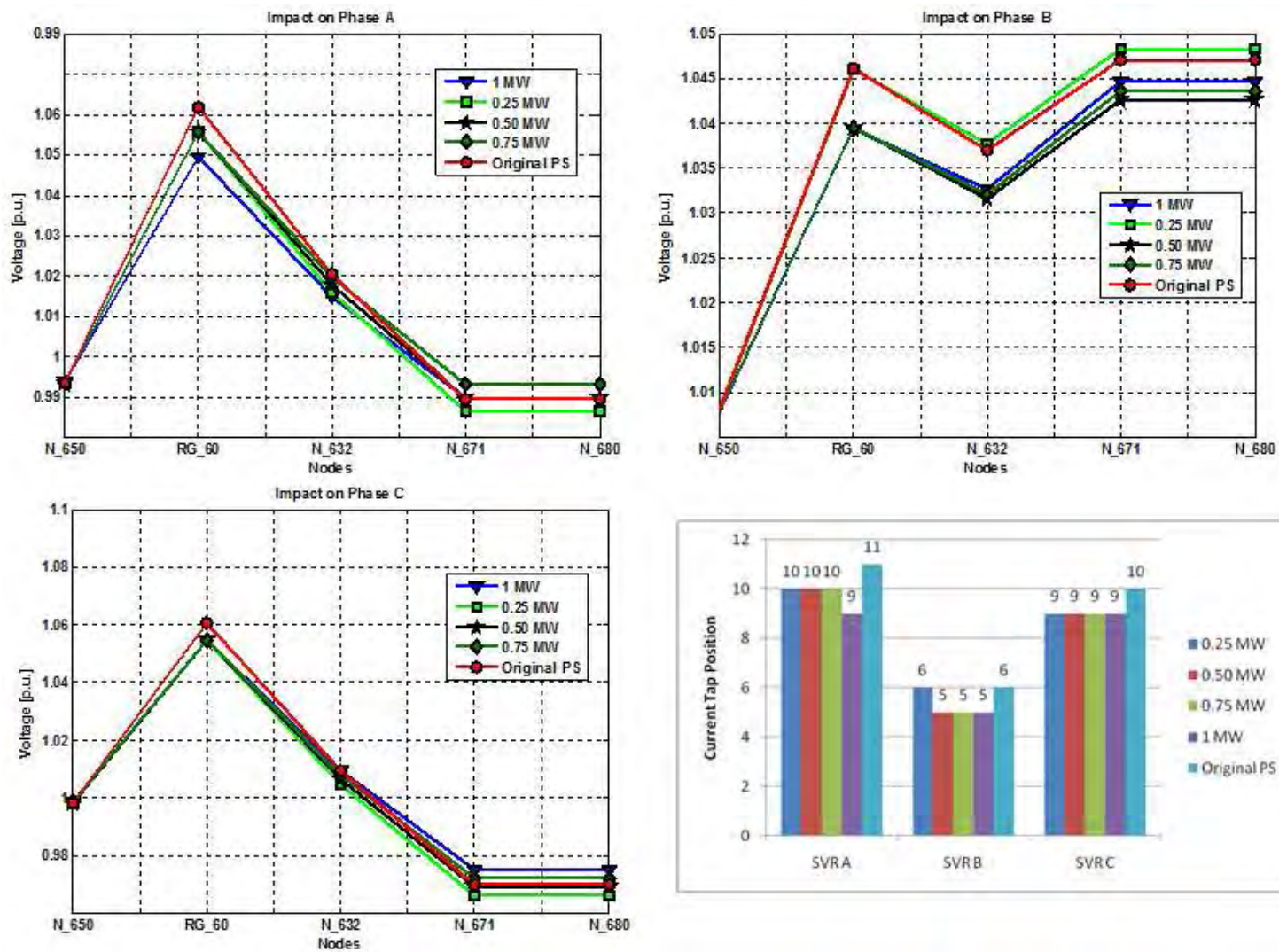
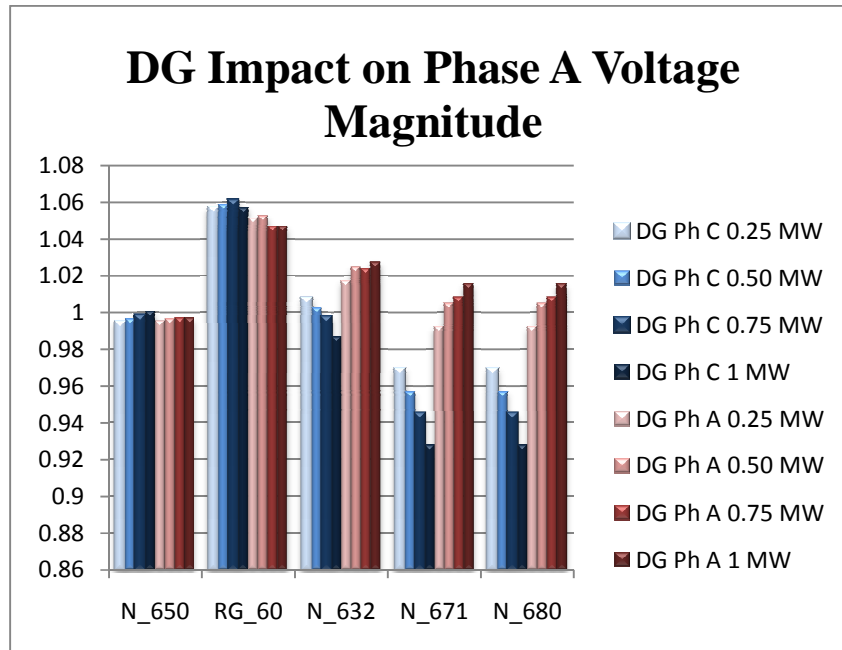
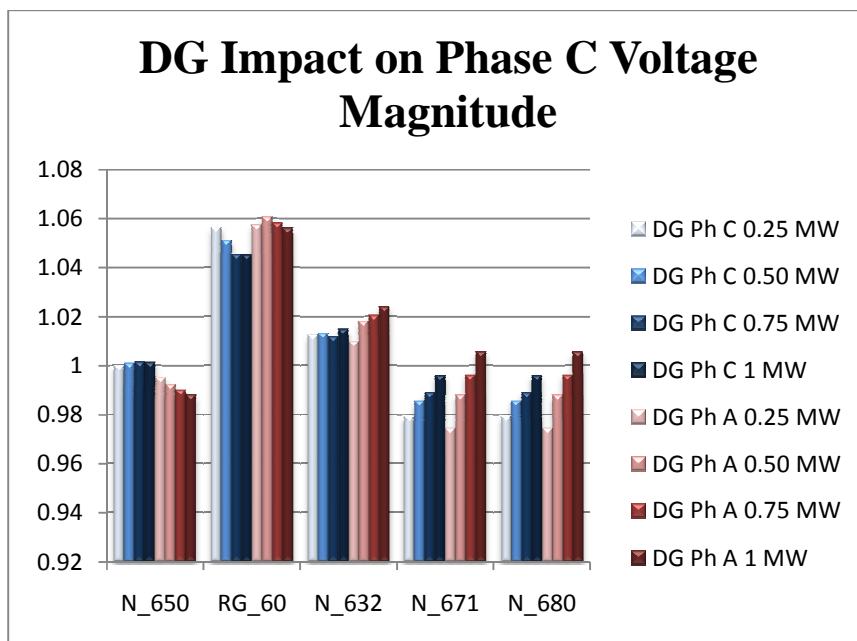


Figure 4. 15: Voltage profile of the Main Feeder and SVR Tap Positions for Three-Phase DG Interconnection

Figures 4.16 and 4.17 summarizes the impact of DG units on phase A and phase C, taking into consideration the voltage magnitude of the main feeder at different penetration levels.



**Figure 4. 16:** Summary of Single-phase DGs Impact on phase A



**Figure 4. 17:** Summary of Single-phase DGs Impact on phase C

The impact of single-phase and three-phase DGs is much related to the settings of the line drop compensator of the step voltage regulator. The voltage regulator tends to stabilize the voltage magnitude at the regulation point, which has been defined by the X and R setting of the line drop compensator. This setting remains constant while the integration of DG changes the impedance equivalent seen by the voltage regulator. The knowledge of the equivalent line impedance in ohms from the generator to the load center is the only parameter needed to determine the required value for the compensator settings. Usually, the load center is located down the primary main feeder after several laterals located upstream. Hence, the current measured by the CT of the regulator is not the current that flows all the way from the regulator to the load center. The only way to determine the equivalent line impedance value is to run a power-flow program of the feeder without the regulator operating. In order to make the per-unit voltage of the compensator voltage relay equal to the per-unit voltage at the regulation point, the per-unit  $R_{set}$  and  $X_{set}$  settings must equal the per-unit equivalent impedance from the regulator output to the regulation point. The line-to-neutral voltage ( $V_{LN}$ ) of the distribution feeder must be chosen as the base line voltage, and the primary rating ( $CT_P$ ) of the current transformer as the base line current.

The integration of single-phase DG reduces the tap position of the voltage regulator improving its flexibility under a major variety of voltage profiles on the feeder, but this effect can be positive or negative in relation to the other phases. Once again the impact depends on the line spacing and the phasing. Therefore, the analysis of the impact of DGs on the voltage regulation considering balanced distribution feeders can be acceptable for the integration of balanced three-phase DG units operating at unity power factor. However, for single-phase DG units a balanced power flow analysis must be neglected. Another critical issue is the impact of single-phase DG taking into consideration the absence of the voltage regulator. This effect can be observed on remotely radial feeders on rural areas.

## **CHAPTER 5**

### **CONCLUSIONS AND FUTURE WORK**

#### **5.1 Conclusions**

Some of the problems associated with interconnecting DG units to a distribution circuit are related to the design of the circuit and its operation; others are related to the analytical tools used to evaluate DG operation. Distribution circuits are designed primarily for radial, one-way flow of power. Distribution line voltage regulators typically are designed to regulate voltage based on a unidirectional flow of power. When DG generators are interconnected to the circuit, two-way flows can result. Most of the load served on a distribution circuit is single-phase. However, most of the analytical tools used to evaluate circuit performance are based on balanced three-phase loads and balanced three-phase line circuit impedances.

Unbalanced phenomena in distribution systems have been the focus of research in recent decades. This work developed a more accurate modeling of unbalanced power systems to determine the impact of DG technologies on voltage regulation. The analysis was conducted with a full three-phase (multi-phase) model because unbalances affect the whole behavior of the distribution system under high penetration of DG. The evaluation of this impact was carried out taking into consideration the total system losses, voltage profiles, and the loading of the distribution lines. A detailed mathematical formulation of line models and voltage dependency of loads was presented in order to achieve a better understanding of the distribution system characteristics. Also, a detailed description of the step voltage regulator control system was presented and related to the three-phase model of transformer banks. The IEEE 13 Node and 4 Node Test Feeders were selected to verify the validity of the proposed models. The complete simulation of the IEEE systems was carried out with the calculation program DIgSILENT. A full comparison between the results obtained with the developed models and the original IEEE systems do not exceed a 3% of difference, which indicates the accuracy of the employed methods to model the unbalanced power system.

The original IEEE 13 Node Test Feeder was modified to analyze the impact of single-phase and three-phase DGs on voltage regulation. The main feeder was selected to measure the impact on the voltage profile because it is the only path with the same line configuration. Each DG was assumed dispatchable at unity power factor, considering individual penetration levels of

5%, 10%, 15%, and 20% of the main substation capacity. For the same penetration level it was found that the impact of single-phase DG on the unbalanced voltage profile of the main feeder is more pronounced than the three-phase DG type. The impacts on the voltage profile from phase-C to phase-A is not the same from phase-A to phase-C regardless the penetration level or location of the DG. Thus, to analyze the real impact of single-phase DG interconnected to distribution system must be necessary to know the correct line spacing and phase location of a particular line segment.

The data provided in the IEEE 13 Node Test Feeder does not have short circuit calculation. An unbalanced short-circuit analysis of the original system was added to the unbalanced power flow simulations in order to show the modeling of overcurrent protective devices. The computation of short-circuit currents for unbalanced faults in a normally balanced three-phase system has traditionally been accomplished by the application of symmetrical components. However, this method is not well suited to a distribution feeder that is inherently unbalanced. The short-circuit calculations were developed considering the *Superposition Method*, which is in terms of system modeling an accurate method. Finally, the correct coordination between the overcurrent protection devices (power fuses and the main substation relay) considering the system unbalanced was presented.

The main contributions of this thesis work are:

- Evaluation of the impact of single-phase and Three-phase DGs on the voltage regulation of an unbalanced power system, taking into consideration the total losses and distribution line loading.
- The correct modeling of overhead and underground lines, three-phase and single phase transformers, voltage dependency of loads, and shunt capacitors.
- Wide description of a Step Type Voltage Regulator and its application in the analysis of distribution systems.

## **5.2 Future Work**

In this thesis a more accurate modeling of unbalanced power system was presented with an emphasis on voltage regulation. The accuracy of the developed model was verified with the benchmarks pointed out by the IEEE Distribution Systems Analysis Subcommittee. It is suggested that future works related to the interconnection of DG technologies be addressed with full three-phase simulations. Impact studies without a correct modeling of unbalanced conditions will lack validity for distribution system researchers. Taking into consideration the work developed in this thesis, the following are future research areas:

1. Impact studies of single-phase DGs on the voltage profile of remote distribution systems. Special attention must be given to the absence of the step voltage regulator.
2. Determine the impact of single-phase DGs on power system losses. Taking into consideration the loading of the feeder which the DG is connected.

## References

- [1] F. Gonzalez-Longatt. (2008, Jun.) Impacto de la Generacion Distribuida en el Comportamiento de los Sistemas de Potencia.
- [2] J. Casazza, "Forgotten Roots," in *Electric Power, 2007* , 2007, pp. 48-83.
- [3] W. H. Kersting, *Distribution System Modeling and Analysis*, L. Grigshy, Ed. CRC Press LLC, 2002.
- [4] W. H. Kersting. (2009, Jun.) <http://www.ieee.org/portal/site>. [Online]. <http://www.ewh.ieee.org/soc/pes/dsacom/testfeeders.html>
- [5] M. H. Brown and R. P. Sedano. (2004, Jun.) Electricity Transmission: A Primer. [Online]. <http://www.oe.energy.gov/DocumentsandMedia/primer.pdf>
- [6] G. J. Miranda, "BE PREPARED! Power industry Deregulation," *Industry Applications Magazine, IEEE*, vol. 9, no. 2, pp. 12-20, Mar. 2003.
- [7] CIRED, Working Group WG04, "Dispersed Generation, Preliminary Report of CIRED," 1999.
- [8] T. Ackermann, G. Anderson, and S. Lennart, "Distributed Generation: a definition," *Electric Power Systems Research*, vol. 57, no. 3, pp. 195-204, Apr. 2001.
- [9] International Energy Agency, *Distributed Generation in Liberalised Electricity Markets*. 2002.
- [10] F. Gonzalez-Longatt and C. Fortoul, "Review of Distributed Generation Concept: Attempt of Unification," in *Proceeding of international Conference on Renewable Energies and Power Quality (ICREPQ 05)*, España, 2005.
- [11] IEEE, "IEEE Standard for Interconnecting Distributed Resources with Electric power systems, IEEE 1547," 2003.
- [12] "Applications of Distributed Resources for Distribution Companies: Business Plans and Strategies," EPRI 1004468, 2003.
- [13] J. Driesen and R. Belmans, "Distributed generation: challenges and possible solutions," in *Power Engineering Society General Meeting, 2006. IEEE*, 2006, p. 8.
- [14] (2009, Sep.) U.S. Department of Energy. [Online]. <http://www.eia.doe.gov/cneaf/electricity/page/prim2/toc2.html#non>
- [15] K. Malmedal, B. Kroposki, and P. K. Sen, "Energy Policy Act of 2005," *Industry Applications Magazine, IEEE*, vol. 13, no. 1, pp. 14-20, Jan. 2007.
- [16] H. B. Puttgen, P. R. MacGregor, and F. C. Lambert, "Distributed Generation: Semantic Hype or the Dawn of a New Era?," *Power and Energy Magazine, IEEE*, vol. 1, no. 1, pp. 22-29, Jan. 2003.
- [17] Renewable Energy Policy Network for the 21st Century. (2007) Renewables 2007 -Global Status Report-. <http://www.ren21.net/publications/default.asp>.
- [18] S. Karki, M. D. Mann, and H. Salehfar, "Substitution and Price Effects of Carbon Tax on CO2 Emissions Reduction from Distributed Energy Resources," in *Power Systems Conference*, 2006, pp. 236-243.
- [19] U.S Department of Energy. (2009, Sep.) Energy Information Administration: Official

Energy Statistics from the U.S. Government. [Online].  
<http://www.eia.doe.gov/cneaf/electricity/epa/epat5p1.html>

- [20] M. T. Doyle, "Reviewing the impacts of distributed generation on distribution system protection," in *Power Engineering Society Summer Meeting, 2002 IEEE*, vol. 1, 2002, pp. 103-105.
- [21] S. Chaitusaney and A. Yokoyama, "An Appropriate Distributed Generation Sizing Considering Recloser-Fuse Coordination," in *Transmission and Distribution Conference and Exhibition: Asia and Pacific, 2005 IEEE/PES*, 2005, pp. 1-6.
- [22] R. C. Dugan and S. K. Price, "Including distributed resources in distribution planning," in *Power Systems Conference and Exposition, 2004. IEEE PES*, vol. 3, 2004, pp. 1694-1698.
- [23] EPRI, "Engineering Guide for Integration of Distributed Generation and Storage into Power Distribution Systems," Technical Report 1000419, 2000.
- [24] R. C. Dugan, "Challenges in considering distributed generation in the analysis and design of distribution systems," in *Power and Energy Society General Meeting - Conversion and Delivery of Electrical Energy in the 21st Century, 2008 IEEE*, 2008, pp. 1-6.
- [25] R. A. Walling, R. Saint, R. C. Dugan, J. Burke, and L. A. Kojovic, "Summary of Distributed Resources Impact on Power Delivery Systems," *Power Delivery, IEEE Transactions on*, vol. 23, no. 3, pp. 1636-1644, Jul. 2008.
- [26] IEEE Standards Coordinating Committee 21. (2008, Dec.) IEEE Application Guide for STD 1547, IEEE Standard for Interconnecting Distributed Resources with Electric Power Systems. IEEEExplore.
- [27] F. A. Viawan and M. Reza, "The impact of synchronous distributed generation on voltage dip and overcurrent protection coordination," in *Future Power Systems, 2005 International Conference on*, 2005, p. 6.
- [28] J. C. Gomez and M. M. Morcos, "Coordination of voltage sag and overcurrent protection in DG systems," *Power Delivery, IEEE Transactions on*, vol. 20, no. 1, pp. 214-218, Jan. 2005.
- [29] L. K. Kumpulainen and K. T. Kauhaniemi, "Analysis of the impact of distributed generation on automatic reclosing," *Power Systems Conference and Exposition, 2004. IEEE PES*, vol. 1, pp. 603-608, Oct. 2004.
- [30] K. Kauhaniemi and L. Kumpulainen, "Impact of distributed generation on the protection of distribution networks," in *Developments in Power System Protection, 2004. Eighth IEE International Conference on*, vol. 1, 2004, pp. 315-318.
- [31] G. Kaur and M. Y. Vaziri, "Effects of distributed generation (DG) interconnections on protection of distribution feeders," in *Power Engineering Society General Meeting, 2006. IEEE*, 2006, p. 8.
- [32] J. L. Blackburn, *Protective Relaying: Principles and Application*, 2nd ed. NY: MARCEL DEKKER, 1998.
- [33] V. Menon and M. H. Nehrir, "A Review of issues regarding the use of distributed generators," in *Power Symposium, 2005. Proceedings of the 37th Annual North American*, 2005, pp. 399-405.
- [34] P. Mahat, C. Zhe, and B. Bak-Jensen, "Review of Islanding Detection Methods for Distributed Generation," in *Electric Utility Deregulation and Restructuring and Power*

- Technologies*, 2008, pp. 2743-2748.
- [35] J. C. Gomez and M. M. Morcos, "Distributed Generation: Exploitation of Islanding Operation Advantages," in *Transmission and Distribution Conference and Exposition: Latin America*, 2008, pp. 1-5.
- [36] W. Y. Zhang, S. Z. Zhu, J. H. Zheng, and H. Zhang, "Impacts of Distributed Generation on Electric Grid and Selecting of Isolation Transformer," in *Transmission and Distribution Conference and Exhibition: Asia and Pacific, 2005 IEEE/PES*, 2005, pp. 1-7.
- [37] R. F. Arritt and R. C. Dugan, "Distributed generation interconnection transformer and grounding selection," in *Power and Energy Society General Meeting - Conversion and Delivery of Electrical Energy in the 21st Century, 2008 IEEE*, 2008, pp. 1-7.
- [38] R. C. Dugan, "Examples of ferroresonance in distribution systems," in *Power Engineering Society General Meeting, 2003, IEEE*, vol. 2, 2003.
- [39] W. H. Kersting, "Radial Distribution Test Feeders," IEEE, 2001.
- [40] P. Kundur, *Power System Stability and Control*, N. J. Balu and M. G. Lauby, Eds. McGraw-Hill, Inc., 1994.
- [41] J. J. Grainger and J. William D. Stevenson, *Power System Analysis*, S. W. Director, Ed. McGraw-Hill, Inc., 1994.
- [42] J. R. Carson, "Wave propagation in overhead wires with ground return," *Bell System technical Journal*, vol. 5, 1926.
- [43] S. J. Chapman, *Electric Machinery Fundamentals*, 3rd ed., E. Ariza H., Ed. Santa Fe de Bogota, Colombia: McGRAW-HILL INTERAMERICANA, S.A., 2000.
- [44] T. A. Short, *Electric Power Distribution Equipment and Systems*. Boca Raton, FL: Taylor & Francis Group, 2006.
- [45] L. L. Grigsby, *Electric Power Transformer Engineering*, J. H. Harlow, Ed. Electric Power Engineering Series, 2004.
- [46] IEEE Power Engineering Society, "IEEE Standard for General Requirements for Liquid-Immersed Distribution, Power and Regulating Transformers," Institute of Electrical and Electronics Engineers Standard C57.12.00-2006, 2007.
- [47] IEEE Power Engineering Society, "IEEE Standard for Terminal Markings and Connections for Distribution and Power Transformers," Institute of Electrical and Electronic Engineers IEEE Std. C57.12.70-2000, 2001.
- [48] Transformers Committee of the IEEE Power Engineering Society, "IEEE Guide for Application of Transformer Connections in Three-phase Distribution Systems," Institute of Electrical and Electronic Engineers IEEE C57.105TM-1978, Reaffirmed 2008.
- [49] W. H. Kersting, "Distribution Feeder Voltage Regulation Control," in *Rural Electric Power Conference*, 2009, pp. C1-7.
- [50] IEEE Power Engineering Society, "IEEE Standard requirements, terminology, and test code for step-voltage regulators," Institute of Electrical and Electronics Engineers IEEE Std. C57.15-1999, 2000.
- [51] W. H. Kersting, "The Modeling and Application of Step Voltage Regulators," in *Power Systems Conference and Exposition*, 2009, pp. 1-8.
- [52] M. W. Davis, R. Broadwater, and J. Hambrick, "Modeling and Testing of Unbalanced

- Loading and Voltage Regulation," National Renewable Energy Laboratory NREL/SR-581-41805, 2007.
- [53] L. R. Araujo, D. R. Penido, S. Carneiro, J. L. Pereira, and P. A. Garcia, "A Comparative Study on the Performance of TCIM Full Newton versus Backward-Forward Power Flow Methods for Large Distribution Systems," in *Power Systems Conference and Exposition*, 2006, pp. 522-526.
- [54] DIgSILENT PowerFactory Version 14.0, "PowerFactory Manual," 2008.
- [55] P. A. Garcia, J. L. Pereira, S. Carneiro, V. M. da Costa, and N. Martins, "Three-Phase Power Flow Calculations Using the Current Injection Method," *Power Systems*, vol. 15, no. 2, pp. 508-514, May 2000.
- [56] Distribution System Analysis Subcommittee, "IEEE 4 Node Test Feeder," Institute of Electrical and Electronics Engineers.
- [57] GE Consumer & Industrial Electrical Distribution, "Distribution System Feeder Overcurrent Protection," General Electric GET-6450, 1997.
- [58] P. M. Anderson, *Power System Protection*, R. F. Hoyt, Ed. NJ: IEEE Press Editorial Board, 1999.
- [59] ABB Power T&D Company Inc., "Type CO Overcurrent Relays," ABB/Westinghouse Description Bulletin 41-101E, 1990.
- [60] General Electric industrial Systems, "Electromechanical Products Catalog," GE Multilin Catalog GEZ-7723F, 2003.
- [61] Power System Relaying Committee of the IEEE Power Engineering Society, "IEEE Standard Inverse-Time Characteristics Equations for Overcurrent Relays," Institute of Electrical and Electronics Engineers Standard C37.112, 1996.
- [62] IEEE Power Engineering Society, "IEEE Standard for Electrical Power System Device Function Numbers, Acronyms, and Contact Designations," Institute of Electrical and Electronics Engineers Standard C37.2, 2008.
- [63] A. Greenwood, *Electrical Transients in Power Systems*, 2nd ed. John Wiley & Sons, inc, 1991.
- [64] IEEE Power Engineering Society, "IEEE Standard Service Conditions and Definitions for High-Voltage Fuses, Distribution Enclosed Single-Pole Air Switches, Fuse Disconnecting Switches, and Accesories," IEEE Standard C37.40, 2003.
- [65] W. H. Kersting and W. H. Phillips, "Distribution System Short Circuit Analysis," in *Energy Conversion Engineering Conference*, 1990, pp. 310-315.
- [66] D. Nedic, B. Graeme, and J. Heath, "A Comparison of Short Circuit Calculation Methods and Guidelines for Distribution Networks," in *19th International Conference on Electricity Distribution*, Viena, 2007.
- [67] Power System Engineering Committee, "IEEE Recommended Practice for Electric Power Distribution for Industrial plants," IEEE Standard 141, 1993.
- [68] I. Kasikci, *Short Circuits in Power Systems: A practical Guide to IEC 60909*. Wiley-VCH, 2002.
- [69] American National Standard Institute, "American National Standard for High Voltage Expulsion and Current-Limiting Type Power Class Fuses and Fuse Disconnecting Switches," IEEE Standard C37.46, 2000.

- [70] S&C Electric Company. (2009, Nov.) S&C Electric Company: Excellence Through Innovation. [Online]. [http://www.sandc.com/support/tccs\\_smd2040.asp](http://www.sandc.com/support/tccs_smd2040.asp)
- [71] J. Vithayathil, *Power Electronics\_Principles and Applications*. McGraw-Hill, 1995.
- [72] M. H. Rashid, *Power Electronics\_Circuits, devices, and applications*, 2nd ed., M. Pompili, Ed. Prentice Hall, Inc, 1993.
- [73] F. Katiraei, R. Iravani, N. Hatziargyriou, and A. Dimeas, "Microgrids Managment\_Controls and Operation Aspects of Microgrids," *IEEE Power and Energy Magazine*, pp. 54-65, May 2008.
- [74] Renewable Energy Policy Network for the 21st Century, "REN21\_Global Statu Report," REN21, 2009.
- [75] R. Hara, H. Kita, T. Tanabe, H. Sugihara, and S. Miwa, "Testing the Technologies\_Demonstration Grid-Connected Photovoltaic Projects in Japan," *IEEE Power and Energy Magazine*, vol. 7, no. 3, pp. 77-85, May 2009.
- [76] W. H. Kersting, "Distribution Feeder Voltage Regulation," 2009.
- [77] W. H. Kersting, "The Computation of Neutral and Dirt Currents and Power Losses," in *Power Systems Conference and Exposition*, 2004, pp. 213-218.
- [78] R. C. Dugan, W. H. Kersting, S. Carneiro, R. F. Arritt, and T. E. Mcdermott, "Roadmap for the IEEE PES test feeders," in *Power Systems Conference and Exposition*, 2009, pp. 1-4.
- [79] T. E. McDermott, "Working Group on Recommended Practice for Distribution System Analysis-P1729," in *Power and Energy Society General Meeting*, 2008, pp. 1-2.
- [80] W. H. Kersting, "Transformer Model Test System," in *Transmission and Distribution Conference and Exposition*, 2003, pp. 1022-1026.
- [81] V. Gurevich, *Electric Relays: Principles and Applications*, M. O. Thurston, Ed. Boca Raton, FL: Taylor & Francis Group, 2006.
- [82] H. H. Zeineldin and J. L. Kirtley, "Islanding Operation of Inverter Based Distributed Generation with Static Load Models," 2008.
- [83] L. F. Ochoa and R. M. Ciric. (2009) Evaluation of Distribution System Losses due to load unbalance. <http://www.montefiore.ulg.ac.be/services/stochastic/pfcc05/papers/fp498.pdf>.